

Protein Precipitation for the Purification of Therapeutic Proteins

by

Christopher W Morris

A thesis submitted for the degree of Doctor of
Engineering in The Department of Biochemical
Engineering, UCL

Abstract

This thesis documents the application of precipitant scouting and analytical tools for the development of a precipitation process for the purification of therapeutic proteins in biopharmaceuticals. Precipitation has the potential to bypass the bottlenecks in productivity experienced with packed bed chromatographic separations, offering a fast, robust first purification step with volume reduction at low cost.

In order to evaluate a large number of precipitation candidates, microscale investigations aided by automated liquid handling robotics were chosen, which conferred precision, speed, and complex experimental design with microliter material requirements and in-line analytics.

A precipitation screening methodology was successfully built onto a Tecan liquid handling platform including product recovery and techniques for measuring soluble protein, liquid volumes, and recovered protein precipitate. The protocol was supplemented with a custom-build Excel VBA driven Tecan control tool. This accelerated progress by freeing up the potential of the liquid handling arm, which was curtailed by system software.

These techniques were then used to characterise effective precipitants for the purification of monoclonal antibodies. Optimal conditions were identified on pure protein models, which were then bridged to process relevant cell culture fluid. Process performance, notably recovery yield and product quality were investigated on the precipitant conditions brought forward. Process integration aspects were explored, by linking precipitation with an anion exchange chromatography step. This led to discussion on future work and process scale up considerations.

Impact Statement

This impact statement serves as a suitable place to reflect on the work presented in this thesis and how it relates to academic and industrial applications. The core subject of precipitation is an established technology, and as stated in this thesis the work was focused on applying precipitation to modern downstream processing challenges. As part of an industrial sponsored doctorate, the investigation of precipitation and development of techniques helped the internal research and development at UCB, and a further doctorate was subsequently carried out, building on the foundations of this work.

A near full-time placement of this engineering doctorate on-site at UCB working as part of a larger team saw opportunities to set up automated high-throughput techniques on the liquid handling platforms for other teams in the company. 96-well plate assays were created for the team in upstream, and over the course of the final 2 years these techniques were employed weekly to a high level of precision and reproducibility by different people, saving time and increasing analytical throughput significantly. These techniques were written up as internal SOPs and it was rewarding to see tangible benefits of the skills developed throughout work detailed in this thesis.

I had the honour of achieving a finalist place in Cogent's UK life sciences student placement of the year award, very kindly nominated by Edith Lecomte-Narrant, due not only to my work at UCB, but also as a result of voluntarily running student open days, tours, and presentations. Regular opportunities to present my work both internally, at regional conferences, and at Recovery 2014 in Rostok were great experiences and I benefitted greatly from the feedback and sharing of ideas.

A silver lining of finalising this engineering doctorate later than planned, is that I have directly seen how industrial experience at UCB combined with academic grounding at UCL have helped me develop a specialist focus in the downstream processing of therapeutic proteins which have concretely led to the successful development of new purification technologies in my current role. The global launch of our new technology of fibre-based chromatography

(planned in the next few months at the time of writing), will have a high impact and I attribute a lot of the contributions I have made to this project to the experience and skills garnered during this doctoral thesis.

I, Christopher Morris confirm that the work presented in this thesis is my own. Where information has been derived from other sources, I confirm that this has been indicated in the thesis.

_____ Date _____

Acknowledgements

“I sometimes try to be miserable so that I may do more work, but find it is a foolish experiment.” William Blake 1757-1827

My first acknowledgement is to my supervisor Nigel, whose steering hand and wisdom guided me through all the various distractions and tangents I would have otherwise wilfully travelled down.

Secondly, a huge thank-you to Stefanos Grammatikos, Edith Lecomte-Narrant, Mari Spitali, Mark Pearce-Higgins and everyone else at UCB who guided me throughout the project. Their help, encouragement, knowledge, and experience have been invaluable.

Finally, I am extremely grateful to my family and friends who have shown inexhaustible encouragement and support throughout.

Table of Contents

Abstract.....	2
Impact Statement	3
Acknowledgements.....	5
Table of Contents.....	6
List of Figures.....	10
List of Tables	12
List of Abbreviations	13
Chapter One: Introduction & Literature Review	14
1.1 Project Relevance.....	14
1.2 Project Aims.....	18
1.3 The Production and Purification of Monoclonal Antibodies	19
1.3.1 Upstream Processing.....	21
1.3.2 Downstream Processing.....	23
1.4 Review of Protein Purification by Precipitation	24
1.4.1 Overview.....	24
1.4.2 Salting-In.....	27
1.4.3 Precipitation by Salting-Out.....	28
1.4.4 Metal Ion Precipitation.....	39
1.4.4 Non-ionic Polymer Precipitation.....	40
1.4.4 Isoelectric Precipitation.....	41
1.4.5 Polyelectrolyte Precipitation	42
1.4.6 Affinity Precipitation	47
1.4.7 Organic Solvent Precipitation	51
1.4.8 Protein Stabilising Agents.....	52
1.4.9 Conclusions & Direction of Research.....	55
1.5 Precipitate Formation & Properties.....	55
1.5.1 DLVO theory and precipitation	55
1.5.2 Precipitate formation – nucleation and growth by diffusion.....	56
1.5.3 Precipitate formation - growth by fluid motion	57
1.5.4 Precipitate conditioning / Camp Number.....	57
1.5.5 Precipitate breakage	58
1.5.6 Precipitate properties.....	59
1.6 The effect of mixing on precipitation	59

1.7	Centrifugation	60
1.8	Filtration.....	60
1.9	Bioprocess Development through Scale Down techniques.....	61
1.10	Conventional Experimental Design vs. Design of Experiments (DoE).....	62
1.11	Data Presentation	66
1.11.1	Sigmoidal Fitting of Precipitation Curves.....	66
1.11.2	Solubility Plots / Precipitation Midpoints.....	67
1.11.3	Fractionation Diagrams.....	69
1.12	Structure of Thesis	70
Chapter Two: Materials & Methods		71
2.1	Material.....	71
2.2	Tecan liquid handling platform.....	72
2.3	Protein quantification by A280nm.....	73
2.4	Precipitate measurement by A600nm	75
2.5	IgG measurement by Protein A HPLC	77
2.6	Protein purity assessment by Protein A HPLC	78
2.7	IgG charge profile measurement by iCE.....	79
2.8	Protein purity assessment by SDS-PAGE.....	80
2.9	Protein purity assessment by Bioanalyzer	81
2.10	Protein purity assessment by Bradford Total Protein	82
2.11	Aggregate profile measurement by SEC HPLC.....	83
2.12	IgG activity measurement by activity ELISA.....	84
2.13	Measuring clarification efficiency of centrifugal separation of precipitate	86
Chapter Three: Automated Precipitation Method Development		87
3.1	Abstract.....	87
3.2	Introduction.....	87
3.3	Tecan Control.....	88
3.3.1	Liquid Handling Arm (LiHa).....	88
3.3.2	Robotic Manipulator Arm (RoMa)	89
3.3.3	Liquid class systems.....	89
3.3.4	Labware and Carriers.....	91
3.3.5	The Excel-Evoware Design Tool	91
3.3.6	High resolution experimentation.....	96
3.3.7	Sampling	97
3.3.8	Supernatant Removal	99
3.3.9	Control of pH	99

3.3.10	Control of Temperature.....	100
3.4	Mixing in Micro-wells	101
3.4.1	Jet Macro Mixing.....	102
3.4.2	Calculating the Reynolds number through the tips.....	102
3.4.3	Calculating required mixing times with Jet Macro Mixing	103
3.4.4	Calculating the critical frequency of plate shaking for exceeding liquid surface tension	104
3.5	Micro-well centrifugation	105
3.6	Micro-well dimensions and pathlength calculations.....	106
3.7	Ionic Strength.....	107
3.8	Volume measurement	108
3.9	The impact of high salt solutions upon 280nm absorbance	110
3.10	Precipitate recovery	113
3.11	The Small Scale Precipitation Screening Methodology.....	114
3.12	Chapter Summary	117
Chapter Four:	Precipitation Screening.....	118
4.1	Abstract.....	118
4.2	Introduction.....	118
4.3	Initial Screening	120
4.4	Precipitation by salting-out.....	125
4.5	The effect of protein concentration upon precipitation performance.....	129
4.6	The effect of pH upon precipitation performance.....	135
4.7	Assessing the impact of different sodium salts upon precipitation.....	137
4.8	Size exclusion chromatography results.....	140
4.9	Activity ELISA results.....	141
4.10	Linking precipitation on pure protein to cell culture fluid.....	144
4.11	Chapter Summary	146
Chapter Five:	Precipitation as a primary purification step.....	148
5.1	Abstract.....	148
5.2	Introduction.....	149
5.3	Screening of precipitants on cell culture fluid	149
5.5	How pH control influences precipitation performance.....	152
5.6	Precipitation on future feed-streams	154
5.7	The impact of feed-stream ionic strength upon precipitation	157
5.8	Investigating precipitation performance with Design of Experiments.....	160
5.8.1	Design	160

5.8.2	Results & Analysis.....	161
5.9	The evaluation of precipitants through Design of Experiments.....	167
5.9.1	Introduction.....	167
5.9.2	Design	167
5.9.3	Results & Analysis.....	168
5.10	Chapter Summary	171
Chapter Six: Process Integration.....		172
6.1	Abstract.....	172
6.2	Introduction.....	173
6.3	Precipitation conditions.....	173
6.4	Buffer exchange step.....	176
6.5	Anion exchange chromatography step.....	177
6.6	Process flow SDS PAGE & Bioanalyzer.....	180
6.7	iCE analysis	185
6.8	Process Integration Considerations	186
6.8.1	Residual conductivity.....	186
6.8.2	Hydrophobic Interaction Chromatography	186
6.8.2	Pre-conditioning the process feed	187
6.8.3	Mixing.....	188
6.8.5	Centrifugal Recovery	189
6.8.8	Recovery through filtration.....	189
6.9	Chapter Summary	190
Chapter Seven: Conclusions and Future Scope of Work.....		191
7.1	Conclusions.....	191
7.1.1	Alternative Applications	191
7.1.2	Scale-Up Considerations.....	192
7.2	Future Expansion of Work.....	193
7.2.1	Key future work	193
7.2.2	Acid pre-conditioning for precipitation	193
7.2.3	Analytical methods	195
7.2.4	Screening on alternative proteins.....	196
7.2.5	Recovery and re-suspension on a UF/DF rig.....	196
7.2.6	Alternative precipitants screening.....	196
7.2.7	The next step.....	197
Chapter Eight: References		198

List of Figures

Figure 1. The schematic structure of an immunoglobulin (IgG) monoclonal antibody (mAb), and detailing the differences in mAb types [21].	20
Figure 2. A standard mAb platform upstream process [7].	22
Figure 3. A typical mAb downstream processing set of unit operations [13][9].	24
Figure 4. The log plot of haemoglobin solubility in ammonium sulphate solutions against molal salt concentration. The solubility, w , is normalised to that of pure water, w_0 . The mathematically derived contributions of the electrostatic (broken line) and the hydrophobic (dash-dot line) are displayed [36].	27
Figure 5. Phase diagram for the crystallisation and precipitation of macromolecules.	29
Figure 6. The schematic of polymer mixing, adsorption, re-conformation, particle aggregation and floc breakup processes in a typical flocculation system [104].	43
Figure 7. The comparison of measured and calculated yield of protein via precipitation in dependence of polyelectrolyte concentration [103].	44
Figure 8. DoE Factorial designs.	65
Figure 9. A three point hyper cube with axial points full factorial design space.	65
Figure 10. Sigmoid fitting of a precipitation curve.	67
Figure 11. The dependence of precipitation transition mid-points on NaCl concentrations for ammonium sulphate precipitations.	68
Figure 12. Enzyme and total protein solubility profiles in the presence of increasing precipitant concentration, taken from [166].	69
Figure 13. Enzyme-total protein fractionation diagram, an alternative presentation format data presented in Figure 12 [166].	69
Figure 14. Tecan system with default equipment layout	72
Figure 15. IgG ₁ standard curve prepared in the 96 well format.	74
Figure 16. The Ammonium Sulphate precipitation profile for pure IgG ₁ .	76
Figure 17. The profile of pure IgG ₁ in the presence of different precipitants and concentrations.	76
Figure 18. Protein A HPLC IgG ₁ calibration curve.	78
Figure 19. Protein A HPLC chromatogram of starting cell culture fluid.	79
Figure 20. iCE analysis generated from a re-solubilised IgG ₁ precipitate	79
Figure 21. Bioanalyzer electropherogram (top) and reciprocal false gel display (bottom and rotated).	81
Figure 22. Bradford total protein assay calibration against purified IgG ₁ .	83
Figure 23. An example size exclusion chromatography chromatogram.	84
Figure 24. An example 4 parameter curve fit to ELISA calibrations.	85
Figure 25. The modular display for the Excel-Tecan Tool.	94
Figure 26. IgG ₁ solubility profiles at different liquid heights.	98
Figure 27. Schematic diagrams of individual micro-well formats.	101
Figure 28. Solution absorbance at 977nm.	109
Figure 29. The effect of increasing Ammonium Sulphate concentration.	111
Figure 30. The effect of increasing Tri-Sodium Citrate concentration.	112
Figure 31. The high throughput screening methodology.	116
Figure 32. Analytical approaches used in a hierarchical screening approach, with number of conditions tested at each level shown.	119
Figure 33. Ammonium Citrate profile for the precipitation of IgG ₁ .	126

Figure 34. Lithium Sulphate profile for the precipitation of IgG ₁ .	127
Figure 35. Tri-Sodium Citrate profile for the precipitation of IgG ₁ .	128
Figure 36. Sodium (mono) Phosphate profile for the precipitation of IgG ₁ .	129
Figure 37. Ammonium sulphate precipitation profiles at different final concentrations of purified IgG ₁ .	130
Figure 38. Tri-sodium citrate precipitation profiles at different final concentrations of purified IgG ₁ .	131
Figure 39. Ammonium sulphate precipitation mid-points against a log plot of IgG ₁ concentration.	133
Figure 40. The impact of pH upon the precipitation performance of ammonium sulphate.	135
Figure 41. The impact of pH upon the precipitation performance of sodium sulphate.	136
Figure 42. The impact of sodium acetate upon the precipitation performance of ammonium sulphate.	138
Figure 43. The impact of tri-sodium citrate upon the precipitation performance of ammonium sulphate.	139
Figure 44. The impact of sodium chloride upon the precipitation performance of ammonium sulphate.	140
Figure 45. SEC Chromatogram for re-solubilised precipitates.	141
Figure 46. Activity ELISA for binding site 1.	142
Figure 47. Activity ELISA for binding site 2.	142
Figure 48. Comparing precipitation of pure and CCCF IgG ₁ based material.	144
Figure 49. The effect of pH on the precipitation profiles with ammonium sulphate.	153
Figure 50. Effect of antibody titre has upon the precipitation profiles with Ammonium Sulphate.	155
Figure 51. Effect of NaCl on the precipitation profiles with ammonium sulphate.	157
Figure 52. Coefficients for DoE model.	161
Figure 53. 4D contour plots showing the recovery yield of IgG ₁ .	162
Figure 54. 4D contour plots showing the recovered purity of IgG ₁ .	163
Figure 55. Sweet spot prediction plots for design space tested.	164
Figure 56. 4D contour plots showing the recovery yield of IgG ₁ .	169
Figure 57. 4D contour plots showing the purity of IgG ₁ .	170
Figure 58. Anion exchange chromatogram for the purification of ammonium sulphate precipitated material.	178
Figure 59. SDS PAGE process flow for ammonium sulphate and sodium citrate driven precipitations.	180
Figure 60. SDS PAGE process flow for lithium sulphate and sodium sulphate.	181
Figure 61. SDS PAGE process flow for the low pH plus sodium sulphate precipitation.	181
Figure 62. SDS PAGE displaying final feed compositions.	182
Figure 63. Non-reduced Bioanalyzer analysis of samples post AEX chromatography false gel image.	183
Figure 64. Isoelectric capillary electrophoresis of samples post precipitation and anion exchange chromatography.	185

List of Tables

Table 1. Monoclonal antibodies and related proteins on the market in (2010) with global sales of blockbuster drugs shown (2012). Adapted from [1] and [7].....	15
Table 2. Hofmeister and Lyotropic series with ion classification into kosmotropes and chaotropes [40][51].....	31
Table 3. Low and High molecular weight PEG properties [71][95][95]	41
Table 4. The application of different polyelectrolytes for the purification of proteins by precipitation.	45
Table 5. Advantages of affinity precipitation.	48
Table 6. Ideal design criteria for affinity macroligands [127].	50
Table 7. Pharmaceutical excipients for use in protein formulations, adapted from [135]. ...	54
Table 8. Liquid Class descriptions.....	90
Table 9. The command break-up for gwl formatted code.....	92
Table 10. A gwl formatted command line for one robotic tip operation	92
Table 11. Main salt precipitants investigated and their corresponding ionic strengths.	107
Table 12. A977nm specific absorption values for different solutions.	110
Table 13. Screening results table on pure protein.....	122
Table 14. Results for both the <i>binding site 1</i> and <i>binding site 2</i> activity assays.....	143
Table 15. Effectiveness of different cation-anion combinations for precipitating IgG ₁	146
Table 16. Performance of various precipitants tested with the screening methodology on pure IgG ₁ and cell culture fluid.....	151
Table 17. Comparison of purity values.....	158
Table 18. The design constraints set out for the DoE for the first experimental run, and then the additional conditions for the second run.	160
Table 19. The design constraints for the DoE first experimental run.	167
Table 20. Performance of precipitation steps on cell culture fluid.	174
Table 21. pH and conductivity tracking throughout precipitation steps.	175
Table 22. Buffer exchange step performance	176
Table 23. AEX column operation regime.	178
Table 24. Anion exchange step performance.....	179
Table 25. Bioanalyzer IgG ₁ purity post anion exchange chromatography.....	183

List of Abbreviations

AEX	Anion Exchange (chromatography)
ADH	Alcohol Dehydrogenase
AS	Ammonium Sulphate
AU	Absorbance Units
BSA	Bovine Serum Albumin
CCCF	Clarified Cell Culture Fluid
CHO	Chinese Hamster Ovary
csv	comma separated values
CV	Column Volume
DoE	Design of Experiments
DF	Diafiltration
DNA	Deoxyribonucleic acid
dsDNA	Double Stranded DNA
DSP	Downstream Process
fAb	Fragment Antigen Binding
ELISA	Enzyme Linked Immunosorbant Assay
EtOH	Ethanol
FT	Flow-through
gwl	general writing language
HCl	Hydrogen Chloride
HCP	Host Cell Protein
HEWL	Hen Egg White Lysozyme
HIC	Hydrophobic Interaction Chromatography
HMW	High Molecular Weight (species)
HPLC	High Pressure Liquid Chromatography
HTPD	High Throughput Process Development
iCE	Isoelectric Capillary Electrophoresis
IgG	Immunoglobulin
LiS	Lithium Sulphate
LMW	Low Molecular Weight (species)
mAb	Monoclonal Antibody
MSDS	Material Data Safety Sheet
MWS	Multiple Wavelength Detector
NaCit	(tri) Sodium Citrate
NaOH	Sodium Hydroxide
NaS	Sodium Sulphate
NEM	N-ethylmaleimide
pHNaS	Low pH step followed by Sodium Sulphate precipitation
PrA	Protein A
pI	Isoelectric point
ppm	Parts per million
ppb	Parts per billion
PPI	Protein-Protein Interactions
Precip.	Precipitated/Precipitation
QbD	Quality by Design
R&D	Research and Development
RO	Reverse Osmosis
SDS PAGE	Sodium Dodecyl Sulphate Polyacrylamide Gel Electrophoresis
SEC	Size Exclusion Chromatography
STAG	System Trailing Air Gap
TAG	Trailing Air Gap
TCA	Tri-Chloro Acetic (acid)
UF	Ultrafiltration
UV	Ultraviolet
WFI	Water For Injection

Chapter One: Introduction & Literature Review

“**Frodo:** I wish the ring had never come to me. I wish none of this had happened.

Gandalf: So do all who live to see such times. But that is not for them to decide. All we have to decide is what to do with the time that is given to us. There are other forces at work in this world Frodo, besides the will of evil. Bilbo was meant to find the Ring. In which case, you were also meant to have it. And that is an encouraging thought.”

J R R Tolkien - The Fellowship of the Ring

1.1 Project Relevance

The biopharmaceutical industry, or more specifically the biotechnology industry has now firmly established itself within the pharmaceutical industry and has seen rapid growth in the last 30 years. Starting with the first licensed biotechnological product, insulin in 1982, there are now over 200 biotechnology products on the market with an estimated 900 more in various stages of clinical developments [1]. Biotechnology utilises bio-molecular engineering or living systems to produce biological based products for the treatment or identification of targets of disease in patients and broadly covers monoclonal antibodies, vaccines, recombinant proteins, gene and cell-based therapies. Biotechnology sales now account for over 20% of all prescription product sales worldwide, up from under 4% in 2002 and this market share is expected to continue to rise [1] with large molecule drugs enjoying much higher clinical success rates than their small molecule counterparts [2].

Table 1 shows monoclonal antibodies (mAbs) that have been shown to target and treat a wide range of clinical indications, ranging from allergies and post-surgery treatments to cancers and rheumatoid arthritis. A recent review of the pharmaceutical industry revealed monoclonal antibodies made up 37% of all biotechnology products in development in 2012; an increase of over 350% over the past 11 years [1], demonstrating how important advances in monoclonal antibody production and purification are.

Developing and bringing a successful product to the market has traditionally been cited to cost around the \$1Billion mark [3][4] taking into account 10-12 years of research and development,

and pipeline failure. However in a recent analysis dividing total R&D spending over the years of the top pharmaceutical companies by their number of approved drugs showed figures ranging from \$3.5b per drug for companies such as Novartis and Amgen to greater than \$10b in the case of AstraZeneca and Sanofi [5]. It should also be noted that these R&D costs are adjusted by a percentage return on investment of typically 11% and are also heavily subsidised under the auspices of tax credits [6]. Although not taking into account products in pipeline development, this is a drastically larger figure and one that emphasises the importance of generating early, comprehensive process understanding of new molecules.

Table 1. Monoclonal antibodies and related proteins on the market in (2010) with global sales of blockbuster drugs shown (2012). Adapted from [1] and [7].

Product	Target	Indication	Antibody type	Company	Year
Monoclonal antibodies					
Orthoclone	CD3	Acute kidney transplant rejection	Murine	Ortho Biotech	
ReoPro	Platelet GPIIb/IIIa	Prevention of blood clot	Murine	Centocor	1986
Rituxan	CD20	Non-Hodgkin's Lymphoma	Chimeric	Genentech/Biogen-Iddec	1994
Panorex	17A-1	Colorectal cancer	Murine	GSK	1997
Zenapax	IL2Ra (CD25)	Acute kidney transplant rejection	Humanised	Hoffman-LeRoche	1995
Simulect	IL2R	Prophylaxis of acute organ rejection	Chimeric	Novartis	1997
Synagis	RSV	Respiratory Syntical Virus	Humanised	Medimmune	1998
Remicade	TNFa	Rheumatoid arthritis	Chimeric	Centocor	1998
Herceptin	Her2	Metastatic breast cancer	Humanised	Genentech	1998
Mylotarg	CD33	Acute myelogenous lymphoma	Humanised	Wyeth-Ayerst	1998
Campath	CD52	B cell chronic lymphocytic leukemia	Humanised	Takeda	2000
Zevalin	CD20	Non-Hodgkin's Lymphoma	Murine	Biogen-Iddec	2001
Humira	TNFa	Rheumatoid arthritis	Humanised	Abbott	2002
Bexxar	CD20	Non-Hodgkin's Lymphoma	Murine	Corixa-GSK	2002
Xoliar	IgE	Allergy	Humanised	Genentech/Novartis	2003
Erbix	EGFR/Her1	Colorectal cancer	Humanised	Bristol-Myers Squibb / Eli Lilly	2004
Avastin	VEGF	Colorectal cancer	Humanised	Genentech	2004
Raptiva	CD11a	Psoriasis	Humanised	Genentech / Xoma	2004
Tysabri	A4 integrin	Multiple sclerosis	Humanised	Biogen-Iddec/Elan	2004
Vectibix	EGFR	Colorectal cancer	Human	Amgen	2006
Solaris	C5 complement	PNH - paroxysmal nocturnal hemoglobinuria	Humanised	Alexion	2007
Stelera	IL12 and IL23	Psoriasis	Human	Centocor	2008
Simponi	TNFa	Rheumatoid arthritis	Human	Centocor	2008
Actemra	IL-6	Rheumatoid arthritis	Humanised	Roche	2009
Monoclonal antibody fragments					
Lucentis	VEGF-A	Age related macular degeneration	Fab'	Genentech	2006
Cimzia	TNFa	Crohn's disease	Pegylated Fab'	UCB	2008
Fc fusion proteins					
Enbrel	TNFa	Rheumatoid arthritis, psoriasis, ankylosing spondylitis	TNFa receptor + IgG1 Fc	Amgen	1998
Amevive	CD2	Psoriasis	LFA3 fused IgG1 Fc	Biogen-Iddec	2003
Orencia	CD80/86	Rheumatoid arthritis	CTLA4 fused to IgG1 Fc	Bristol-Myers Squibb	2005
Arcalyst	IL-1	CAPS - Cryoprin Associated Periodic Syndrom	IL-1 receptor IgG1 Fc	Regeneron	2007

Developing techniques to speed up process development allows for drugs to reach the market faster, reducing development costs whilst improving the benefit to patients, and this can be achieved through microscale bioprocessing [8].

Motivation

Mammalian cell-culture now regularly reach titres of monoclonal antibody expression in excess of 5 grams per litre [7][9]. This has been achieved through high expression systems and cell line development techniques [10][11] in conjunction with media and cell culture process optimisation. Improvement in titre brings economy of scale to upstream processing; as the productivity per unit volume increases. However, these economies of scale do not always translate easily to downstream processing, and especially purification resins can prove a bottleneck.

There is evidence that traditional downstream processing techniques can struggle to match the advances made in upstream processing [12], and with future titres exceeding 10g/L anticipated these challenges are expected to become more pronounced. Purification with chromatographic resins is determined by the mass of product to be purified, rather than volume. However a good case can be made that for large scale manufacturing of recombinant therapeutics there is no need to deviate from platform chromatography and filtration unit operations since cost of goods reduce well with scale [13].

The priority for downstream process design is to maintain a high product yield whilst achieving a desirable level of purification. Speed of process development, good throughput, process robustness and ease of scale up are also important factors. Recovery and purification of therapeutic proteins from cell culture is a key aspect of the entire production process, contributing from 40% to as much as 80% of the total manufacturing costs [14]. The space and volume requirements for downstream operations include buffers, cleaning and sanitisation, which increase in proportion to the mass of product to be purified. Technology, equipment, and facility limitations are an issue with downstream processing capacity; hence

traditional downstream processing techniques can struggle to match advancements made in upstream processing [12].

Challenges

Recovering a single protein fraction from fermentation broth is complicated by low target protein concentrations and selectively separating this protein from other biomolecules in solution. Additionally, recovery steps need to avoid extremes in conditions to preserve the activity of the protein [15]. An effective purification process must remove process related impurities such as host cell proteins, DNA, media additives as well as product related components; high molecular weight species and aggregates. Suitable viral clearance is essential to act as a contingency for an undetected contamination [16]. The difficulties in achieving cost efficient larger scale chromatographic separations in biopharmaceutical processes to match increasing upstream titres [17] have opened the way for the inclusion of selective but scalable protein precipitation methods which offer significant throughput potential [7].

The production and processing of therapeutic proteins such as monoclonal antibodies faces a range of purification challenges; reducing costs, achieving higher throughput, robust process development and the integration of upstream and downstream technologies.

Proposed solution

Precipitation offers an older technology to a modern challenge, where the constraints of traditional fixed bed chromatographic separations could be effectively bypassed. The challenges faced will be whether precipitation can match chromatography with favourable yields and levels of purification whilst offering significantly improved process throughputs and cost-savings and this provides the backdrop to the thesis.

1.2 Project Aims

The work presented in this thesis aims to design an automated high throughput screening methodology for the rapid screening of precipitants and hence to identify alternative purification strategies to the traditional approach of Protein A chromatography for the purification of monoclonal antibodies (mAbs).

Central to this study is the assertion that precipitation, a well-established technique but one that traditionally displays limited performance compared to chromatography, can provide a viable alternative in future bioprocess designs.

To investigate this assertion a precipitant screening study will be performed, with the objective to optimise performance. The study will be achieved through application of scale down methods using automated liquid handling techniques.

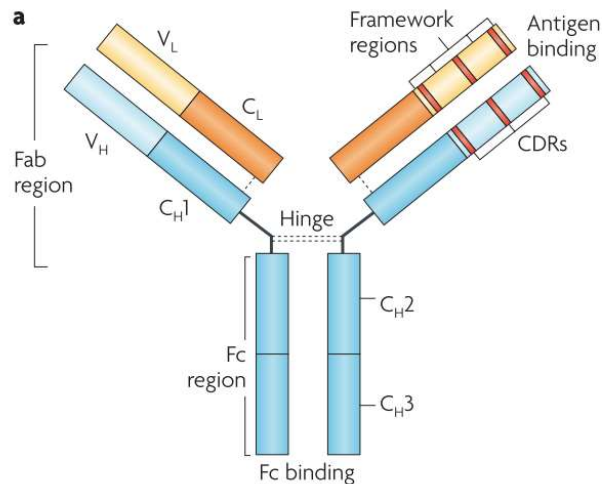
Project milestones for this thesis include:

- 1) The development of a high throughput automated methodology for the evaluation of precipitation, centrifugal recovery and re-suspension of precipitates
- 2) Identifying optimal precipitation conditions for the early clarification of mAbs from clarified cell culture process fluid
- 3) Characterising the scale-up of the microscale method to bench scale operation
- 4) Integrating the precipitation step with a traditional packed bed chromatographic separation

1.3 The Production and Purification of Monoclonal Antibodies

This section will focus on the platform approach to the production and purification of humanised IgG monoclonal antibodies expressed through a mammalian Chinese Hamster Ovary (CHO) cell line. Mammalian platforms are the expression system of choice for the production of mAbs as they possess the full capability of efficiently translating, assembling and modifying high titres of antibodies whilst successfully secreting the assembled antibodies extracellularly [9].

Monoclonal antibodies, mAbs, are monospecific antibodies produced by identical clones of a unique parental immune cell. Monoclonal antibodies exhibit monovalent affinity, binding to same target epitope, part of the antigen recognisable by the immune system. Due to their variable binding regions, mAbs have the near limitless potential of being able to detect or purify almost any substance [18]. Monoclonal antibodies, classed under therapeutic proteins offer distinct advantages over small molecule pharmaceuticals. They benefit from higher specificities, longer serum half-lives and can be specifically designed for novel therapeutic targets whilst imparting little or no immunological response in patients [19][20].



Types of mAbs

Murine	Entirely murine amino acids	'o' = mouse e.g. mur <u>o</u> monab
Chimeric	Human constant (C) + murine variable (V) regions	'xi' = chimeric e.g. ritux <u>i</u> mab
Humanized	Murine complementarity determining regions (CDRs)	'zu' = humanized e.g. alemtu <u>z</u> umab
Human	Entirely human amino acids	'u' = human e.g. adalimu <u>u</u> mab

Figure 1. The schematic structure of an immunoglobulin (IgG) monoclonal antibody (mAb), and detailing the differences in mAb types [21].

The complementary-determining regions (CDRs) of a mAb within the Fab' region bind to specific targets, leading to antagonistic or signalling responses. The fraction crystallisable, Fc, region of a mAb consists of a hinge and constant heavy domains of CH2 and CH3, and can be utilised for complementary binding for Fc receptors [21]. The general progression from murine mAbs (see Figure 1), to chimeric mAbs with murine variable V regions grafted onto human constant C regions, to humanised mAbs of a human IgG scaffold modified with murine CDR regions and finally to the most recent, fully human mAbs has brought about reduced immunogenicity and an improved risk-benefit ratio [21]. This is exemplified by current mAbs achieving clinical success rates of around 20% which are noticeably higher than the average 5% rate achieved by small molecules [22].

1.3.1 Upstream Processing

Figure 2 displays a typical mAb upstream process. Cells are first thawed from a vial, then expanded through a stage of inoculum steps, which are further expanded through a series of seed bioreactors before transferring to the main production bioreactor where mAb is extracellularly expressed into the medium. Primary recovery is often covered under upstream processing, with centrifugation followed by depth filtration remaining as the main set of unit operations for clarifying the cell culture fluid from the broth by removing cells and cell debris [7].

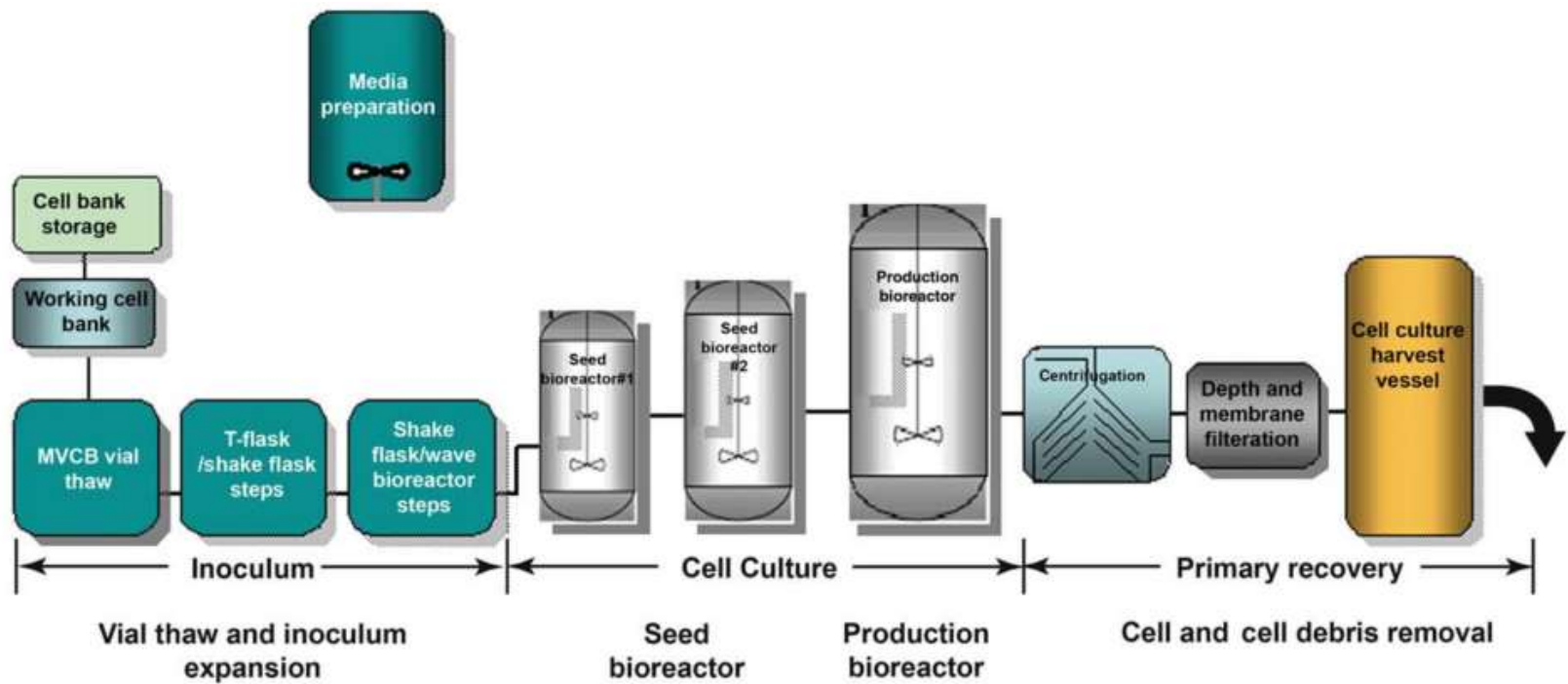


Figure 2. A standard mAb platform upstream process [7]

1.3.2 Downstream Processing

Downstream processing is the term for all unit operations run after the upstream production steps of manufacture. The large scale approach for the purification of monoclonal antibodies is currently dominated by chromatographic separations. A typical sequence of purification steps involves Protein A affinity chromatography followed by one or two polishing steps using size exclusion, hydrophobic interaction or ion exchange chromatography [23]. The combinations of steps is designed to remove contaminant proteins from the initial cell and media soup to parts per million (ppm) levels and DNA to parts per billion (ppb) [9], resulting in a purified therapeutic protein.

Protein A (PrA) affinity chromatography is the workhorse of downstream processing due to the high physiochemical selective binding to monoclonal antibodies exhibited by the ligand [16]. PrA chromatography is run in bind/elute mode; as the clarified cell culture fluid is passed through the stationary resin, mAb product binds to the immobilised ligand with high affinity whilst the majority of impurities flow through the resin stationary phase and are separated. Bound product can then be eluted off the column by lowering the pH of the mobile phase, decreasing the hydrophobic binding between ligand and protein by increasing the electrostatic repulsion [16]. Product can then be collected in the elution pool, typically followed by a low pH viral inactivation step before continuation to subsequent downstream processing steps. The application of PrA chromatography to high titre feed-streams can lead to notable bottlenecks. Protein A resins achieve binding capacities ranging typically between 20-50g of mAb per litre of resin, meaning that as upstream productivity increases, existing columns require higher levels of cycling or new, larger columns need to be introduced at increased capital expense. With resin costs regularly reaching in excess of £10,000/L this shifts the focus to the use of smaller columns utilised with higher cycle numbers, reducing process throughput. Protein A chromatography as a single step typically contributes to 50% of total cost of goods [13]. Higher cycling has the knock-on effect of greater buffer usage and all associated operations such as storage tanks and filtration capacity.

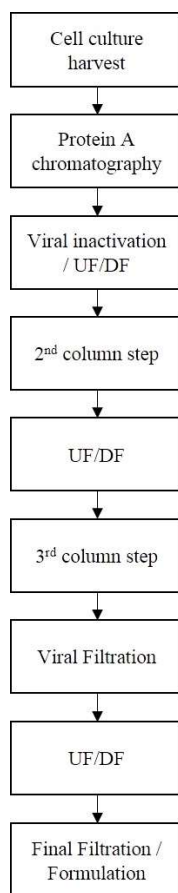


Figure 3. A typical mAb downstream processing set of unit operations [13][9]

With mammalian cell culture-derived antibodies, the downstream process must also have capacity for suitable viral clearance. As displayed in Figure 3, two viral inactivation/ removal steps are incorporated into the process flow. The low pH hold viral inactivation step is typically performed by adjusting the protein A eluate pool, with the viral filtration step performed after the chromatographic separations. Ultrafiltration/diafiltration steps are utilised for product concentration and adjusting the buffer/pH suitable for the next purification step.

1.4 Review of Protein Purification by Precipitation

1.4.1 Overview

Precipitation is said to occur when a soluble substance in solution becomes insoluble. Precipitation can be induced by a change in the chemical or physical environmental conditions.

Precipitate recovery requires a simple solid-liquid separation such as filtration or centrifugation, so precipitation of a target molecule can be a powerful tool in bio-separations [24].

The main advantages offered by precipitation is that it is relatively inexpensive, can be carried out using simple equipment, can be run in continuous mode, and forms a protein solid which has been shown to retain stability in long term storage [25]. Traditional precipitation steps are tolerant to variations in process feed-streams, and as such are used in early bioprocess separations to deal with impurities such as nucleic acids and lipids.

The application of precipitation for the purification and recovery of proteins is common in the milk and blood industries. The precipitation of milk by a range of acids has been shown to fractionate casein effectively [26][27][28]. One of the largest scale applications of protein precipitation, however, is probably the fractionation of human blood by ethanol [29][30]. This is based on a series of precipitation steps manipulated by temperature and the addition of ethanol. Due to the volumes of liquid involved traditional chromatography may be unsuitable for processing at this scale [31]. Although chromatography is frequently the main approach for downstream operations, precipitation offers a good preliminary step for processing crude streams, decreasing the load on following chromatography steps, and thus increasing the separation power.

A protein's solubility is a function of its physical characteristics; the number, size and distribution of hydrophobic residues, charged, and polar groups on its surface. A protein can be brought out of solution, out of its soluble state, and precipitated by a range of approaches; the pH, ionic strength, and temperature can be changed, as can the properties of the solvent by addition of a precipitating agent. The challenge with selective protein precipitation is that the conditions required to form a precipitate depend upon a range of factors: pH, temperature, protein properties, solvent properties, and the chemical composition of precipitant. Hence optimising a precipitation process and establishing process reliability and robustness can be a difficult challenge.

Precipitating agents can be broadly split into three main categories: salts, water-miscible organic solvents and high molecular weight polymers [32]. These all act in accordance with the model of preferential exclusion proposed [33], whereby the thermodynamically unfavourable interactions between protein and precipitant (the preferentially excluded solvent) are minimised once the protein is in a precipitated state, due to the reduced interface of the protein and solvent.

They have been split into slightly more specific categories based on chemical properties of precipitants and possible mechanisms of action:

1. Precipitation by salting-out through high concentration salts
2. Metal Ion precipitation
3. Non-ionic polymer precipitation
4. Isoelectric precipitation by reducing protein net charge to zero
5. Polyelectrolyte precipitation / flocculation
6. Affinity precipitation
7. Precipitation by organic solvent addition

These categories of precipitant will be discussed in detail.

1.4.2 Salting-In

Although not a precipitation technique it is important to understand the effect low salt concentrations can exert upon proteins in solution. At low salt concentrations typically ranging from 0 to 500mM, proteins and other polyelectrolytes can be stabilised in solution, through non-specific electrostatic interactions. Proteins are surrounded by the salt counter-ions and this screening leads to a decrease in the electrostatic free energy of the protein and the increased activity of the solvent, resulting in increased overall solubility [34].

Examples of effective salting-in salts include: barium chloride, calcium chloride, magnesium chloride, and nickel (II) chloride, [35]. These all show little preferential hydration towards proteins but can often act as protein destabilisers at higher concentrations[34].

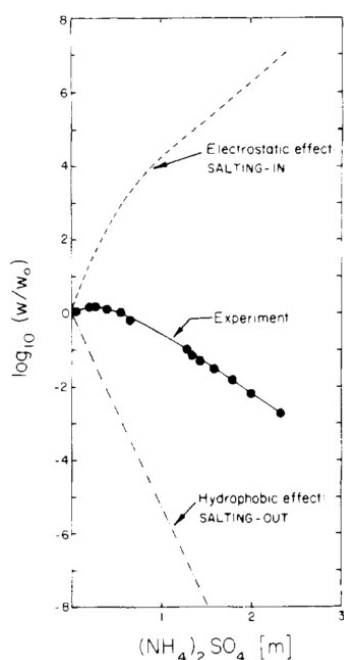


Figure 4. The log plot of haemoglobin solubility in ammonium sulphate solutions against molal salt concentration. The solubility, w , is normalised to that of pure water, w_0 . The mathematically derived contributions of the electrostatic (broken line) and the hydrophobic (dash-dot line) are displayed [36].

Figure 4 displays how salting-in can improve protein solubility at low concentrations before being superseded by the more dominant salt-out hydrophobic effects the higher salt molarities. Salting-in is not a precipitation technique as it increases the overall solubility of proteins in

solutions yet needs to be factored when considering low ionic strength conditions and dilution steps.

Proteins in some cases can be salted-in at high salt concentrations, solutions containing divalent cations have been demonstrated to increase lysozyme solubility at high concentrations [37]. Protein solubility in these cases is at a minimum in intermediate salt concentrations, and hence for precipitation screening studies it will be important to test a wide range of concentrations of a new precipitant to evaluate it fully.

1.4.3 Precipitation by Salting-Out

Precipitation of a target molecule can occur with the addition of salts. With protein precipitation, the protein is usually not denatured, and activity can be recovered upon re-dissolving the pellet. In addition these salts can also stabilise proteins against denaturation, proteolysis or bacterial contamination [35].

Precipitation by addition of a salt is termed 'salting out'. Salting out works on the nature of the hydrophobicity of the surface of proteins; most hydrophobic groups predominate in the centre of the protein, but some are found externally. These interact with water molecules to add order and structure. With salt addition, water solvates the salt ions. As the salt concentration increases, water is removed from around the protein, eventually exposing the hydrophobic patches. These hydrophobic patches on the proteins interact with one another, resulting in aggregation.

Proteins with larger or more numerous hydrophobic patches will aggregate and precipitate faster than those with smaller or fewer patches, allowing for protein fractionation. Hence, apart from the size and shape of the protein, the number and distribution of charges, hydrophobic residues, and non-ionic polar groups it possesses determines the concentration of salt required to form precipitates [35].

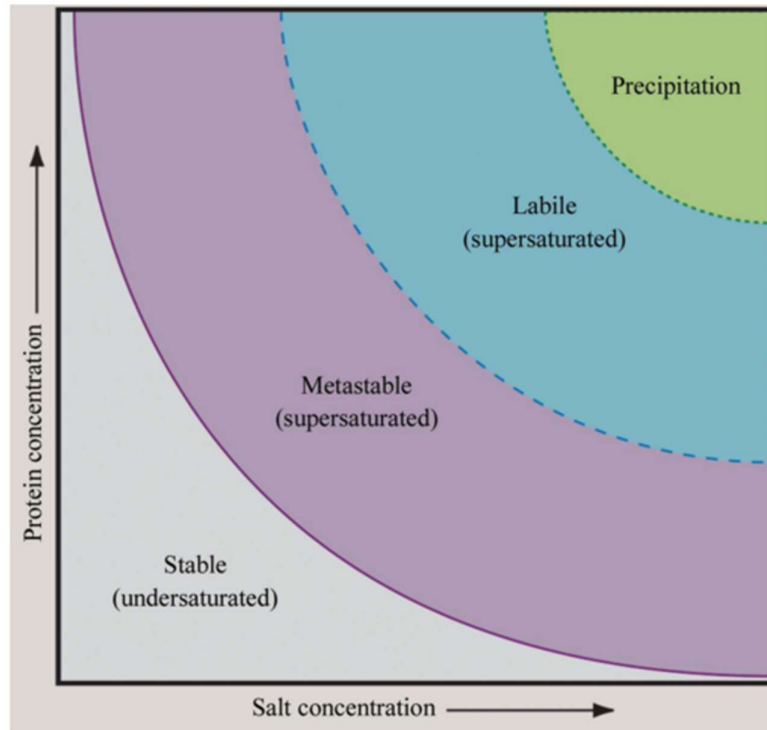


Figure 5. Phase diagram for the crystallisation and precipitation of macromolecules.

Based upon protein concentration and salt (or other precipitant) concentration [38].

Figure 5 displays a typical macromolecule phase diagram with respect to the influence of protein and precipitant concentration. It also succinctly displays non-precipitating but crystallising conditions. The solubility diagram divides into regions of under-saturation, super-saturation and precipitation. Metastable regions can see nuclei crystal growth, but no nucleation. Labile regions can expect to see both nuclei growth and nucleation. The figure could be viewed as a probability diagram, with precipitation the most likely region to see a full protein phase change

The Hofmeister series

Neutral salts were first observed to precipitate proteins out of solution over 125 years ago [39], with salts ranked by their ability to salt-in or salt-out protein relative to their overall ionic strength [40]. The effectiveness of a salt to cause precipitation is primarily driven by the choice of anion, followed by the cation. Anions are the more dominant force, and as such the

Hofmeister series focuses on these. Since this discovery, this series has been extensively reviewed and tested on a wide range of biological phenomena[41][42][43][44].

Salts at the top (left) of the Hofmeister series create a high surface tension, lower the solubility of hydrocarbons, and exhibit high salting out (lowering protein denaturation and conferring high protein stability). They are described as anti-chaotropic salts. Progressing down the Hofmeister series decreases surface tension, increases the solubility of hydrocarbons, starts to salt-in, increases protein denaturation and lowers protein stability.

The Lyotropic series

The lyotropic series is an alternative ranking system to the Hofmeister series allowing for compounds to be ranked according to their interaction with water, although the two are typically synonymous. Highly lyotropic ions interact strongly with water, cause large hydration numbers, and are referred to as structure making kosmotropes, where water molecules surrounding the ions have little variance in character to bulk water. Low ranking lyotropic salts are conversely termed chaotropes due to the disruptive influence they exert upon surrounding water molecules, reducing overall organised structure[45]. Hofmeister and Lyotropic series are usually synergistic, with a few notable exceptions. Multivalent cations for example are high on the lyotropic scale (kosmotropic), yet have a low effectiveness at salting out and so sit lower down on the Hofmeister series [45].

When the solution pH exceeds that of the isoelectric point (pI) of the protein, the general trend of increased salting-out performance of an ion in accordance with the Hofmeister series occurs. This has been described as when “salt ions sequester water molecules and prevent them from forming favourable hydrogen bonds with the protein surface”[46]. This drives proteins to form intermolecular protein-protein interactions, leading to aggregation and/or precipitation pathways. It is when solution pH is below the protein pI that the reverse has been found to be true. A reverse-lyotropic series has been observed with lysozyme at below its pI, with SCN^- found to be an effective crystallising agent and notably SO_4^{2-} was ineffective[47][48]. Above the pI, there is also the suggestion that positively charged arginine groups on the protein surface exhibit strong binding interactions with chaotropic anions.

Below the pI, anions are counter-ions, and above the pI they are described as co-ions [49]. The lyotropic series observed again with hen egg white derived lysozyme (HEWL) at pH below the pI was shown to follow NaSCN<NaI<NaCl, with the reverse at pH above the pI of NaCl<NaI<NaSCN for repulsive double layer forces [50]. Investigating how these trends found with HEWL translate to immunoglobulins will be interesting, especially since most operating conditions will be found at below the pI of the protein for the monoclonal antibody under investigation in this thesis.

Table 2. Hofmeister and Lyotropic series with ion classification into kosmotropes and chaotropes [40][51].

Anion series	Protein Stabilising Kosmotropes	Protein Destabilising Chaotropes
	$C_6H_5O_7^{3-} > SO_4^{2-} > HPO_4^{2-} > CH_3COO^- > F^- > Cl^- > Br^- > NO_3^- > I^- > ClO_4^- > SCN^-$	
Cation series	Protein Destabilising Kosmotropes	Protein Stabilising Chaotropes
	$Mg^{2+} < Li^+ < Na^+ < K^+ < NH_4^+ < (CH_3)_4N^+$	

	Kosmotropic ions	Chaotropic ions
Size	Small	Large
Surface charge density	High	Low
Hydration	Strong	Weak
Water structure effect	Structure making	Structure breaking

Table 2 displays how different ions affect protein solubility and stability. The most effective salts for salting-out have been found to be multi-charged anions such as sulphates, phosphates, and citrates. However, for cations it is the monovalency of salts such as NH_4^+ and Na^+ that have been found to promote precipitate formation the best. Ammonium sulphate, $(NH_4)_2SO_4$, is a very effective salting-out agent as it is comprised of a high-ranking anion and cation. Going down (across) the Hofmeister series, there is an increase in the salt's chaotropic nature, which can bind and interact directly with the protein and have a destabilising effect.

When precipitating crude mixtures, the aggregates that form will often be a mixture of several proteins; the nature of the precipitation extract will be determined by the concentration and type of salt used. Salting-out precipitation agents are typically ammonium or sodium

sulphates, citrates, and phosphates [52]. The solubility of a salt is a key consideration, since concentrations of several moles can be required to salt-out a protein. By contrast to isoelectric precipitation, increasing the temperature increases the level of precipitation; however, salting out is typically done at 4°C to decrease the risk of inactivation (e.g. proteases). Lower solubilities of salts will be found at lower temperatures, so there is a trade-off which will need to be understood.

The decrease in protein solubility with increasing salt concentration has been described by the Cohn equation:

$$\text{Log}S = \beta - KI$$

Equation 1.1 The Cohn Equation, where S is the protein solubility (g/L), β the protein solubility constant, K the salting-out constant and I is the ionic strength of precipitant (M) [51][52][53].

Ammonium Acetate

Ammonium acetate was first shown to precipitate proteins by Hofmeister [55], has mainly been referred to as a good crystallisation agent [56][57], yet more recently briefly mentioned as a successful precipitant of IgG₁ [32]. This salt should be investigated as a salting-out candidate as it displays good solubility from the NH₄⁺ ions and moderate salting out capability from the acetate ions.

Ammonium Citrate

Ammonium citrate has been briefly mentioned as a precipitant used in macromolecular crystallisation [56]. It has also been covered in a broad citrate patent [58], with no experimental details revealed eluding to its performance and characteristics. Again, as with ammonium phosphate, it is more commonly cited as a protein crystallisation agent [57][56] and its potential for protein salting-out is not well characterised.

Ammonium Phosphate

Ammonium phosphate (as well as lithium sulphate) was found to be a medium effective precipitant in the precipitation of bacterial lipase, with a higher ionic strength required

compared to the conventional ammonium sulphate to effectively precipitate and recover lipase [59]. Aside from brief mentions as a potential protein crystallisation agent [60][57][56], ammonium phosphate remains a relatively unexplored precipitant for immunoglobulins.

Ammonium Sulphate

Ammonium sulphate (AS) is by far the most established protein precipitation in the literature. It has had numerous applications for over 125 years, starting with the early observations by Hofmeister [39] for the salting-out behaviour of different cation/anion combinations with proteins, to enzyme precipitations from yeast [53][52], then to more advanced applications such as joint precipitations with caprylic acid [61] or with synthetic affinity polymers [62]. Ammonium sulphate, $(\text{NH}_4)_2\text{SO}_4$, is an effective, cheap and soluble salt. Ammonium sulphate precipitation is a widely used method for preparative protein separation due to it being rapid, simple and easily scalable to large volumes [63]. Again, the temperature at which the precipitation occurs is of importance; the higher the temperature the lower the solubility of the protein, but this also increases the level of denaturation. Slow addition of the ammonium sulphate with good mixing is important, especially if the salt solution is approaching saturation [64].

Ammonium sulphate offers a high solubility in water, up to 4.1M (54.17g/100mL) in ambient conditions combined with a high ionic strength of 3M/1M $(\text{NH}_4)_2\text{SO}_4$, making it ideal for salting out proteins. Ammonium sulphate has been shown to precipitate at concentrations of 1.2M and above [65], however this will be dependent upon protein charge, size, shape, and concentration, as well as pH, temperature, and a host of additional process conditions [66]. Ammonium sulphate is slightly acidic, but can be easily prepared into buffer systems of a reasonable pH range and has been established to maintain protein structure and function during precipitation and upon recovery [65][67][68]. Under more alkaline conditions (pH >8) ammonium sulphate is prone to release ammonia. An alternative salt such as sodium citrate can be used if a higher operating pH is required.

Ammonium sulphate has been shown to effectively precipitate lysozyme [64][68][41], alcohol dehydrogenase [52], α -chymotrypsin [41][69], and fumarase [53]. Historically lysozyme has

been a good protein to work with as it is cheap and commercially available however it is an order of magnitude lower in molecular weight compared to fully glycosylated antibodies (~14.7kDa compared to ~150kDa). More relevantly, ammonium sulphate has also been shown to successfully precipitate bacterial derived Fab' with structure and function retained upon recovery of the precipitate [65].

Ammonium sulphate precipitation has been able to achieve an 80% yield of IgG from crude mammalian serum, following an initial cut with caprylic acid [70]. However, as with most salts, it can lack the specificity and it can be difficult to achieve clear cut fractionation of complex protein mixtures [71]. Ammonium sulphate can present costly disposal issues when used at large scale applications [72]. Salting out often requires large volumes of precipitant stock; this can mean unfavourable dilutions of the protein feed volume [32]. This can be challenging for further downstream processes with larger process volumes leading to either longer process times or the need for higher capacity equipment. Longer process times can be detrimental to the stability of the target protein, and along with larger downstream process equipment, increase the production costs.

Lithium Citrate

Lithium Citrate, $\text{Li}_3\text{C}_6\text{H}_5\text{O}_7$, is expected to perform well as a salting-out agent based on the positioning of lithium and citrate ions in the Hofmeister series, however no prior mention of this salt applied to protein purification has been found. The good solubility of lithium in water and its dehydration characteristics make this salt theoretically very effective.

Lithium Phosphate

Lithium is rarely referenced as a cation partner to the phosphate salt, with a literature review into the finding only mention of its use for protein crystallisation. Lithium phosphate has been referred to as a potential precipitant option out of a list of other phosphate salts; sodium phosphate, potassium phosphate, rubidium phosphate and caesium phosphate, with no experimental data shown to back up this claim [73].

Lithium Sulphate

The uses of lithium sulphate have typically been limited to protein crystallisation [57][74][75], with concentrations in the range of 0.2M, far from the range where protein precipitation can initiate. Lithium sulphate has shown effective precipitation of IgY from chicken egg yolks [76], with yields of pure IgY reaching 94±5% yield from the complex egg yolk feed. This work was based on a previous methodology which use sodium sulphate as the precipitant at for egg protein purification[77]. An early mention in one table by Hofmeister also indicated its application for precipitation [39]. Lithium sulphate was found by Hofmeister to be remarkable when compared to the other lithium salts investigated, lithium nitrate, and lithium chloride which built insoluble protein components akin to calcium salts which were irreversible[55]. Issues may arise with using a heavy metal sulphate salt.

Sodium Acetate

Sodium acetate's role appears to be predominantly as a buffer system, with few references for its application for protein salting-out. In a multi precipitant screening study, 80% saturation sodium acetate was found to precipitate >95% IgG at pH 8.0 only, with no precipitation observed at the lower pH of 5.5 [32]. A pH dependency and a high saturation requirement to precipitate proteins are non-ideal characteristics, which are to be expected from the acetate anion's positioning in the salting-out series.

Sodium Citrate

Sodium citrate (abbreviated to NaCit) is a common and well established precipitant, with a naturally higher pH in solution of 8-8.25 and is a good choice for proteins with high pI values[32]. Citrate is theoretically the best anion for salting-out and combined with the high solubility of Na⁺ it is of no surprise this salt is one of the most common precipitants used.

In the patent, 'Protein purification by citrate precipitation', [58], the broad claim is made for any citrate salt precipitation, separation and recovery of any protein from a mixed starting material. The authors claim the step offers a marked reduction in the volume of starting

material by precipitating the antibody and re-suspending it in a smaller volume prior to chromatography steps. In addition to volume reduction, citrate salts offer partial purification of the protein of interest from other contaminants in the cell culture harvest. The patent claims for any citrate salt by only specifically mentions disodium citrate ($\text{Na}_2\text{HC}_6\text{H}_5\text{O}_7$) as the salt investigated. The advantage citrate salts offer over traditional approaches is that apparently ammonium sulphate is corrosive and prone to releasing gaseous ammonia, whilst polyethylene glycol (PEG) is viscous and the precipitate is hard to recover. 0.5 M disodium citrate was the minimum concentration found to precipitate the antibody investigated with concentrations increasing in 0.1M increments up to 1.0M mentioned. To reduce the required citrate concentration, there is the option for the addition of alternative salts such as ammonium sulphate. For recovery of the precipitate anything in the art could be used, centrifugation, filtration or tangential flow filtration (TFF) for example. Residual salts in the precipitate were removed using a PEG wash buffer between 0.25-50kD in size (typically 3-10kD) from a stock concentration of 35% at typically 5, 10 or 15 % final volume which was applied in 1-10x wash buffer to precipitate volume “thereby allowing the protein to be captured by ion exchange, hydrophobicity and mixed mode affinity resins”. Performance was revealed to range from a minimum of 50% antibody yield to 95%, with the precipitate containing levels of protein contaminants no higher than $2\mu\text{g/ml}$, however the antibody concentration was not stated so this value as a standalone has little value. The patent claims for a 4 fold reduction in process volume, a residual conductivity of less than 20mS/cm and optimised recovery between 80 to 98% of target antibody.

A broad patent covered precipitation, then dialysis for recovery of proteins from a crude mixture mentions sodium citrate as a suitable candidate [78]. The patent focus was on sodium sulphate however “the choice of the salting-out agent will depend on the objective of retention or removal of a particular protein or set of proteins” which should be investigated further as this statement indicates that there is scope for specificities from different salt ions.

A patent claiming for an aqueous two-phase extraction applied using sodium citrate and PEG between 1.5-6 kDa, for the purification of IgGs in general shows the versatility of sodium

citrate [79]. The claim also covers the use of alternative strongly hydrated salts (phosphate, citrate and sulphate). Instances of PEG-citrate precipitation of protein can also be found in literature as well [80][32].

$\text{Na}_3\text{C}_6\text{H}_5\text{O}_7$ was shown to successfully precipitate IgG with near-complete recovery with at 50% saturation, pH 8.0 and 80% saturation at pH 5.5 [32]. This would be likely due to the pH being closer to the pI of the protein under investigation.

Sodium Phosphate

NaH_2PO_4 , sodium mono-phosphate is not clearly listed as a precipitant, however the phosphate salt has been frequently suggested to be effective based on the salting-out series [51][73]. Nonetheless, with the high solubility of Na^+ ions, the mono-phosphate variant should be investigated (the mono-sodium phosphate salt has a much more limited solubility in water).

Sodium Sulphate

Sodium Sulphate, Na_2SO_4 , was one of the first protein precipitants to be identified by Hofmeister [39]. Sodium Sulphate has been shown as an effective precipitant of IgG from blood plasma. 6N (2M) Na_2SO_4 was added by constant stirring to 300ml blood plasma. Complete retention of the target IgG in the precipitate was achieved with 25% loss (removal) of albumin achieved [78]. It has also been shown to effectively precipitate IgG from egg yolk [77][81], fibrinogen [82] and filamentous bacteriophage from *Escherichia coli* [66]. Ovine polyclonal antibodies have been successfully precipitated and recovered from blood plasma, with 18% w/v Na_2SO_4 , non-buffered. The precipitated flocs were recovered by centrifugation, with albumin the main protein contaminant removed [83].

Sodium sulphate offers the interesting properties of being near insoluble at 0°C , crystallising as a decahydrate [84]. From a process point of view this can be exploited "...if 50g of anhydrous Na_2SO_4 are (sic) added to 100g of water at 32°C a saturated solution is formed, and if a protein is present it is completely precipitated and may be filtered off. If this saturated solution is now cooled to 0°C it separates into 110g of $\text{Na}_2\text{SO}_4 \cdot 10\text{H}_2\text{O}$ and 40g of 4% Na_2SO_4

solution. The water-soluble constituents originally present in the 100g of water are now contained in 40g and free from protein.”

The water bonding of $\text{Na}_2\text{SO}_4 \cdot 10\text{H}_2\text{O}$ saw marked increased in viscosity with the addition of the polyelectrolyte saccharose was added to water in the presence of “water absorbing” sodium sulphate [85]. Using saccharose addition to measure the salting-out behaviour of different salts by observing viscosity trends could be an interesting additional tool for precipitant selection. Sodium sulphate is a well characterised precipitate, with a proven track record of good performance and a candidate worth exploring.

Dual salt precipitation

The combination of salts can often improve process performance by exploiting their different properties. For example, dual salt precipitation of Fab’ with ammonium sulphate and sodium citrate was shown to exert a “*synergistic or antagonistic*” effect upon protein profiles, resulting in good purification and near-complete recovery of target protein [86].

The differences in lyotropic values of salts has been exploited in a hydrophobic interaction chromatography (HIC) step, by using a second salt for improving the separation resolution [87]. With HIC performance operating on the cusp of precipitation conditions, the implication is that in order to achieve better selectivity through precipitation, a main salt could be adjusted via a second “*finesse*” salt.

Summary of precipitation by salting-out

Salts offer a cheap, robust, and effective primary purification step for therapeutic proteins. Understanding and controlling key process conditions can results in improved selectivity and yield, with the mechanism of precipitation suggesting higher productivities with improved upstream processing titres. The performance different salts can exhibit will be investigated in detail, as well as the potential for synergistic effects.

1.4.4 Metal Ion Precipitation

The binding of positively charged metal ions to proteins can reduce protein solubility by altering its isoelectric point (pI). Strong binding metal ions also displace protons from binding sites, leading to an overall reduction in pH. It is this dual action which can lead to the state change of proteins from soluble to insoluble [88]. This is a different mechanism of action compared to salts; however, there is scope for a synergy if the two are applied together. Zinc metal ions have been shown to be the more effective metal ion precipitants, however calcium ions have also been effective [89].

Zinc Chloride

Zinc chloride has effectively precipitated and led to the recovery of porcine urokinase, plasminogen activator FK2P, and human-interleukin-1 β driven specifically by the zinc ions and not by salting-out directly. [90]. Precipitations with full target recovery and activity were achieved in as low as 2mM zinc. Zinc and copper form relatively stable complexes with histidine and cysteine residues – possibly via imidazole and thiol exposed groups. Zinc ions can reduce the pI of the protein, for example 0.2M ZnCl₂ was found to reduce the isoelectric point of albumin from 4.7 to 4.5 [54]. This could be a powerful tool in controlling protein characteristics. This salt could operate as both a standalone precipitant and as a co-precipitant but may only work for specific molecules and not apply well as a platform approach.

Zinc Sulphate

Zinc sulphate was established as good precipitant of proteins (measured by absorbance at 280nm) from human, dog, rat, and mouse plasma with yields greater than 95% from a stock of 10% w/v at precipitant to plasma ratios ranging from 1:1 to 4:1 [88].

1.4.4 Non-ionic Polymer Precipitation

Polyethylene Glycol (PEG)

Polyethylene glycol, PEG, is a non-ionic polymer with several applications for the isolation of biological materials. It can concentrate biological components including viruses, by dialysis, be used in liquid-liquid extraction in aqueous 2-phase mixtures, and more notably as a precipitant [91]. PEG is non-flammable, uncharged, non-toxic, and relatively inexpensive. Concentrations of 10-20% w/v are required to precipitate most proteins. However, PEG solutions are highly viscous, so liquid handling can be a challenge as well as achieving good mixing conditions. It is the most popular non-ionic polymer cited in literature.

PEG is understood to precipitate by sterically excluding proteins by competing for space in the solvent, hence proteins concentrate together in 'pockets' and then precipitate out of solution once the solubility limit is exceeded [54][92]. Thermodynamically, PEG increases protein chemical potential, so when this potential exceeds that of the solid state then precipitates form [93]. PEG, like a lot of other compounds ranging from amino acids, salts, glycerol and 2-methyl-2,4-pentanediol (MPD), has been shown to be preferentially excluded from the domain of proteins in aqueous solution [92], and when they are present in high concentrations proteins are preferentially hydrated. Hence the steric exclusion of PEG can lead to preferential hydration of the protein molecules, whilst maintaining protein structure and function [94]. However since PEG interacts with proteins via hydrophobic interactions, and these can destabilise protein structure, there is the potential for long term protein damage in aqueous and solid state [92].

The efficiency of protein fractionation increases with the molecular weight, (or chain length) of the polymer [71]. Compared to other high molecular weight polymers, PEG is the least viscous, so liquid handling is easier and causes virtually no denaturing of proteins at room temperature.

Table 3. Low and High molecular weight PEG properties [71][95][95]

Low MW PEG	High MW PEG
Less-compact precipitates	Compact precipitates
Low viscosity	High viscosity
High concentration PEG	Low concentration PEG
High specificity	Low specificity
Easier removal/recovery	Harder removal/recovery

6000 (units g/mol) tested against a range of proteins; carboxyhaemoglobin, ovalbumin and BSA (bovine serum albumin) as well as brome grass mosaic virus, has demonstrated that PEG precipitation can be described with the Cohn equation. More recently PEGs ranging between 3350-9000 g/mol [96][97][98][99] have been shown to effectively precipitate IgG from clarified cell culture fluid with good yield and recovery.

PEG can be removed by ultrafiltration, provided its molecular weight differs from that of the target protein. PEG, unlike salts, does not actively interfere with purification steps such as ion exchange or affinity chromatography [35].

1.4.4 Isoelectric Precipitation

Precipitating by pH adjustment is wholly dependent on a proteins isoelectric point. Isoelectric precipitation of proteins depends upon low salt concentrations – with an ionic strength close to zero. Under these conditions the electrostatic forces between molecules may not be strong enough to keep protein molecules apart, allowing for precipitates to form. Proteins typically exhibit lowest solubility around their isoelectric point (pI). At pH above the pI, the surface of a protein is predominantly negatively charged and similarly charged molecules will repel each other. Below the pI, the surface of a protein becomes predominantly positively charged. An overall molecule charge of zero keeps repulsive electrostatic forces to a minimum, possibly

allowing for hydrophobic attraction and resulting in precipitate formation. This has been termed isoelectric precipitation [100].

Isoelectric precipitation can be further complicated by complex, crude feed streams; different proteins with similar properties can aggregate together. Isoelectric precipitation can be improved by decreasing protein solubility. This can be done by adding a solute such as polyethylene glycol, or an organic solvent with pH control can form successful precipitates. Most precipitation techniques mentioned in this literature review employ some aspect of isoelectric precipitation in conjunction with a primary mechanism of precipitation. However, IgM has been shown to precipitate effectively and recover at close to its pI at pH 6.0-6.1 with good recovery [101].

1.4.5 Polyelectrolyte Precipitation

Polyelectrolytes are polymers containing ionisable groups which dissociate into charged polymer chains and counter ions in solution [102]. These dissociated polymers can then form, via a bridging action [59], into insoluble complexes with oppositely charged proteins [103]. Precipitation of proteins by polyelectrolytes works by a different mechanism to preferential dehydration, first with the formation of the protein-polyelectrolyte complex, then with the formation of larger floc protein particles [104]. Globular proteins can form stable complexes with synthetic or natural polymers, forming water-soluble or insoluble coacervates depending on solution conditions [105].

Precipitate recovery by the standard centrifugation / filtration can be performed, with the solid precipitate recoverable through re-dissolving in a different pH or an elevated ionic strength [102]. Similar to non-ionic precipitation approaches, polyelectrolyte precipitation needs the optimisation and control of solution pH and ionic strength as well as polyelectrolyte type, molecular weight, concentration for the effective formation of a polyelectrolyte-protein complex [23].

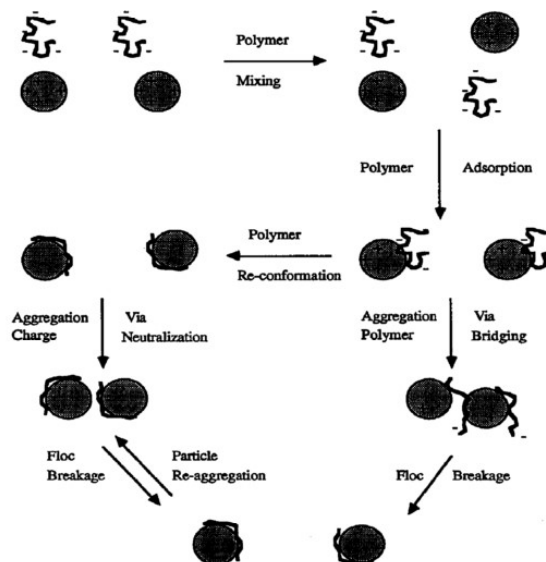


Figure 6. The schematic of polymer mixing, adsorption, re-conformation, particle aggregation and floc breakup processes in a typical flocculation system [104].

The application of polyelectrolytes to precipitate proteins has been used for over 60 years [106], yet have received much greater attention recently with the industry looking towards alternatives to chromatographic separation [7]. Precipitation by anionic polyelectrolytes has the potential to be applied as a platform approach to a wide range of monoclonal antibodies without the need for much process change, as HCPs are typically the precipitation target [23]. Precipitation by polyelectrolytes offers the advantages of good selectivity with low material requirements compared to salts and PEGs [104].

The solubility of many polyelectrolyte complexes is determined by pH; small changes in pH result in a sharp and reversible transition from its soluble state to an insoluble state. Polyelectrolytes have been successfully shown to exhibit reversible solubility profiles [105]. However polyelectrolytes run the risk of denaturing proteins as the mechanism of action does not exclude water molecules as seen with salting-out and non-ionic polymer precipitation [59]. Caprylic acid for example has been shown to reduce the affinity of some antibodies; for example it has been found to be unsuitable for murine IgA and IgG₃ [107].

Unlike precipitation by salting out and non-ionic polymers, there no direct linearity between the concentration of polyelectrolytes in solution and the fraction of protein precipitated.

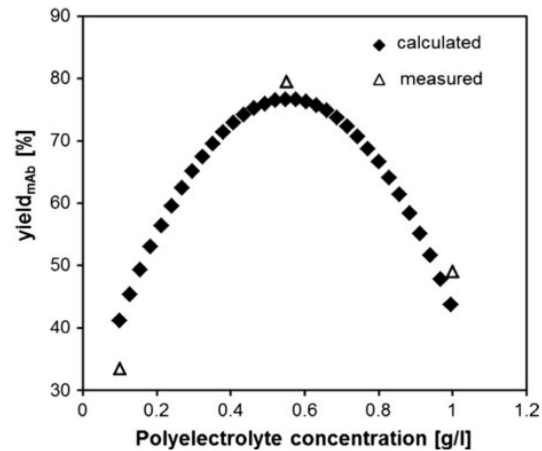


Figure 7. The comparison of measured and calculated yield of protein via precipitation in dependence of polyelectrolyte concentration [103].

As depicted in Figure 7, excess of the polyelectrolyte can lead to a reduction in the protein fraction precipitated, this trend has been observed with polyacrylic acid, polystyrene sulfonic acid, polyanetholesulfonic acid, polyalanine, and polyvinyl sulfonic acid [102][23]. For screening studies, it is important to explore a wide range of concentrations before ruling out a new polymer as a precipitant.

Ionic strength has a strong impact on polyelectrolyte precipitation. For example PVS performance was seen to reduce above 1.5-1.6 mS/cm [23]. Increasing the molecular weight polymers can reduce sensitivity to ionic strength [23].

Polyelectrolytes can be expensive, even at the low concentrations required [15] meaning that recovery and re-use of the material needs to be considered. Good process understanding is essential, as optimum polymer concentrations are defined as a mass fraction of the protein, for example at a specific ratio of 0.04g of carboxymethylcellulose to 1g of protein [15]. Hence process feed stream variations must be accommodated by changes in polyelectrolyte precipitant concentrations, and possibly pH and the addition or exclusion of cofactors.

Table 4. The application of different polyelectrolytes for the purification of proteins by precipitation.

Polyelectrolyte	Precipitation Applications
Chitosan	BSA [108]
Polymethacrylic acid (PMA)	BSA[106]
Polyvinylamine (PVA)	BSA[106], mAb [109]
Polyalanine (PAA)	mAb [109],
Polyacrylic Acid (PAC)	mAb [23], mAb [102], BSA [110], HEWL [111]
Polyethyleneimine (PEI)	mAb [109]
Poly(4-vinylpyridine) (P4VP)	mAb [109]
Poly(N-methyl vinyl amine) (PMVA)	mAb [109]
Poly(diallyldimethylammonium chloride) (PDADMAC)	BSA [112], β -lactoglobulin [112], γ -globulin [112], ribonuclease A [113]
Poly(dimethyldiallylammonium chloride) (PDMDAAC)	BSA [113], Bovine Pancreas Ribonuclease [113] HEWL [114]
Polyanetholesulfonic acid (PASA)	mAb [102]
Spermine	mAb [109]
Polystyrene Sulfonic Acid (PSS)	mAb [23], mAb [102]
Polyvinyl Sulfonic Acid (PVS)	mAb [23], mAb [102]
Sodium bis-(2-ethylhexyl) sulfosuccinate (AOT)	Lysozyme [114]

Table 4 displays a range of polyelectrolytes which have been documented to purify proteins by precipitation. The application can either be for positive precipitation (the target molecule stated) or negative precipitation (precipitation and removal of impurities whilst retaining the target molecule in solution). Ultrafiltration membranes can successfully recover/remove the polyelectrolyte from their protein of interest [110]. Proteins are recovered in the permeate fluid, with the polyelectrolyte fraction separated in the retentate.

Summary of polyelectrolytes as precipitants

The following factors affect protein removal and fractionation efficiency: Increased ionic strength leads to lower protein removal efficiencies as this avoids shielding the electrostatic interactions between host cell proteins and polyamines [15][115]. Higher molecular weight polyelectrolytes allow the precipitation to be carried out under higher ionic strengths [115]. Approaching the pI of the protein, charge neutralisation of the antibody reduces the strength of interaction between antibody and polyelectrolyte, reducing the extent of precipitation [23]. Increasing the pH shows an improved impurity clearance, generally closer to the pI of the protein [23]. Protein removal increases with dosage to an optimum – which promotes good bridging and precipitation of proteins whilst avoiding re-dissolution – further addition of polymer past this point decreases precipitation efficiency[15][115]. Good mixing conditions are paramount, especially with incremental precipitant addition [15]. There is great scope for combining polyelectrolytes with charged surfactants for advanced purification techniques [116][117].

Precipitation of proteins by polyelectrolytes promises to be an exciting avenue to investigate, however precise conductivity and pH control would be required to develop a suitable high throughput process development (HTPD) scale down screening methodology. There is potential to combine a negative polyelectrolyte precipitation step followed by a positive salting-out step.

1.4.6 Affinity Precipitation

Traditional precipitation can be a very effective non-specific pre-treatment operation to chromatography that can operate at large scale [118]. The protein of interest is not selectively precipitated out of solution from other proteins in a crude mixture. Affinity precipitation has a higher specificity, which can reduce the bulk load on downstream processing steps notably chromatographic separations.

Affinity binding mechanism

Affinity chromatography utilises biological interactions to affect binding of specific solutes. A solid phase polymer resin is conjugated to antibodies, antigens or dyes which can bind a specific solute from a mixture. The target molecule is extracted from the liquid phase and specifically bound to the solid phase of the chromatography column. The ligands are capable of selectively retaining and separating the target molecules even from a diluted and complex feed stream. The target molecule can then be eluted and recovered by a change in pH [119] or salt concentration [120], or by addition of a chaotropic agent or displacer /competing agent [25].

Affinity precipitation offers an attractive alternative, since solid liquid separations are well characterised and understood. With affinity precipitation the ligand is bound to a soluble carrier, forming a macro-ligand. The target protein and the water-soluble macroligand can then form a complex which precipitates out of solution leaving the contaminants behind. Complex binding occurs in the homogeneous aqueous phase, meaning mass transfer resistance and issues with steric hindrance are avoided [121].

Affinity precipitation can bypass the fundamental disadvantages of affinity chromatography which can include column fouling, scale up, flow rate limitations, as well as the slow association rate of the target protein with the immobilised bio-specific ligand, caused by diffusion limitations as well as the steric hindrances of the porous bead stationary phase [122], [119].

Table 5. Advantages of affinity precipitation.

Collated from the following: [123][119][124][121][125].

Key Attributes	Description
No need for solid supports	The affinity molecules do not need to be immobilised in solution. Spacers used in chromatography aren't required.
High ligand utilisation	The affinity ligand in the homogeneous phase is more effective and rapid compared to affinity chromatography.
Selective precipitation	Specific multimeric proteins can be selectively precipitated.
Low capital cost	Little or no additional equipment is required.
Low polymer consumption	Recycling of polymer can also be an option.
Scalable process	Precipitation in general can be applied to large process volumes.
Sequential Precipitation	Multi-step precipitation, where different components can be precipitated out step-wise. Sequential recovery of multiple components possible.
High MW ligands	High molecular weight ligands can be effective precipitants when in the homogeneous phase.
Primary purification step	Affinity precipitation can be carried out on large volumes of crude extract.
No fouling issues	Affinity precipitation is not subject to batch variation as a consequence of solid-phase affinity matrix fouling.
Low polymer concentrations	In the range of 0.1-0.5% so non-specific adsorption of proteins on the polymer is low.
Purification & volume reduction	Affinity precipitation can purify the feed stream as well as reduce the process volume. Hence reducing the number of subsequent downstream processing steps required.

There are two different mechanisms for precipitation via macroligands, depending upon their structure and function:

Primary Effect Precipitation

Homo-bifunctional ligands are a synthesis of two identical ligand molecules bound to a spacer molecule, forming bis-ligands. Provided the spacer molecule is long enough and the protein-ligand binding is of enough strength, then a precipitate can form in crude mixture containing a multi-subunit protein which interacts with the immobilised ligand, due to the simultaneous bis-ligand interaction [126]. Provided the ligand and molecule are present at a suitable concentration ratio, the macro-ligand can cross-link, forming a three-dimensional structure with the target protein, growing in size until the aggregated material becomes insoluble and

precipitates out of solution. Primary effect precipitation is a direct function of the affinity relationship between the multivalent enzyme and the bi-functional ligand.

This affinity ligand mode of action is limited by the fact that macroligands require multiple ligand binding sites in the same protein. This allows the ligand/protein complex to complete a structure with a sufficiently greater density difference to that of water, forming a precipitate. Hence primary effect precipitation is suitable only for the precipitation and purification of multimeric proteins. The limited number of bis-ligands apparently reduces the application of primary effect affinity precipitation techniques to dehydrogenases [24].

Secondary Effect Affinity Precipitation (Hetero-bifunctional Ligands)

In primary effect precipitation, precipitation and affinity interactions are directly linked. This method is simple but less robust; it is much more sensitive to environmental conditions and requires good process control and optimisation. With secondary (or indirect) affinity precipitation the affinity and precipitation actions are no longer linked, which carries the advantage of controlling and performing each action independently. The molecule will consist of two key building blocks: a polymeric substance that responds to an environmental stimulus, so that it can phase change from water soluble to insoluble upon external stimulus, and an affinity ligand, which specifically binds to the target molecule. This hetero-bifunctional complex has been termed an affinity macro-ligand (AML). A significant advantage is that precipitation occurs independently of the amount of target (protein) molecules present, which can be a big issue with homo-bifunctional ligands. Hence there is the potential for greater process robustness as the extent of precipitation is not primarily linked to feed stream properties [127].

Table 6. Ideal design criteria for affinity macroligands [127].

The majority of these characteristics could apply to most precipitants, aside for the need to recovery cheaper materials, phase change upon stimulus and reactive groups for ligand binding.

Contain reactive groups for ligand binding	Give complete phase separation upon external stimulus	Have a sharp and well characterised transition between phases
Form compact precipitates	Exclude trapping of impurities	Easily re-solubilised
Soluble/Insoluble under different conditions	Good recovery of precipitating agent	Commercially available / Low Cost

From Table 6 it would be a challenge to identify candidates which achieve all of the specified criteria, so a ranking tool would allow for a progressive precipitant selection strategy.

Bis-Dyes offer an alternative to biological affinity ligands; they are chemically and biologically stable, they are easily attachable to solid supports and they are readily available at a low cost [128]. An example of Bis-Dyes include Bis-Cibracon blue [129], Procion blue H-B [123] and C.I. Reactive Blue 2 [128]. However, binding will be wholly dependent on protein structure with difficulty in devising a platform process step.

Metal chelate affinity precipitation has also shown promise for the effective affinity precipitation and purification of protein, however performance can be thermo-responsive, requiring temperatures often unsuitable for biologics [130][131].

Affinity precipitation is an attractive technique; however it falls out of the scope of this work which is to develop a platform precipitation purification approach for a range of therapeutic proteins.

1.4.7 Organic Solvent Precipitation

Adding water-miscible organic solvents such as acetone and ethanol can result in protein precipitation. Organic solvent addition lowers the dielectric constant of the solution, reducing its solvating power. This decreases the solubility of a protein in solution, allowing for aggregation by electrostatic attraction. The factors influencing organic solvent precipitation are similar to those of isoelectric precipitation; precipitation with organic solvents can be achieved in conjunction with salting-out [35], and more readily occurs close to the pI of the protein. Protein size is also an influence; a larger protein can be precipitated in the presence of a lower organic solvent concentration than that of a smaller protein with similar properties. Hydrophobic proteins, however, are not precipitated by organic solvents. For these proteins an increase in solubility is observed; the organic solvent displaces water molecules from around the hydrophobic patches of the protein, increasing solubility.

The best case example of organic solvent precipitation is the fractionation of human blood by ethanol [29][30]. The meat industry also utilises protein precipitation on a large scale. Blood processed by the meat industry in the UK alone amounts to around 100,000 tonnes per year. Key plasma proteins such as albumin, globulins and fibrinogen can be effectively precipitated by ethanol and PEG [132]. Precipitation is the purification method of choice due its high throughput capacity and cost-effectiveness, especially when compared to more expensive purification methods such as chromatography.

Precipitation with alcohol tends to cause protein denaturation unless the conditions, especially temperature, are well regulated [71]. Operations tend to be carried out at 0°C or below, the freezing point of the solution is typically much lower. Organic solvent addition to solution increases the temperature - due to the negative ΔH_o of hydration of the solvent molecules. When precipitating with organic solvents, great care must be taken to avoid operating above 10°C. At higher temperatures, protein conformation can experience sudden changes, exposing organic solvent molecules to the interior of the proteins, disrupting hydrophobic interactions and causing them to denature [35]. Low operating temperatures can be achieved by adding

pre-cooled organic solvent, slowly and under good mixing conditions, with the feed solution held in an ice-salt bath. Precipitation rates can also be promoted at a lower temperature [72]. The more commonly used solvents are ethanol and acetone, but also used are methanol, propan-1-ol, propan-2-ol and ketones. Longer chain alcohols can cause a greater level of denaturation. Safety is a big consideration when precipitating with organic solvents; especially for large scale processes; the solvent needs to be non-toxic, with a flashpoint above 20°C – which rules out dioxans and ethers. Most enzymes have been found to precipitate in the range of 20 to 50% organic solvent. Above 50% solvent only proteins smaller than 50kDa remain in solution [133].

Summary of organic solvent precipitation

The reliance of effective alcohol precipitation upon key feed properties such as a high protein concentrations and low ionic strengths indicates poor potential for good process robustness. Organic solvent precipitation could be an issue with high throughput automation techniques; firstly, the liquids involved will have varying viscosities which would need to be accommodated by the robotic liquid handling arms. Secondly operational temperatures as low as 0°C are difficult to implement and maintain, adding considerable cost to the experiments. Health & safety issues with flammability and toxicity also reduce the attractiveness of precipitation using organic solvents. Alcohol precipitation may be well established as an effective way to fractionally precipitate in the blood industry, but there is a lack of specificity and large volumes are required. Coupled with the aforementioned issues it would be wise not to investigate alcohols too intensively.

1.4.8 Protein Stabilising Agents

Whilst not strictly under the guise of precipitation, addressing the impact stabilising compounds, which are present in complex feed such as cell culture fluid, have upon protein solubility profiles will be important for characterising precipitation.

The polyols glucose, sucrose, raffinose, glycerol and sorbitol all reduced the propensity for BSA to aggregate/precipitate with PEG [93]. Similar patterns have been observed with polysorbate, arginine, glycine, dextrose, sucrose, trehalose, glycerol and sorbitol all reducing the aggregation of mAbs [134]. The impact these stabilising agents have upon precipitation profiles will need to be suitably characterised in order to build a robust purification method capable of maintaining performance with varying feed-streams passed on from the upstream processes.

Table 7 summarises protein-excipient interactions, and demonstrates the influence a wide range of compounds can have upon protein stability and performance [135]. In terms of precipitation, understanding which agents are present in the cell culture fluid and how to control these will be important to achieve robust precipitation techniques. Additionally, if denaturation is observed with a precipitant then use of such stabilising agents could potentially fix the problem.

Table 7. Pharmaceutical excipients for use in protein formulations, adapted from [135].

Category	Representative examples	General comments	Cautionary comments
Buffering agents	Citrate, acetate, histidine, phosphate, tris	Maintain solution pH Buffer-ion specific interactions with proteins	pH may change with temperature crystallisation during freezing decomposition during storage
Amino acids	Histidine, arginine, glycine, proline, lysine, methionine	Specific interaction with proteins Antioxidant (His, Met)	
Osmolytes	Sucrose, trehalose, sorbitol, glycine, proline, glutamate, glycerol, urea	Natural compounds that stabilise proteins and macromolecules against environmental stress (temperature, dehydration)	High concentration often required for stabilisation Many additional osmolytes have been identified, but not currently approved for use as excipients Destabilising effects also reported
Sugars and carbohydrates	Sucrose, trehalose, sorbitol, mannitol, glucose, lactose	Protein stabiliser in liquid and lyophilised states Tonicifying agents Lactose as a carrier for inhaled drugs Dextrose solutions during IV administration	Reducing sugars react with proteins to form glycated proteins Non-reducing sugars can hydrolyse forming reducing sugars Impurities such as metals and 5-HMF
Proteins and polymers	HSA, gelatine, PVP, PLGA, PEG	Competitive inhibitor of protein adsorption Lyophilisation bulking agents Drug delivery vehicles	Trend towards use of recombinant sources of HSA and gelatins Drug delivery polymers may not be compatible with protein drugs
Salts	Sodium chloride, potassium chloride, sodium sulphate	Tonicifying agents Stabilising or destabilising effects on proteins, especially with anions (Hofmeister salt series)	Concentration dependent effects Trace metals can cause oxidation May be corrosive to metal surfaces Lowers Tg' of solution (may affect lyophilisation)
Surfactants	Polysorbate 20 and 80	Competitive inhibitor of protein adsorption Competitive inhibitor of protein surface denaturation Liposomes as drug delivery vehicles	Concentration dependent effects Peroxidases can cause oxidation May degrade during storage Complex behaviour due to micelle formation
Chelators and anti-oxidants	EDTA, DTPA, amino acids (His, Met), ethanol	Bind metal ions Free radical scavengers	Certain anti-oxidants such as ascorbic acid and glutathione lead to protein instability Light exposure accelerates oxidation
Preservatives	Benzyl alcohol, m-cresol, phenol	Prevents microbial growth in multi-dose formulations	Inverse concentration dependent effects on protein destabilisation vs. antimicrobial effectiveness
Specific ligands	Metals, ligands, amino acids, polyanions	Binds protein and stabilises native conformation against induced unfolding Binding may also affect protein's conformational flexibility	May involve use of novel excipients or an excipient with biological activity

1.4.9 Conclusions & Direction of Research

Investigating precipitation by salting-out will be the main focus of work throughout this thesis. This decision was based on the range of relatively unexplored salts for their potential to purify monoclonal antibodies from process cell culture fluid. The key factors affecting precipitant choice should be based on the recoverable target protein yield, the level of purification achievable, the effect upon protein structural stability, operational ease of use, process time and cost.

Developing a high throughput screening methodology will allow a wide range of candidates to be tested under a varying process conditions and testing on different salts should test the limits of this approach suitably. The methodology will need to be capable of handling viscous, saturated salt solutions with the potential for future investigations looking at non-ionic and charged polymers.

1.5 Precipitate Formation & Properties

By understanding how precipitation conditions affect particle formation and growth means that final characteristics such as particle size distribution, mechanical strength and density can be controlled [25]. Achieving large, dense precipitates makes the filtration or centrifugal recovery easier. Small particles can lead to poor solid/liquid clarification issues and low densities will result in a reduced process volume reduction. Poor mechanical strength can lead to product loss during recovery. Precipitate formation has traditionally been described to develop through five non-discrete stages; 1) initial mixing, 2) nucleation, 3) growth by diffusion, 4) growth by fluid motion, 5) ageing [100][136]. These mechanisms are driven by the precipitant exerting favourable protein-protein interactions.

1.5.1 DLVO theory and precipitation

Protein suspensions have traditionally been characterised using the Derjaguin-London-Verwey-Overbeek (DLVO) theory. It describes forces of attraction and repulsion and allows

for an energy barrier for aggregation to be identified. DLVO theory has been shown to apply well to dilute electrolyte solutions; however its relevance to describing precipitation conditions can be limited; the ionic strength dependent term is the electric double-layer potential, and this becomes negligible at concentrations where salting-out is observed [47]. The DLVO model does not take into account anisotropic interactions, salvation forces, or specific ion effects [45][137], and as a general rule cannot be applied to solutions with an ionic strength exceeding 100mM [138]. DLVO theory remains a useful tool for understanding protein-protein interactions and may apply to low ionic strength reactions, such as with polyelectrolytes.

Initial Mixing

This is the mixing required to achieve homogeneity upon addition of all the components required to precipitate. Traditionally this is upon addition of the precipitant to the protein feed, although for microscale methods this may well be upon addition of the feed to the pre-prepared precipitant conditions. For effective mixing precipitant and product molecules need to be brought into contact as quickly as possible, with mixing between eddies assumed to be instantaneous, and mixing within eddies diffusion limited [139][140].

1.5.2 Precipitate formation – nucleation and growth by diffusion

Nucleation is defined as the formation of ultramicroscopic sized particles. For particles to form, the solution needs to be supersaturated. The rate of nucleation increases exponentially with increasing levels of super-saturation, until reaching the super-saturation limit [25]. Too high a high a rate of nucleation leads to a high concentration of aggregate nuclei, which leads to fine precipitates, as growth is spread out across too many seed-sites. Keeping saturation to reasonable levels will therefore result in optimal early precipitate characteristics [141].

For protein solutions, random motion from molecule thermal energy leads to collisions, and the association of proteins from these collisions is promoted by the removal of hydration and electrical barriers by the conditions imparted by the precipitant [142]. Nucleation is driven by Brownian motion, and this perikinetic growth leads to primary particles sizes of around 0.2 μ m, in the case of isoelectrically precipitated soya proteins [143]. For precipitation by salts or non-

ionic polymers it would initially seem that operating at high precipitant concentrations would be ideal (discounting the capture of additional impurities), however high super-saturations tend to form colloidal precipitates, gels or highly solvated precipitates, so for precipitation via salts or non-ionic polymers there will be a compromise between a fast rate of nucleation and the ease of precipitate recovery, as well as selectivity.

1.5.3 Precipitate formation - growth by fluid motion

Precipitate particle growth is limited by diffusion after the nucleation stage and will only be defined by fluid motion after particles accrue diameters between 0.1-10 μm , depending on high or low shear conditions respectively. The growth rate can then be said to be orthokinetic, as these larger particles require additional kinetic energy to overcome aggregation energy barriers [140]. Aggregate particle growth rate becomes dependent on \bar{G} , the mean velocity gradient, and the concentration of particles [144]. The mean velocity gradient is a well-established metric for defining mixing conditions in batch stirred vessels, under the constraints of a turbulent flow regime and using a Rushton impeller [145].

$$\bar{G} = (P/V\mu)^{0.5}$$

Equation 1.2 The mean velocity gradient (s^{-1}), where P is the power input (W), V is the volume, (m^3) and μ the viscosity (Nm^{-2}s) [145].

1.5.4 Precipitate conditioning / Camp Number

Aging of fine precipitate particles under well-mixed conditions results in a decrease in particle number and an increase in size/strength.

$$Ca = \bar{G}t$$

Equation 1.3 Camp number (dimensionless), a function of mean velocity gradient, \bar{G} (s^{-1}) and time (s) [146].

Camp number describes the precipitate ageing process; aggregate-aggregate collisions are expected to increase with higher shear rates and longer residence times. These increased collisions effectively ‘polish’ the aggregates, decreasing porosity and hence increasing overall strength and density [147]. The ageing and polishing of aggregates decrease the collision effectiveness of aggregates, hence decreasing the rate of larger particle formation. A camp number exceeding 1×10^5 is a good indication of strong precipitate particles suitable for good separation [146]. Large aggregates formed under the effects of low shear have been found to require a much longer aging time to match the particle strengths achieved by smaller, high shear-formed aggregates. Centrifugation efficiency is proportional to the square of mean particle size, so by controlling precipitation conditions with regard to precipitate particle size, process yields can be improved. Almost counter-intuitively, the best precipitate characteristics can be attained from a high shear mixing conditions, and this should be considered when looking to scale up and industrialise a precipitation step.

1.5.5 Precipitate breakage

Hydrodynamic forces can affect precipitate particle breakup during and after formation. Breakage can occur during mixing, settling, recovery and at gas-liquid interfaces. Breakage has been attributed to the following: 1) deformation due to the pressure differences across the particle, 2) primary particle and large particle erosion by hydrodynamic shear and 3) fragmentation due to collisions between particles [139]. Hydrodynamic forces are widely believed to dominate other forms of breakage [100] and as such understanding how mixing conditions affect hydrodynamic shear is important for desirable precipitate formation.

By discounting particle collisions, breakage can be described by the forces acting upon the particle:

$$N_{force} = \frac{\text{force acting on particle}}{\text{force binding the particle}}$$

Equation 1.4 The force number which is a dimensionless ratio of the forces acting on and binding the particle.

The rate of breakage is a function of the magnitude of a dimensionless force number (N_{force}), the frequency the force number value exceeds particle unity and the concentration of precipitate particles [100]. To maintain large precipitate particles for easier solid/liquid separations, it is therefore important to ensure the particle strength exceeds that of external forces acting upon it.

1.5.6 Precipitate properties

Protein precipitates can exhibit complex rheology which can impact upon the solid/liquid separation and may not dewater readily. This can form sticky protein sludges, frequently viscoelastic in nature. Time dependent behaviour can also be observed, with structural breakdown or formation actions leading to thixotropic or rheopectic characteristics [142].

1.6 The effect of mixing on precipitation

With the primary objective to form protein aggregates of maximum size and strength for ease of recovery, the design of a mixing regime needs to be well thought out. Potential damage to proteins and precipitates can be minimised by avoiding high localised concentrations of precipitant, which can be achieved in turn by an efficient and effective mixing regime. Precipitation reactor design, mixing conditions and its mode of operation have all been shown to affect the physical properties of protein aggregates such as size, strength and rheology [148][140]. Impellers of greater diameter and rotational speed achieve faster tip speeds and consequently these localised high regions of energy dissipation at the tip-liquid interface increases the amount of shear aggregates are exposed to. Hence the rate of shear generated from the impeller type and speed should be minimised following the nucleation stage, in order to effect efficient orthokinetic growth. The aggregated particle then should be aged under suitable mixing conditions to maximise strength [142]. Precipitation is usually carried out in

a batch mode in stirred tanks, aggregates settle to the bottom of the tank, the top liquid phase is siphoned off and the aggregate slurry is fed to a solid/liquid separator.

1.7 Centrifugation

For the case of precipitate recovery, centrifugation clarifies the solid protein precipitate from the liquid phase according to respective density differences. Centrifugation offers a fast, semi-continuous throughput with low contamination risks and as such remains the mainstay of primary clarification approaches for therapeutic proteins [16]. Yield from the centrifugation step will be dependent on good phase separation, ideally resulting in good clarification and a dry precipitate from good dewatering. Small aggregate particle sizes, the degree of precipitate hydration and compressibility of the precipitate all add to the challenge of effective centrifugal separation, requiring high centrifugal forces [149]. Maximising dewatering is paramount as wet protein sludges will retain more impurity-rich supernatant, which would then require additional washing steps leading to product loss [142]. It is therefore important to integrate the design of protein precipitate formation and the mode of centrifugal recovery [148].

1.8 Filtration

Although mAb precipitates from PEG precipitation has been previously shown to be successfully recovered by filtration in the micro-well format [98], this will not be utilised for the capture of precipitates in this thesis. This was decided due to the challenges identified in preliminary work, with high salt solutions failing to filter through the membranes tested. In addition, protein precipitates are compressible and can lead to fouling issues with membrane separation. Alternative, less hydrophobic membranes could have been investigated; yet separation by centrifugation was selected for work throughout this thesis since operation was simpler, faster and therefore more suited for a high throughput screening methodology.

1.9 Bioprocess Development through Scale Down techniques

Microscale bioprocessing techniques can enable accelerated process development. The advantages of automated scale-down experimentation are well established; offering reduced material, time and manpower requirements through parallel experimentation [17] whilst enabling the rapid identification and selection of optimised conditions through high throughput analytical techniques [97]. Microscale experimentation means that early process development can yield a much more comprehensive process understanding, with more variables explored for the same material and time requirements. Provided the conditions tested successfully mimic larger scale conditions based on core engineering principles [150], scale-down of bioprocess operations is a powerful tool for deriving critical process parameters building a process on solid foundations.

Microscale processing applies to micro-well systems and microfluidics. Throughout this thesis the focus will be on micro-well systems; the scale-down mimics of batch operations in small volumes ranging between 50 μ L to 1000 μ L. Micro-titre plates consist of identical wells with micro-litre capacities, varying in number and geometry. Micro-titre plates are a great time-saving solution to processing large sample numbers; they possess a standard layout, negating the need for labelling, and storage can be much more convenient. Operations such as mixing and centrifugation allow for parallel operation, avoiding issues of time-delays from sequential operations and analysis [151].

Micro-titre based high throughput process development techniques have traditionally been based around fermentation operations [152][153][154][155] and primary recovery steps such as filtration [156][150] and centrifugation [157][149]. Regarding downstream processing unit operations in HTPD, chromatographic steps have been developed utilising early batch screening of slurry resins, then transferring to miniaturised columns [158]. Both stages can be performed using automated liquid handling platforms, and analysis is carried out in the micro-titre plate format. This allows for a rational approach whereby scouting of suitable process conditions can be followed by process fine-tuning before scaling up these findings to

laboratory scale [159]. Microplates have successfully been used to investigate protein stability [160][161] as well as refolding from inclusion bodies [162].

Precipitation screening in the HT format has shown early promise, with the precipitation and recovery of IgG1 with PEG via centrifugation [96] and IgG4 with PEG via filtration [156] demonstrated, as well as the initial precipitation of Fab' with ammonium sulphate [65].

A high degree of repetition is required with sample manipulation and liquid transfers, with this burden increasing with larger sample numbers. Compounding this is the need for calibration standards and controls prepared by sequential dilution from a starting stock standard. These operations can be sped up and optimised by utilising automated robotic liquid handling systems. These systems require considerable capital investment, and dedicated time programming and transferring manual protocols to the system. Automation offers the dual benefits of increased precision and accuracy of results whilst the capacity to operate at smaller scales enables markedly reduced material requirements and hence the ability to address issues of precipitant selection much earlier in the development pathway than is currently possible [151]. Automated approaches have been shown to increase precipitation and instrument utilisation to between 3-fold and 4 fold compared to the same manual approach [163][151]. The compounding benefit of automation is the freeing up on skilled analysts for other activities.

1.10 Conventional Experimental Design vs. Design of Experiments (DoE)

High throughput format experiments offer a certain amount of experimental decadence; a large number of experimental conditions can be explored with high repeat values, standards and controls with rapid experimental runtimes whilst requiring minimal materials. For early screening experiments this enables more comprehensive one or two-factor at a time experiments to be run. The majority of early work produced in this thesis has been approached this way and has helped build up a strong understanding. Firstly, screening each key parameter over a wide range with multiple points establishes the full operating range and builds up information on the upper and lower limits of operation. Secondly, for developing the high

throughput screening methodology the running of multiple conditions in triplicate helped to validate trends and understand experimental variation due to liquid handling, sampling and analytical approaches. Finally, the majority of early work was focused on fitting precipitation curves to different conditions tested in order to understand the effect key parameters had upon mAb solubility and hence propensity to precipitate, and large sample numbers brought confidence to these trends.

The disadvantages of one or two factor-at-a-time experiments can be mitigated by the fast processing times and low material requirements of the micro-scale format accelerated on a liquid handling platform. It is well suited for early screening with fast and simple analytical measurements, however when investigating more complex feed-streams which require more expensive and slower analytics a more efficient experimental approach became apparent.

Design of Experiments

Design of experiments (DoE) is an approach ensuring the selected experiments produce the maximum amount of relevant information, thus speeding up experimentation. It is the procedure of designing a set of experiments to represent and answer a well framed question. DoE is well suited to the development of new products and processes as well as the optimisation of existing products and processes. The DoE methodology provides a framework for the experimenter to set an experimental objective, devise and then execute a set of experiments which achieve the objectives established. It requires fewer experimental runs than other approaches to achieve the same data output as all variables are changed simultaneously to cover the design space in the most efficient way possible [164].

It can reveal the most useful and precise information about the studied system, since the joint influences of multiple factors can be assessed. DoE offers the best approach to monitoring systems influenced by multiple factors and provides a framework to analyse these factor responses and determines which effects are real, and which can be discounted as statistical noise. Reliable process design spaces of these explored systems can then be generated, from which constructive findings and conclusions may be drawn.

There are three main stages to the design of experiments approach: firstly there is screening, whereby the most influential factors for a process are identified along with appropriate ranges. Secondly optimisation, where once the influential factors have been identified, the optimum operating conditions can be identified. Finally, robustness testing, this is the stage where factors can be assessed to improve process robustness, so change can be accommodated more readily without the process falling out of specification.

Full factorial design of experiments

Full factorial designs allow for relatively few experimental runs required per investigated factor. In a full factorial design, all combinations of upper and lower values are included. Variables are given user-defined maximum and minimum values based on pre-existing knowledge which are typified by plus and minus signs when displayed in a table format [164]. For x variables, the number of experiments is typically $2x + 3$, with three or more midpoints included. They are very effective for looking at 2-4 factors and can be readily upgraded with future additional experimental runs to form composite designs which are useful in process optimisation. Figure 8 displays the increasing number of experiments required to run factorial designs for two, three and four variables. Centre point experiments are not shown, but should always be included in designs as these can identify non-linear relationships, with repeats increasing the model validity [165]. For experimental designs looking at five factors or more, full factorial designs become less than ideal due to the number of conditions incurred, especially if duplicate/triplicates are run. Fractional factorial designs then become more suitable, requiring fewer runs but with the drawback of possible confounding between main effects and interaction effects [164].

Two Variables			Three Variables				Four Variables				
Exp. No.	Variables		Exp. No.	Variables			Exp. No.	Variables			
	Factor 1	Factor 2		Factor 1	Factor 2	Factor 3		Factor 1	Factor 2	Factor 3	Factor 4
1	-	-	1	-	-	-	1	-	-	-	-
2	+	-	2	+	-	-	2	+	-	-	-
3	-	+	3	-	+	-	3	-	+	-	-
4	+	+	4	+	+	-	4	+	+	-	-
			5	-	-	+	5	-	-	+	-
			6	+	-	+	6	+	-	+	-
			7	-	+	+	7	-	+	+	-
			8	+	+	+	8	+	+	+	-
							9	-	-	-	+
							10	+	-	-	+
							11	-	+	-	+
							12	+	+	-	+
							13	-	-	+	+
							14	+	-	+	+
							15	-	+	+	+
							16	+	+	+	+

Figure 8. DoE Factorial designs.

Plus signs are the upper value and minus the lower. All variables are changed simultaneously, resulting in an experimental design with controlled, unique combinations of variable labels [165].

Design mode for precipitation screening

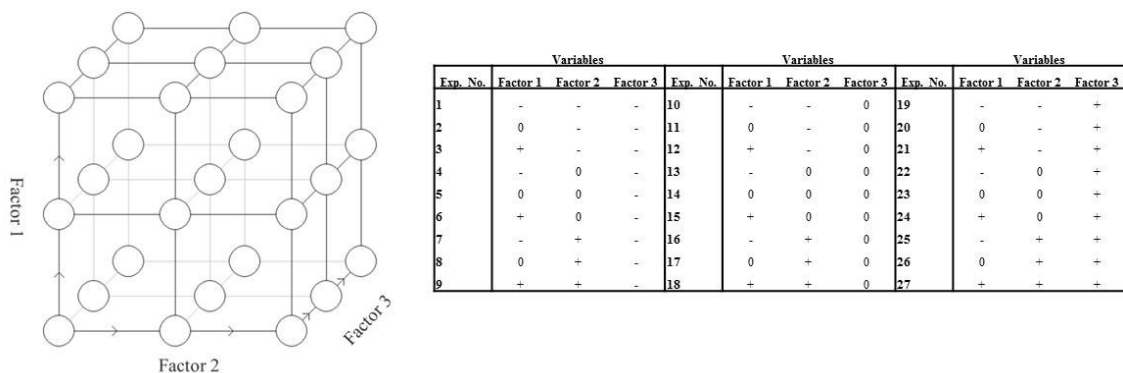


Figure 9. A three point hyper cube with axial points full factorial design space.

Figure 9 displays a three factor, hyper cube with axial points, full factorial design space. It is a much more experimentally intensive design space than 2-point low-high factorial designs, requiring 27 unique experimental points. The rationale for running low, middle and high values for all iterations of factors is that a more robust model can be built. This can be easily accommodated in the automated microplate format; with experiments run in duplicate or triplicate there is still space for standards and controls whilst still only requiring one plate. It should be noted that first developing a scale down methodology using one or two-factor at a time experimental designs builds strong foundations to base DoE designs upon. Since design

spaces are reliant upon the accuracy of results generated, there needs to be confidence in the methodology established in advance to ensure results obtained are meaningful.

1.11 Data Presentation

1.11.1 Sigmoidal Fitting of Precipitation Curves

Precipitation data (the fraction of protein precipitated plotted against the precipitant concentration) can be fitted to a sigmoidal curve function, which for this work will be through OriginPro version 9.1 [OriginLab Corporation, Northampton, MA]. The sigmoidal expression can be used to fit precipitation curves and to predict performance with varying conditions:

$$f = f_0 + \frac{f_{max} - f_0}{1 + \exp^{-B([A] - [A]_{1/2})}}$$

Equation 1.5 Sigmoidal precipitation curve fitting. Where f is the fraction of protein precipitated, f_0 is the bottom plateau, typically zero where no protein has been precipitated, f_{max} is the top plateau, B is the slope at the midpoint, $[A]$ is the salt concentration and $[A]_{1/2}$ the salt concentration at the midpoint, where 50% of protein has been precipitated.

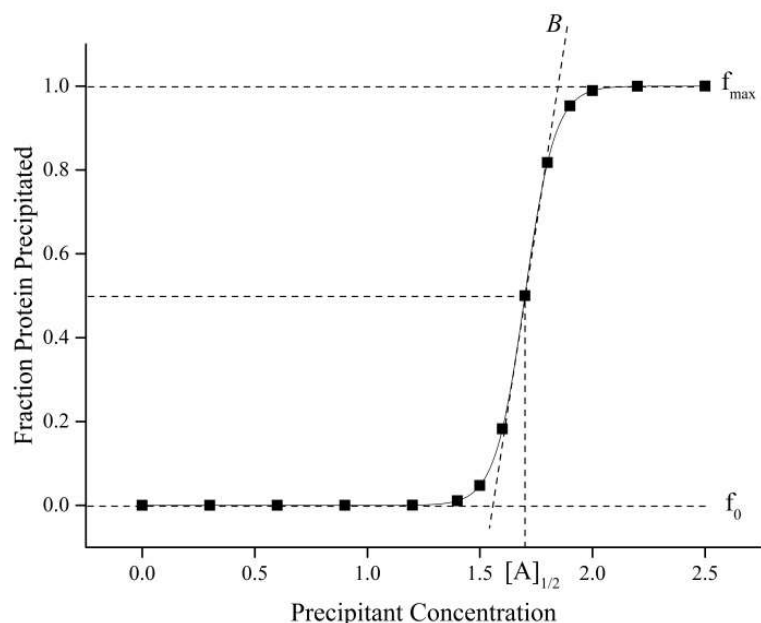


Figure 10. Sigmoid fitting of a precipitation curve.

Graph shown is of an idealised data set with terms from equation 1.5 displayed.

Figure 10 displays a theoretical data set based on an ammonium sulphate precipitation profile.

The precipitation mid-point, $[A]_{1/2}$ informs us at what point 50% of protein has been precipitated, the B term is how sharp a transition from soluble to insoluble has occurred and f_{\max} the maximum fraction of protein precipitated from solution under the conditions tested, f_0 is expected to be zero and would prompt investigation if not this value.

This allows the precipitation midpoints to be calculated which can be used to understand protein behaviour under different conditions [65] and extrapolated to understand the limits of solubility [96]. In this paper the fitting allowed for models to capture when precipitation starts to occur, and the minimum precipitant concentration required to achieve complete precipitation of the protein under specific process conditions.

1.11.2 Solubility Plots / Precipitation Midpoints

In order to evaluate the performance of different conditions upon protein precipitation, the $[A]_{1/2}$, precipitation midpoints from the solubility plots can be isolated and plotted against the

investigated variables. Figure 11 shows how the ammonium sulphate concentrations corresponding to the transitional precipitation midpoints are found to depend linearly upon sodium chloride concentration, and to a good extent protein concentration for both alcohol dehydrogenase (ADH) and hen egg white lysozyme (HEWL). This global fitting has been shown to build up a more complete description of the data [65].

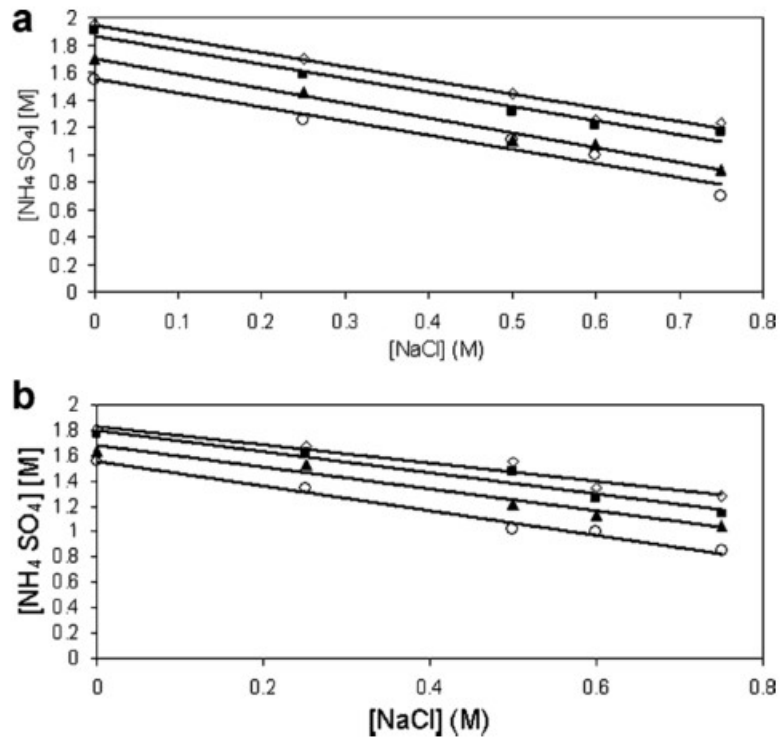


Figure 11. The dependence of precipitation transition mid-points on NaCl concentrations for ammonium sulphate precipitations.

A) displays the profile for HEWL at (\diamond) 4 mg/mL, (\blacksquare) 5 mg/mL (\blacktriangle) 7.5 mg/mL and (\circ) 10mg/mL, B) ADH (\diamond) 4mg/mL, (\blacksquare) 7.5mg/mL, (\blacktriangle) 10mg/mL and (\circ) 12.5mg/mL [65].

For total (impurity) protein solubility profiles no model exists to capture this amalgamation of multiple host cell proteins, unless all individual fractions are analysed and modelled then collated, which adds serious complication [166]. Therefore, sigmoidal fitting and mid-point analysis is reserved solely for the target protein under investigation.

1.11.3 Fractionation Diagrams

Fractionation diagrams offer an alternative method for representing the purification of a target protein relative to total contaminating protein, providing a clear way of comparing yield and purity [166]. Figure 12 displays theoretical product (enzyme) and total protein solubility profiles in the presence of increasing precipitant concentrations, whilst Figure 13 displays the same data as a fractionation diagram. Fractionation diagrams remove the precipitation concentrations between the enzyme and protein solubilities by plotting them against each other.

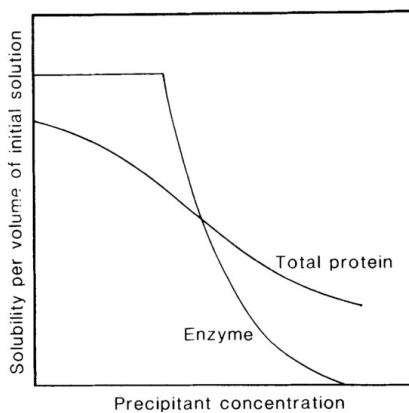


Figure 12. Enzyme and total protein solubility profiles in the presence of increasing precipitant concentration, taken from [166]

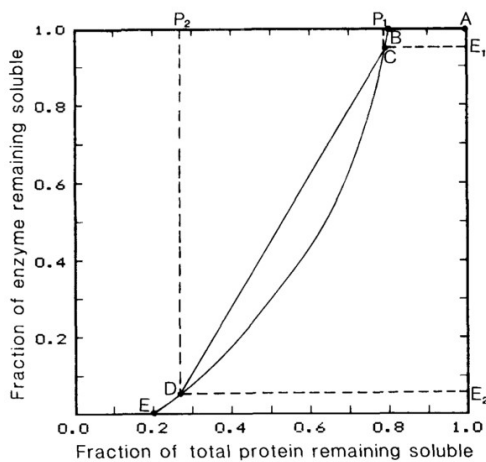


Figure 13. Enzyme-total protein fractionation diagram, an alternative presentation format data presented in Figure 12 [166]

The downside of plotting precipitation solubility data as fractionation diagrams are that the precipitant concentrations are not displayed, so conditions must be cross-referenced against a different data format.

1.12 Structure of Thesis

The work presented in this thesis aims to develop an effective microscale precipitation screening methodology for the rapid identification of suitable precipitation conditions for the early purification of the mAbs.

Chapter Two details the materials and generic methods used throughout the work in this thesis. In Chapter Three, the micro-scale precipitation methodology is developed, with the focus on automation and process control. The work in Chapter Four then tests this methodology by screening a range of precipitants on purified IgG₁ in order to rapidly build up understanding. Linking studies on cell culture fluid are then performed. Understanding built from pure protein studies is then applied to process cell culture fluid in Chapter Five, with the focus on both recovery yield and product purity. In Chapter Six the potential integration of precipitation with orthogonal chromatographic separations is explored, linking with an anion exchange chromatography step. Chapter Seven concludes the work throughout the thesis and sets out future experimental work to build what has been presented.

Chapter Two: Materials & Methods

“Insanity: doing the same thing over and over again and expecting different results”

Albert Einstein (attributed) – who clearly did not work in the biological sciences

This chapter describes the main materials and analytical procedures used. Details pertaining to specific experiments are described in their appropriate chapters.

All chemicals were of analytical grade and sourced from Sigma-Aldrich Ltd (Poole, UK). Water was obtained by reverse osmosis (RO) (Millipore, Hertfordshire, UK). 96-well flat bottom Corning Costar® UV Micro-well plates and Corning 96 well 2mL, V-bottom deep well plates were sourced from Corning (Leicestershire, UK).

2.1 Material

A purified humanised 150kDa monoclonal antibody was provided by UCB Pharma (Slough, UK) at 80.1mg/ml IgG₁ concentration in a well-defined formulation buffer (personal communication, UCB Pharma). Clarified cell culture supernatant (CCCF) was also provided at a defined IgG₁ concentration. The clarification involved a sequence of centrifugation, depth filtration and 0.22µm sterile filtration to achieve an essentially particle free feedstock.

The cell culture fluid was composed of a range of well characterised components, known to the author for the consideration of how could affect precipitation performance, but redacted for the thesis. Material was stored in small volumes, 50mL for cell culture fluid and 1mL purified IgG₁, to avoid issues of thawing and refreezing. Material was stored at -80°C and the required amount was thawed on the day of experimentation, for extended studies material was stored at 2-8°C for no greater than 4 days.

2.2 Tecan liquid handling platform

A Tecan Freedom EVO® 200 series liquid handling system was employed for the majority of work presented (Tecan, UK). The system is modular in design and highly customisable. Figure 14 shows the deck layout used with key systems and labware carriers labelled. The Liquid Handling Arm (LiHa) was installed with 8 fixed, 1mL stainless steel tips with integrated liquid conductivity sensors. Tips are flushed and washed with RO water in the wash station. The Robotic Manipulator Arm (RoMa) extends the use of the Tecan work deck by enabling the transportation of microplates and other labware types quickly and efficiently between deck, storage and peripheral devices such as the orbital shaker (TeShake) and Tecan Infinite® 200 series plate reader.

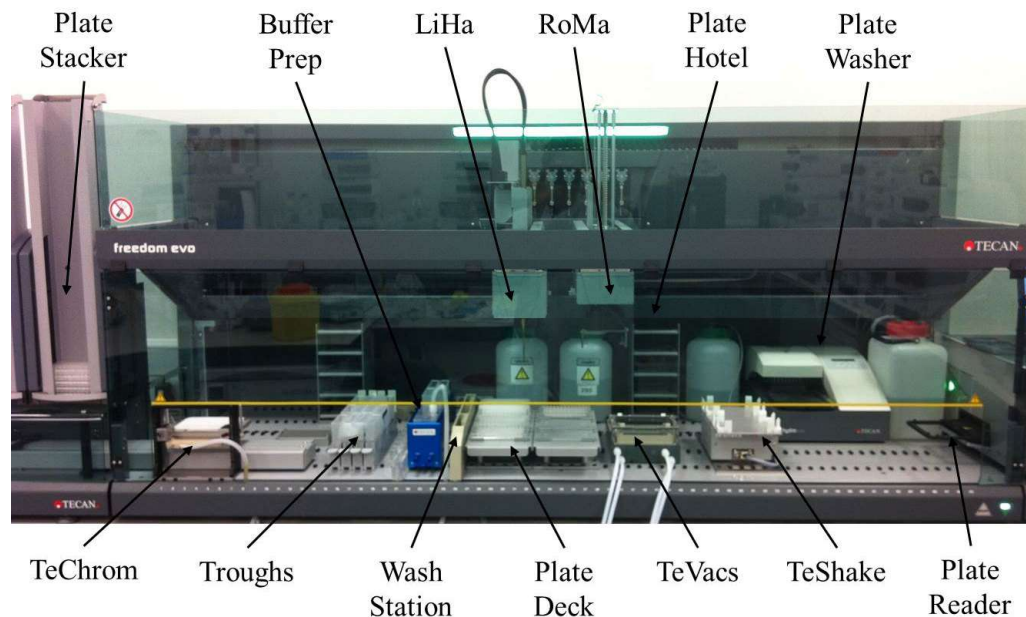


Figure 14. Tecan system with default equipment layout

There was capacity for twelve 100mL liquid troughs, for containing stock solutions and feed material. Not shown in Figure 14 but also available were a range of Eppendorf and Falcon tube carriers capable of housing between 8 and 16 vessels per rack. The 2 plate deck carriers were set out suited for 24, 96 or 384 well layouts. Additional system functionality not used

included the Plate Stacker, Plate Hotels, the TeChom (chromatography system), TeVacs (plate vacuum separator), automatic Buffer Prep and Plate Washer systems. More specific details and operating conditions will be covered in Chapter 3.

2.3 Protein quantification by A280nm

For pure protein studies, the Beer-Lambert law was used to determine IgG₁ concentration. Concentrations of IgG₁ in pure protein stocks were determined at A280nm in Corning UV transparent plates with a Tecan™ Infinite® 200 series plate reader (Tecan, UK). The extinction coefficient of the IgG₁ investigated was $\epsilon = 1.56 \text{ mL}\cdot\text{mg}^{-1}\cdot\text{cm}^{-1}$, (personal communication, UCB Pharma). For protein measurements in the 96 well format, the path length of samples measured would vary depending on the liquid volumes measured, hence sample measurements were fixed to 300 μL . With the path-length fixed, the equation could be simplified and rearranged to find the protein concentration:

$$c = \frac{A_{280}}{\epsilon_{280}}$$

Equation 2.1 The absorbance, A, (AU) at a given wavelength of light is determined by the specific molar extinction coefficient, ϵ ($\text{mL}\cdot\text{mg}^{-1}\cdot\text{cm}^{-1}$) and substance concentration, c (mg/mL).

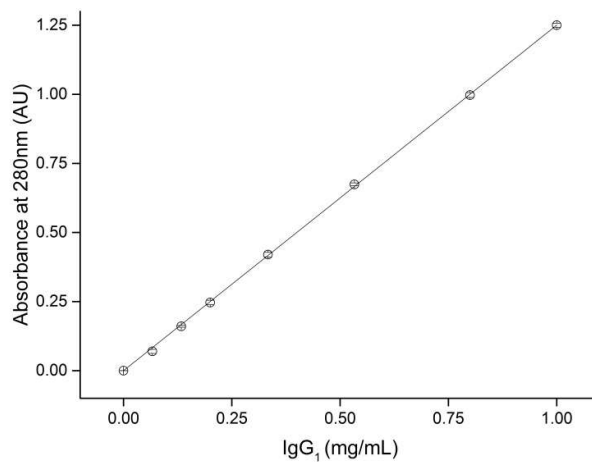


Figure 15. IgG₁ standard curve prepared in the 96 well format.

The extinction coefficient for a fixed 300 μ L volume was determined to be 1.25 AU.mg⁻¹.mL ($R^2 = 0.9998$). Triplicate preparations of protein standard were prepared; the standard deviation of measurements is plotted.

Figure 15 displays a typical IgG₁ standard curve generated by automated liquid handling. Space permitting, a fresh standard curve was prepared for each set of experiment runs, with little variation observed from the absorbance coefficient in 300 μ L.

In proteins it is the amino acids tyrosine, tryptophan and to a lesser extent phenylalanine as well as disulphide bonds which absorb strongly at 280nm. Changes in 2^o, 3^o and 4^o protein structure can also affect absorbance so care should be taken to ensure pH, ionic strength, and temperature remain controlled.

This assay cannot differentiate between different proteins, hence is only a viable approach for studies on fully purified material. Cell culture fluid contains a wide range of components including HCPs, DNA and media additives which can all distort values, and hence a more specific assay is required to differentiate between IgG₁ and other species. For example, DNA can absorb up to ten times more strongly at 280nm than proteins at equal concentration, so even small amounts can have a strongly distorting effect. Spectroscopy remains a quick, cheap and simple assay for early analytics.

2.4 Precipitate measurement by A600nm

It has been shown that fraction of protein precipitated can be determined by correlating the absorbance at 600nm to the mass of protein precipitated [65]. Figure 16 displays the effectiveness of two approaches for determining protein precipitation: direct measurements at 280nm were found to be the most accurate, whilst absorbance measurements at 600nm were included throughout the scale-down methodology to check the extent of precipitation; determining if the system stabilised and can be assumed to be at equilibrium. Absorbance readings at 600nm were also used to measure the extent of re-suspension of precipitated pellets, whereby any absorbance at 600nm after the re-solubilisation would be indicative of incomplete re-suspension of solid protein and prompt further investigation. Measuring the absorbance at 600nm was a rapid, qualitative, non-intrusive and effective tool for understanding the extent of precipitation. However, at increasing precipitant concentrations a trend of reduced solids absorbance was observed. For example in Figure 16, precipitating conditions with ammonium sulphate above 2.0M saw a drop in the A600nm value, even though the fraction of IgG₁ precipitated out of the liquid phase remained complete. This can be explained from observing that as more dense precipitates form, by greater preferential dehydration, the light path length is less obstructed compared to the cloudier precipitate emulsion and a greater transmission is recorded.

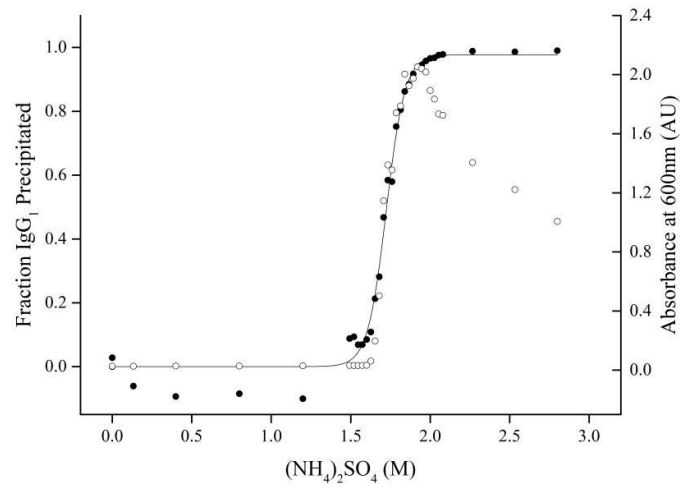


Figure 16. The Ammonium Sulphate precipitation profile for pure IgG₁.

Performed at a final concentration of 3.35mg/mL. Fraction of IgG₁ precipitated (●) determined by the protein absorbance at 280nm can be seen to match well to the solids measured at 600nm (○).

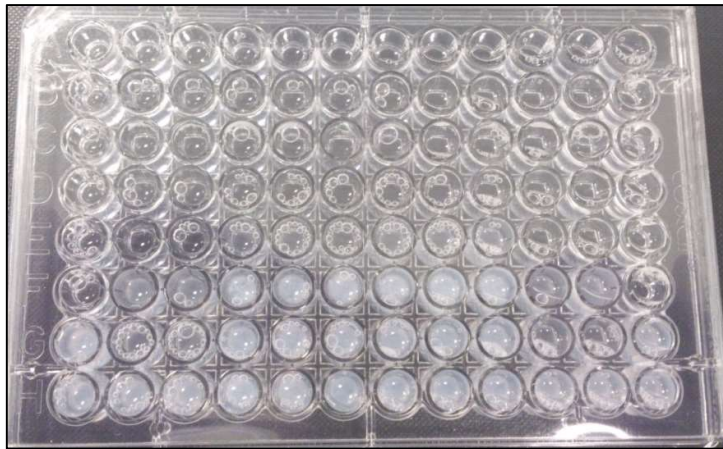


Figure 17. The profile of pure IgG₁ in the presence of different precipitants and concentrations.

Photo captured after the initial jet-macro mixing stage. Clear solutions suggest non-precipitating environments whilst cloudy white emulsions are indicative of precipitation, absorbing strongly at 600nm.

Figure 17 displays a typical 96 well micro-titre plate which is assessed by absorbance at 600nm. In this instance the photo captured the plate post the jet macro mixing stage and hence air bubbles can be observed. These have the tendency to affect absorbance values measured in the plate reader, and as such A600nm readings are taken in multiple sets of readings to

ensure a representative result. Air bubbles were dispersed after sustained orbital shaking and were not found to affect subsequent measurements.

2.5 IgG measurement by Protein A HPLC

IgG₁ concentration was determined using a Protein A column (PA Immuno detection sensor cartridge 2.1 mm (D) x 30 mm (L) Applied Biosystems, Life Technologies) on an Agilent 1200 series HPLC (High Pressure Liquid Chromatography) system (Agilent, Berkshire, UK) and analysed with Empower data analysis software (Waters, Milford, US).

Samples were run at 2mL/min at 30°C for 7 minutes per sample in a 96-well plate format. Buffer A was phosphate buffered saline, pH 7.40 (± 0.05) and the elution buffer B was phosphate buffered saline, adjusted to pH 2.70 (± 0.05) with 85% w/v phosphoric acid. Samples are loaded, then mobile phase A is run for 2 minutes, during which all non-binding proteins pass through the PrA column. Mobile phase B is then run for 2 minutes, with bound protein eluting off the column. 3 minutes, or 6mL of mobile phase A was then run to re-equilibrate the column. The maximum system pressure limit was set throughout to be 400 bar. Sampling was set to 200 μ L/min draw and eject speeds, with a 2 second equilibration time and five times the injection volume sample flush out volume. The multiple wavelength detector (MWD) was set to a single wavelength of 280nm with a bandwidth of 16. Each plate included a 6-point standard curve based on the IgG₁ standard. Standard injections of 35 μ g IgG₁ were run every 10 samples to validate column performance. The HPLC was configured to run up to 296 well plates per run. Plates were sealed with silicone or aluminium foil lids to avoid evaporation liquid losses with the HPLC sampling needle piercing the septum to acquire samples. Concentrations were determined by integrating the peaks, converting to mass of protein by linear regression and then dividing by the injection volume.

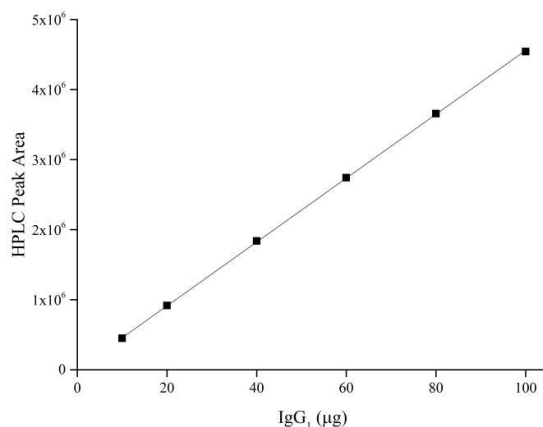


Figure 18. Protein A HPLC IgG₁ calibration curve.

Standard 6-point calibration curve, each point measured in triplicate, 46600 P.A/µg, $R^2 = 0.99998$.

Protein A HPLC has been used as the workhorse analytical tool for most work run on cell culture fluid. Its specific binding to the Fc region on immunoglobulins allows for a simple and quick assay to determine IgG₁ recovery yields.

2.6 Protein purity assessment by Protein A HPLC

For analysis of precipitate purity, the flow-through peaks from the protein A HPLC column of re-solubilised precipitates were integrated as an initial identifier of remaining impurities. Although not a specific assay, the rationale was that any substances absorbing at 280nm not binding to the Protein A HPLC column would be captured in the assay flow-through (FT) and could be used as a quick metric for performance:

$$Purity = \frac{C_I}{C_I + C_F}$$

Equation 2.2 Precipitate purity (%) can be determined from C_I , the measured concentration of IgG₁ (mg/mL) by integrating the eluted peak and C_F , the concentration of impurities (mg/mL) measured from integrating the flow-through peak both from the Protein A HPLC assay against the IgG₁ standard curve.

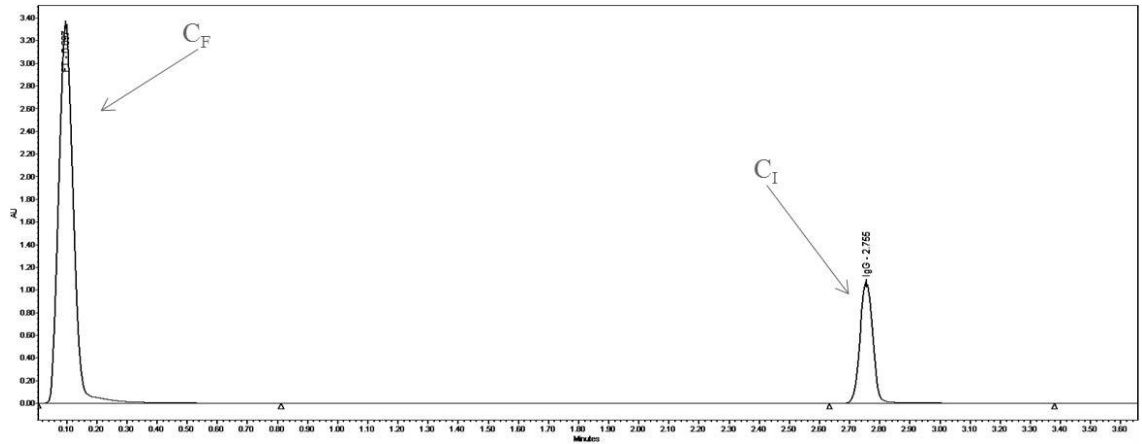


Figure 19. Protein A HPLC chromatogram of starting cell culture fluid.

25 μ L of material at a defined IgG₁ titre. The C_F, impurity flow-through is detected at 0.1min with the IgG₁ peak eluted and detected at 2.75 minutes. Concentrations were determined by integrating the peaks, converting to mass of protein by linear regression and then dividing by the injection volume.

Since PrA HPLC was run to quantify the IgG₁ peak, evaluating the flow-through peak required no additional resources and provided additional information about the overall purity of the material under investigation.

2.7 IgG charge profile measurement by iCE

Imaged Capillary Electrophoresis (iCE) was run on re-solubilised pure IgG₁ precipitates to determine the charge profile of the protein as a determinant of product quality retention. An iCE system with Alcott 720NV auto-sampler was utilised (Protein Simple, Santa Clara, CA, USA). Samples were run in the 96 well plate format with 30 μ L 2mg/mL samples prepared in 150 μ L HPLC grade water, 105 μ L 1% methyl cellulose, 12 μ L pharmalytes (pH 3-10), 1.5 μ L lower pI marker and 1.5 μ L upper pI marker. Samples were pre-focused for 1 minute at 1.5kV before being focused at 3kV for 6 minutes at a controlled auto-sampler temperature of 18 $^{\circ}$ C.

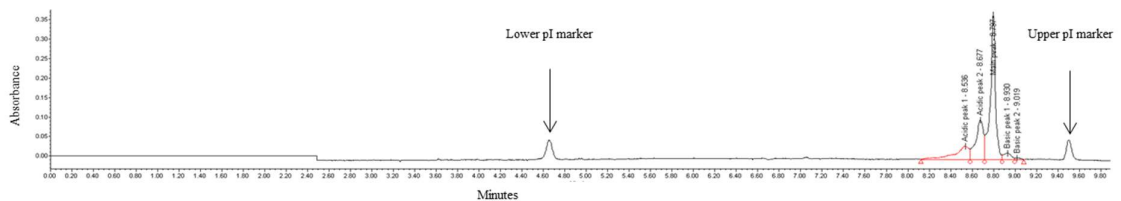


Figure 20. iCE analysis generated from a re-solubilised IgG₁ precipitate

Charge profiles were expressed in terms of acidic, main and basic peak percentages as the sum of the total peak area. The method was sensitive to residual salts so samples were buffer exchanged with 50mM phosphate buffer, pH 7.0 for 2-3 volumes in Eppendorf spin tubes until conductivity was less than 5mS/cm.

2.8 Protein purity assessment by SDS-PAGE

Reduced and non-reduced sodium dodecyl sulphate polyacrylamide gel electrophoresis (SDS PAGE) were run on samples using 1.5mm x 10 or 15 channel NuPAGE® 4-12% Bis-Tris Precast Gels (Life Technologies). A Mark 12™ unstained standard protein ladder (Life Technologies), IgG1 standard and cell culture fluid sample were included on each gel. 20µL preparations consisting of 8µL sample and deionised water, either 2µL NEM (N-ethylmaleimide) or 2µL NUPAGE® 10x reducing agent and finally 10µL NuPAGE® 2x Sample Buffer were mixed, treated at 85°C for 4 minutes and then centrifuged at 13,600rpm on bench scale centrifuge for 30 seconds. Channels were loaded with either 5 or 10µg of protein depending on Antibody treatment with NEM prior to SDS-PAGE reduces the formation of half antibodies by akylation of free cysteine residues, avoiding auto-reduction. Gels were run at 150kV, 35mA for 90 minutes. Faster protocols at higher voltages were avoided to mitigate the risk of gel ‘burning’ by residual salts from the precipitation step. Gels were stained in 0.1% Coomassie R-250 in 40% ethanol and 10% acetic acid for 1-3 hours. Background staining of the gel was removed by diffusion in 10% ethanol and 7.5% acetic acid, with the solution changed after 1 hour, to speed up the process then allowed to stand for typically 16 hours. Gels were scanned and used for early visual inspection work. Band densitometry was an option for semi-quantification of protein fractions; however alternative, more effective assays were used instead. SDS PAGE was not ideally suited to the high throughput nature of precipitation studies, so its main application was for early proof of concept work in understanding performance under different precipitating conditions.

2.9 Protein purity assessment by Bioanalyzer

Product purity was assessed using electrophoresis under non-reduced conditions. This was performed using an Agilent 2100 Bioanalyzer (Agilent, Berkshire, UK) with Agilent Protein 230 Quick Kits which included micro-fluidic chips. Reagents including a fluorescent gel-dye mix, de-staining solution and a protein ladder were first loaded onto the chip, followed by 8 μ L of samples and standards denatured by sodium dodecyl sulphate, SDS. Proteins were then separated by an electric field through the chip channels based on molecular size, allowing for separation of IgG₁ and impurities. The relative abundance of each protein species was plotted as electropherograms by the software based on the fluorescent intensity of the dye bound molecules against time. This data could be translated to more familiar gel-like images for visual analysis, both modes of presentation are depicted in Figure 21. Protein sizing was achieved by comparing to a ladder with the range of 4.5 to 240kDa, allowing for IgG₁ purity to be calculated by relating its peak area to the total peak area of all proteins generated from the electropherograms.

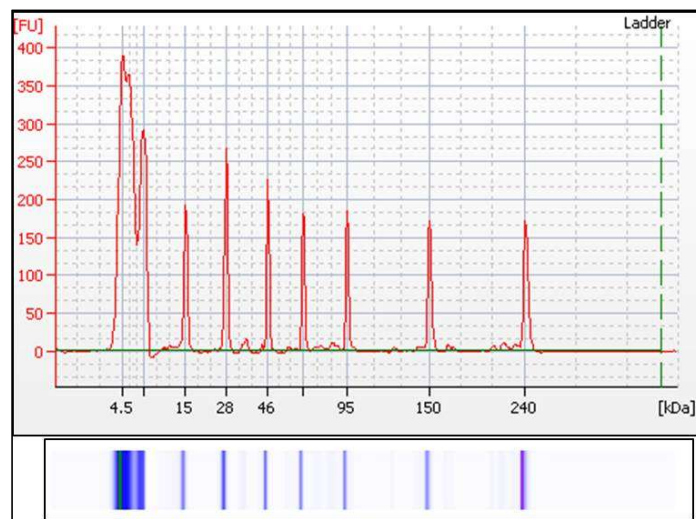


Figure 21. Bioanalyzer electropherogram (top) and reciprocal false gel display (bottom and rotated). Displayed is a protein ladder. SDS-PAGE like protein bands are built from the fluorescent unit absorbance peaks.

Bioanalyzer enabled semi-high throughput screening, as each microfluidic chip could run 10 samples and had a total processing time of 20 minutes. Samples were pre-diluted utilising the Tecan liquid handling system, so less than 10 minutes of manual sample prep were required. At 2-3 minutes per sample, Bioanalyzer electrophoresis becomes a powerful tool for assessment of work done on cell culture fluid.

2.10 Protein purity assessment by Bradford Total Protein

Bradford reagent (Sigma Aldrich, Poole, UK) was selected to determine the concentration of proteins in solution. Proteins bind to the dye Brilliant Blue G forming a complex which shifts the maximum absorbance of dye from 465nm to 595nm, with absorption proportional to the concentration of protein present within a range between 0.1-1.4mg/mL with a BSA standard. A sample dilution plate was prepared before the transferring samples to the assay plate. Utilising an Excel-Evoware Tool spreadsheet, typically 10-50 μ L of each sample was transferred to a new 96 well flat bottom Corning Costar® UV Micro-well plates, and diluted with 50mM phosphate buffer, pH 7.0 to bring protein concentration within range of the assay. A 7-8 point standard curve was prepared from a 1.00 mg/mL IgG₁ standard, along with a starting cell culture fluid control. All liquid volumes were mixed with the robotic liquid handling tips. In a fresh UV micro-well plate, 10-20 μ L of all samples, standards and controls were dispensed across the plate followed by 250 μ L of Bradford Reagent to each well. Liquid volumes were mixed by liquid handling robot and then incubated at room temperature for 15 minutes before transferral to the Tecan plate reader. Absorbance readings at 595nm were taken three times, at 10-minute intervals objective to determine the most stable measurement.

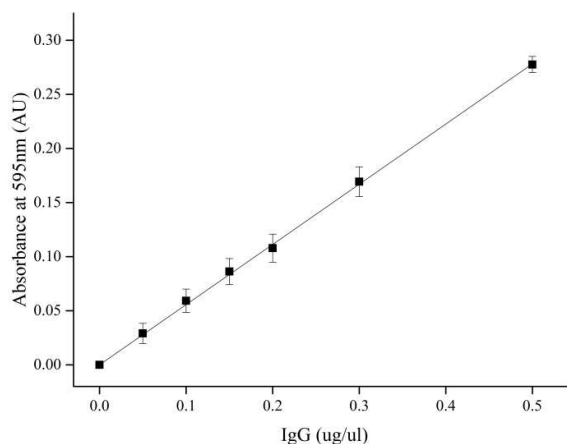


Figure 22. Bradford total protein assay calibration against purified IgG₁.

Linear correlation of $5.88 \times 10^{-1} \text{ AU}_{595} \cdot \mu\text{L} \mu\text{g}^{-1} \text{ IgG}_1$, $R^2=0.9997$. Triplicate preparations were prepared with standard deviation displayed.

Figure 22 displays a typical Bradford assay calibration curve against IgG₁ standard. Bovine serum albumin (BSA) is traditionally used to correlate total protein concentrations, however since 40 to 80% of total protein in samples is expected to be the product IgG₁ it was rational to relate all proteins to this standard. Bradford total protein assay was used for initial assessment of total protein concentrations in the recovered protein precipitates. Its application for high throughput screening on precipitated conditions was found to be limited. Residual salt concentrations were prone to adversely affect absorbance values and adding a buffer exchange step to the 96 well plate format was possible however would have markedly reduced the throughput of operations. The alternative early assays of Protein A HPLC flow-through analysis and Bioanalyzer gel electrophoresis were found produce more reliable findings. It remains a good application for assessing non-salt driven precipitation.

2.11 Aggregate profile measurement by SEC HPLC

Size exclusion chromatography (SEC) enabled protein samples to be analysed based on size. Re-solubilised precipitate samples were analysed by Gel Permeation HPLC using a 7.8mm x 300mm reverse phase TSK gel G3000SWXL (Tosoh Bioscience, Stuttgart, Germany) column

in an Agilent 1200 series HPLC system (Agilent, Berkshire, UK). A 15-minute method was run at 1mL/min at 25°C. IgG₁ monomer was identified as the main peak based on a molecular weight standard at 150kDa, and percentage monomer was calculated by dividing this by the sum total of all peak areas. The mobile phase buffer used was a 200mM phosphate buffer at pH 7.00 (±0.05). Target sample loading was set at 50µg of protein.

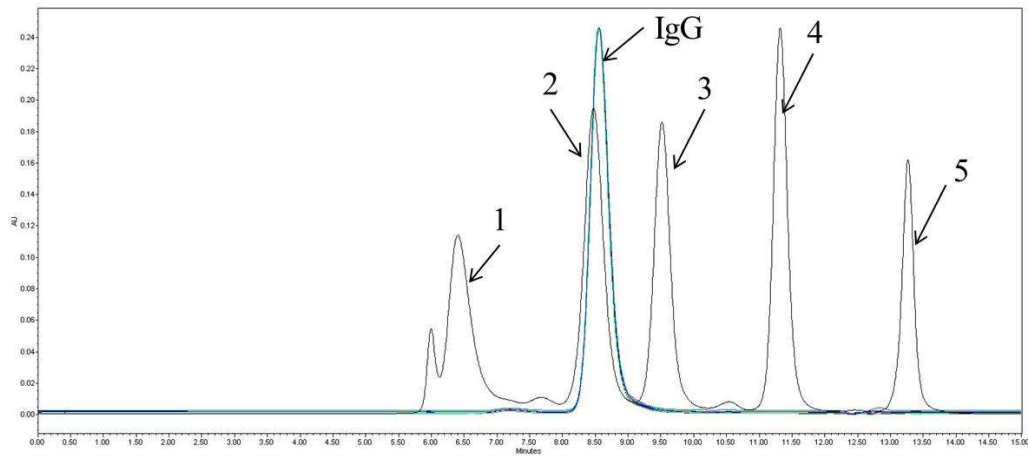


Figure 23. An example size exclusion chromatography chromatogram.

A molecular weight standard (BEH200 SEC Protein Standard Mix, Waters) is overlaid on a purified IgG₁ material. The main peak at 8.60 minutes is the monomer protein profile. Analytes include 1) Thyroglobulin, 669kDa 2) IgG, 150kDa 3) BSA, 66.4kDa 4) Myoglobin 17kDa and 5) Uracil 0.112kDa.

Size exclusion chromatography is a useful tool for assessing the protein profiles following recovery and re-suspension of the protein precipitate. It is a more time intensive assay however, since requiring 15 minutes to run each sample, a full 96 well format plate including standards and controls can take in excess of 24 hours to process and as such is not ideally suited for high throughput screening as it can cause a bottleneck unless multiple HPLC systems are employed.

2.12 IgG activity measurement by activity ELISA

To test for IgG₁ function after recovery of the precipitate samples were run internally at UCB for a test on activity. A dual binding enzyme linked immunosorbant assay (ELISA) was

performed, testing for two different functionalities on the immunoglobulin. A plate was run for each binding assay. On each plate three reference standards from independent preparations were used, with all three reference standards used to separate the percentage activity of each sample tested. The % activity was calculated by dividing the C parameter of the reference standard curve by the C parameter of each sample curve. Each sample had three values for percentage activity, and a geometric mean for those results was also calculated.

$$y = D + \frac{A - D}{1 + \left(\frac{x}{C}\right)^B}$$

Equation 2.3 The 4-parameter curve fit for the activity ELISA calibration curve. Whereby y is the measured absorbance at 450nm (AU), D is the upper absorbance value (AU), A the lower value (AU) and C is concentration at the midpoint of the curve (ng/mL), and B is the power exponent.

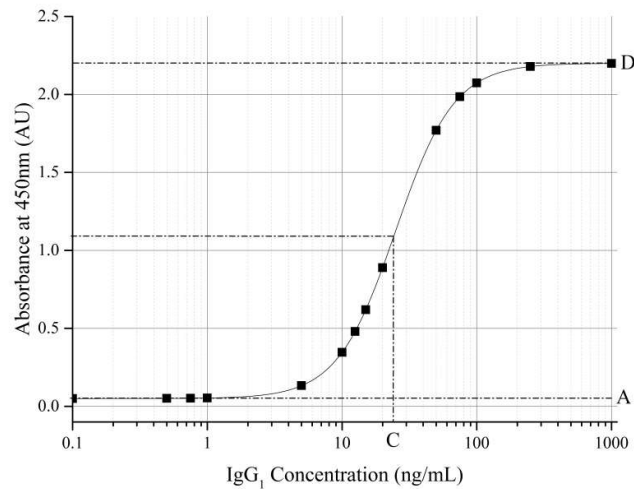


Figure 24. An example 4 parameter curve fit to ELISA calibrations.

A, C and D terms in equation 2.4 are displayed on the graph.

2.13 Measuring clarification efficiency of centrifugal separation of precipitate

Centrifuge performance was evaluated by measuring the degree of clarification achieved in the supernatant:

$$C = \left[1 - \left(\frac{OD_s - OD_0}{OD_f - OD_0} \right) \right] \times 100$$

Equation 2.4 Clarification of the supernatant, C (%) can be calculated from the optical density values measured at 600nm wavelength. Where OD_s is the supernatant sample (AU), OD_f is the feed material (AU), in this case the precipitated protein, and OD_0 is the supernatant after an extended centrifugation operation (AU), as a best-case scenario.

Centrifugation separation efficiency was tested during method development and intermittently during experimentation to ensure precipitation yields were not being adversely affected by the centrifugal recovery operation. Clarification typically exceeded 99% for the lab scale plate centrifugation assays on pure protein which was indicative of good solid/liquid phase separation.

Chapter Three: Automated Precipitation Method Development

“The whole is greater than the sum of its parts”

Aristotle

3.1 Abstract

This chapter details how precipitation screening was applied to the micro-well format and accelerated through liquid handling automation. Development work is presented explaining how operating system conditions were established through robust testing on analytical techniques to measure soluble protein, liquid volumes, effective centrifugal recovery and re-suspension of the precipitate. A custom-built Excel-Tecan design tool was constructed in order to facilitate high throughput screening and complex experimental designs involving multi-component solutions.

The work presented in this chapter includes the fully automated screening procedures including full assay preparation and analysis in the case of on-deck spectroscopy. Liquid volume transfer involving precision control was augmented with the Excel control tool, enabling even complex full factorial designs to be carried out in less than two hours. Liquid volume detection, robotic tip liquid conductivity feedback on supernatant removal, and understanding of absorbance spectroscopy has aided in this approach.

3.2 Introduction

A very broad remit was initially assigned to this project to investigate precipitation as an alternative to PrA chromatography for new therapeutic proteins in development. In order to fashion this objective into an investigation suited for a research thesis, it was decided from the onset to focus on the microscale and look at a wide range of precipitants. This was perceived to be the best approach to build up a comprehensive understanding of its performance and in doing so allow for a more considered and universal appraisal of precipitation from a manufacturing perspective.

The application of automation can markedly reduce labour requirements, whilst improving operational and analytical accuracy [167]. As stated earlier, automation has previously been shown to improve experimental throughput by 3-4 fold [163][151], and provided analytical techniques are not step-limiting this has the potential to speed up early bioprocess development by the same scale. To unashamedly say that this thesis is “standing on the shoulders of giants”, microscale experimentation played greatly to the strengths of The Department of Biochemical Engineering at UCL, so strong foundations on mixing, scale up and automation were already laid. This chapter covers how different techniques have been sourced, amalgamated, and applied to precipitation studies through automation.

3.3 Tecan Control

The Tecan system used had two robotic arms installed, a liquid handling and robotic manipulator arm.

3.3.1 Liquid Handling Arm (LiHa)

The liquid handling arm (LiHa) consisted of eight independently controlled fixed tips. Distance between pipetting tips can range from 9mm to up to 38mm allowing for flexibility for different labware formats. Each had a maximum volume capacity of 990 μ L, with system liquid driven movements. Space inside the tips can be filled with system liquid, air gaps and samples with multiple compartmentalised for multiple aspirate/dispense operations. The fixed tips were fitted with integrated conductivity probes, so for typical liquid aspirate commands, liquid level tracking meant the tips moved down until they detected liquid, then aspirated whilst moving down to accommodate the volume removed. As default, tips descended 2mm further below this liquid level to avoid aspirating air.

Due to the nature of fixed tips instead of disposable tips, cleaning and maintenance was very important. At the beginning of each script, a 20mL short flush (solely passing liquid through the tips) plus 20mL deep flush of liquid (whereby fluid passed through and around the outside of the tips), or \sim 40 tip volumes of RO water was run. The exterior of the tips were carefully

wiped down after every run to remove any potential salt build up which could corrode the materials over time. A maintenance operation carried out included a 50mL flush of caustic 0.1M NaOH, followed by 50mL RO water, then 50mL 20% EtOH and the 50mL RO water through each tip. No indication of carryover between washes was observed, if this was the case a more thorough wash stage would have been devised.

3.3.2 Robotic Manipulator Arm (RoMa)

The main function of the robotic arm was to bring labware into the operational range of the LiHa and also to transfer between devices on deck. All movements can be programmed with X (horizontal), Y (depth), Z (height) and R (rotation) co-ordinates, with the grip distance and force adjustable so as to accommodate various labware geometries. The main use for the RoMa within this thesis was to move plates to and from the orbital shaker and the plate reader, aiding in overall automation and reducing manual intervention. The RoMa can also be used to cycle labware through the plate stacker, so if the centrifugation step could be automated by using an on-deck centrifuge then near-continuous operation of multiple plates could be run without any manual intervention. The system was pre-built with automatic 'Transfer-To' commands, however custom vectors were designed for most movements as these proved to be more reliable at picking up and controllably placing labware in the correct places and avoiding potential collisions with labware and carriers on the deck.

3.3.3 Liquid class systems

Each liquid handling operation through Evoware could be assigned different liquid classes. Liquid classes define how the robotic tips handle the liquids, adjusting for differences in physical properties and ensuring accuracy and reproducibility of operations. Table 8 displays the main liquid classes used throughout. Conditions were set based on preliminary work. The delay time after aspiration was how long the tips are suspended at Zstart above the source labware. This time was increased for more viscous fluids so that any possible liquid bound to the outside of the tips would have opportunity to drip off. System trailing air gap (STAG), the

air cushion placed between system liquid and sample in the system, were kept constant, whilst trailing air gaps (TAG), the air cushion between the liquid and the end of the tip pipette, was increased to 20 μ L, with the more viscous fluids. This was to combat occasional dripping and liquid loss which was sometimes observed under the default setting.

An increase in liquid breakoff speed during dispense ensured that any residual ‘drip’ (up to several microliters) with viscous fluids was ejected forcibly. The majority of these settings were established through experimental trial and error; changes were made until the issues disappeared. This is no different from how liquid handling from manual pipetting would be done, except more conscious thought was needed to teach the robotic system how to react like a human would. Optimal conditions were initially identified by emulating the action manually first then mimicking on the system.

Table 8. Liquid Class descriptions

	Water	Fast Water	Viscous	High Viscous
Conductivity (-)	High	High	Low	Low
Aspirate Speed (μLs⁻¹)	150	600	100	100
Aspirate Delay (ms)	200	200	600	2000
STAG (μL)	20	20	20	20
TAG (μL)	10	10	20	20
Liquid Level Detection tracking (mm)	+2	+2	+2	+2
Dispense Speed (μLs⁻¹)	600	600	600	600
Breakoff Speed (μLs⁻¹)	150	150	150	600
Dispense Delay (ms)	0	0	400	400

Water was the default liquid class on the system and was perfectly effective for most non-viscous liquid handling operations. The *Fast Water* liquid class was used for speeding up simple non-viscous liquid operations. It was used to speed up repetitive tasks such as dispensing Bradford reagent to all wells across a plate or creating blends of buffer systems in a plate before any reaction takes place. The *Viscous* class was set for most commands run through the Excel-Evoware Tool, so that all aspirate and dispense commands could accommodate the lowest common denominator at the sacrifice of pipetting speed. *High Viscous* was used for screening on PEGs and other liquids requiring complex handling.

3.3.4 Labware and Carriers

Carriers were the housing units for each piece of labware, for example *MTP 3Pos* is a plate carrier which has capacity for micro-well plates in predefined locations (1, 2, & 3), the imaginatively named *Eppendorf 16 Pos* is a housing unit for 16 Eppendorfs and so on and so forth. Geometric dimensions could be edited, and this allowed for customised carriers to be added. Labware can be defined as any equipment which fits onto these carriers. In order for the system to locate labware on the deck, X, Y, and Z coordinates are attached to each individual piece of carrier and labware. Relative referencing is applied to the labware so that the system always updates these locations. As mentioned in the materials and methods chapter, the main labware used through the system included Corning UV transparent flat bottom, round 96 well plates, with a maximum capacity of 360 μ L and Corning V-shaped bottom, square 96 well plates, with a 2000 μ L per well hold volume.

Each labware could be assigned 4 z-co-ordinates to which the liquid handling arm referred to, named as travel, start, dispense and max. Z-travel is the height co-ordinate set where liquid handling tips first move into position over the labware and revert to once the command line has been executed. Z-Start moves the tips into the labware. Z-dispense is then the lowered position which just hovers above the well liquid level and Z-max is the height tips are moved to just avoid touching the base of the labware. These co-ordinates have default settings for each pre-programmed labware system, and as with the X and Y co-ordinates, relative referencing, so that they will adjust according to which carrier the labware is based on. The speed the tips move between these different Z-heights could be adjusted to increase or decrease contact time with the liquid if so desired.

3.3.5 The Excel-Evoware Design Tool

Liquid handling robots, such as the Tecan Evoware 200 system offer fast, accurate and complex liquid transfer between a wide range of labware and equipment. It became apparent early on however that the Evoware software had limitations when looking towards more

complex experimental designs. As it stood, each liquid aspirate command operation was confined to a block of 8 tips all aspirating from different sites on the same labware location. The volume aspirated was set by default to the same amount for all tips, so to control individual volumes each tip had to be manually updated. The same limitations applied to dispense operations. For simple operations this wasn't too time consuming, however to create the experimental designs required for high throughput screening of large numbers of different variables there emerged a clear need for a more flexible control system.

Evoware code

Evoware read and executed instructions written in general writing language, .gwl. The format of the code was broken up into sets shown in Table 9.

Table 9. The command break-up for gwl formatted code

Action	Rack Label	Rack ID	Rack Type	Position	Tube ID	Volume	Ext	Ext
A; Aspirate	MTP 1	;	x96 Well UV Microplate	1	;	50	;	;
D; Dispense	DWP 1	;	x96 2ml Deep Well	96	;	50	;	;
W; Flush	;	;	;	;	;	;	;	;
B; Break	;	;	;	;	;	;	;	;

For example, a gwl formatted command to aspirate 50µL from a 96 well microplate in well 1 to a deep well plate in well 96 with a wash step afterwards would need to be written in the order displayed in Table 10.:

Table 10. A gwl formatted command line for one robotic tip operation

A;MTP 1;;x96 Well UV Microplate;1;;50;;;
D;DWP 1;;x96 2ml Deep Well;96;;50;;;
W;,,,,,,,,,,,,;

The *action* command defines whether the tip will aspirate, dispense, wash or break. Wash commands on fixed tip systems can be set when the script is loaded, allowing for variable cleaning regimes suitable for the task. A *wash* command sent to a disposable robotic tip system will discard the used tips and pick up new ones. *Break* is a less common command which can control blocks of operation within a script, and is a useful tool for controlling liquid handling sequences when the sequence or timing needs to be controlled, for example instead of the automatic 8 commands, sets of 6 using only 6 tips could be run. The rack label is the

user assigned name to the specific labware/rack type which links to its physical dimensions characterised through Evoware. The rack type therefore defines what type of labware has been selected. If there are multiple labware of the same type on the deck, it is the rack label which differentiates between them (e.g. MTP 1, MTP 2). Position is the location on the labware which the tip on the LiHa (Liquid Handling arm) will move to, so a 96 well plate will have positions 1-96, whereas a 100ml trough will only have positions one to eight, these positions are defined through the rack type selection. Volume is quantity of liquid in μL which is either aspirated or dispensed. A semi-colon separator is used between each operation and for every blank command not utilised.

Evoware already had a function to convert a comma separated values (csv) file into the raw code in the general writing language (gwl), which could be read and executed on the deck for liquid handling operations. This means that in Excel or another software package capable to saving to the csv format, each operation could be defined in a column, with Evoware extracting from each user-specified column the code and compiling it into the gwl format. However, this system also has its limitations since designing a 96 well plate layout with multiple liquid components, with for example 3 aspirate, 1 dispense and 1 wash command per tip would result in 480 inputs in every column. Visualising the design space and even checking for errors was found to be very difficult and labour intensive. Knowing how complex some experimental designs may become, especially when applying DoE principles, there was a definite need to improve upon the current system.

Creating the control tool

Microsoft Excel was the software package selected to create scripts for the Tecan liquid handling platform to run. Matlab was also considered, however since most computer systems have Excel pre-installed and people are more *au fait* with how it works, it made sense to select the most accessible option. Files could be password protected and given limited editing privileges, meaning only fields which were meant to be changed could, bequeathing all background calculations and references immunity from user error. Since plate reader systems

can also export results to Excel, the extra benefit was that results can be processed on the spreadsheet and analysis could be sped up by direct referencing the results to the experiment design.

A 96 ‘well’ visual layout was designed since the majority of operations would be micro-titre plate based. Figure 25 displays a simplified summary of the experimental design space. Each block represents the inputs and/or calculations for an 8x12, 96 well layout. This layout was specified for 3 aspirate commands followed by 1 dispense then 1 wash per tip, which met the experimental requirements of typically buffer, precipitant and a second precipitant /solution. For more complex liquid handling performances, the interface could be expanded, however it was simpler to execute a second spreadsheet and ensure all conditions were balanced and combined together. The concentration calculator translated the volumes of each different liquid added into the final concentrations taking into account the total volume.

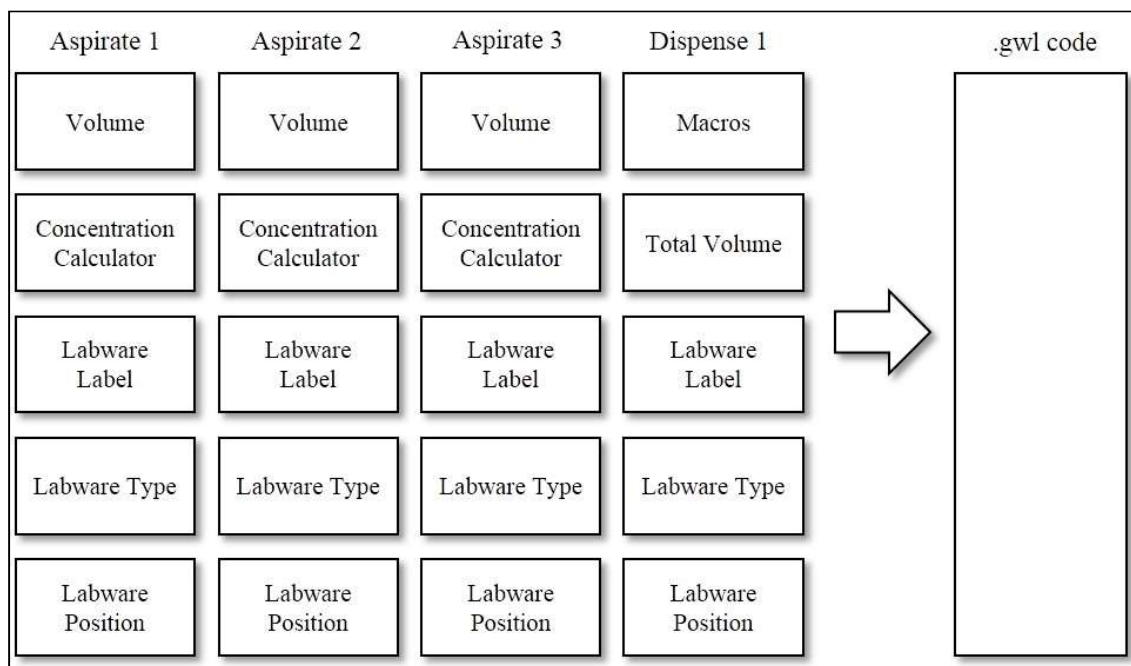


Figure 25. The modular display for the Excel-Tecan Tool.

Excel-Tecan Tool Features

A number of features were imbedded into the spreadsheet, these included drop down lists with pre-populated labware names and types assigned to cells; since all descriptions need to be case sensitive for Evoware to locate the labware name and type these were pre-defined to reduce user error. The lists could be updated when new labware names and types are needed. The ability to transfer to and from any labware/equipment added to the system made this a flexible operation, aiding the completion of multiple different operations in one spreadsheet command. There were also hover-over green question boxes in every module box, detailing instructions for users.

For quick calculations balanced total volume equations always added up to the set volume unless manually edited, with concentration calculators so the final system concentration of each liquid could be shown taking into account the stock conditions and total working volume. For each liquid source there are sum total boxes to show the amount of liquid required to ensure there is enough for the tips to pick up allowing for the user to ensure enough material is made-up prior to experimentation. Also included were 'load bars' to quickly give an overview of how much liquid is being aspirated from which liquid and tip position, which helped with error recognition and visualisation of the design space. Although trivial, pastel colours were chosen to separate each command line and add clarity to what could be an information overload. For faster utilisation, the Excel-Tecan tool is VBA (Microsoft Visual Basic) macro command driven to automatically extract the code, open a new notepad file, and paste the code into the notepad. The user could then save the commands as a gwl file, ready for loading and executed through Evoware. The picture top right of the spreadsheet executes this macro command when clicked, with options to select the full 96 or partial lines of script. For alternative layouts, the labware positions for the dispense operation could be easily changed, effectively making it 96 commands which can be applied to any format. For example, a 384 well format could be designed by running 4 sets of 96 commands, or a reduced 16 sets could be used if dispensing to a single rack of Eppendorfs. These additional functionalities were added to over the course of the project from feedback from other users.

Future potential upgrades could include a macro driven well randomiser, mitigating the risk that results were dependent upon well positioning within the plate. Liquid class control can be added, allowing for each tip and sub-action within that tip to be assigned different liquid classes. This would be especially useful when handling with liquids of varying viscosities and densities, and there is space for this additional command in the extension section of the code. The Excel-Evoware tool was built from an Excel Macro-Enabled Template, allowing for easy generation of new experimental designs into new files without affecting the original file. All 96 well experiments, unless otherwise stated, were executed through this tool. Effort was taken to simplify and make use as intuitive as possible. Although it was initially time intensive to set up the spreadsheet, the Excel-Evoware Tool quickly repaid the early investment and ensured even the most complicated of plate designs could be designed and executed in under 20 minutes.

3.3.6 High resolution experimentation

An additional advantage of running experiment design through the Excel script with multiple aspirate commands was that combinations from two or more stock solutions could lead to accurate small incremental increases in experimental factors, without needing to use smaller liquid volumes. For example in a 100 μ L working volume, using a stock solution of 4.00M ammonium sulphate and using the lowest suitable liquid handling increments of 5 μ L, the best resolution achievable would be 200mM. If combined with a second stock solution of 100mM ammonium sulphate, the resolution achievable can be as low as 5mM salt whilst still being able to reach high saturation conditions capable of promoting precipitation. The question remains whether this level of accuracy is overshadowed by other forms of experimental error; however as will be demonstrated in Chapter Four, high experimental resolution could capture the precipitation curves of proteins very clearly and show excellent experimental fit. This could just as well be achieved manually, however would be very time consuming and the chance of operator error is high when assigned such an intricate and monotonous task. In

principle this is very simple concept but is worth mentioning when considering how its application is broadened through automation and improved control.

3.3.7 Sampling

For sample transfers from the initial reaction plate, standard tip aspirations 2mm below the liquid level with tracking was used. A study was run to determine if analysing the top layer of liquid for protein solubility curves was representative of the remaining supernatant fraction, and also to understand the 'salting in' phenomena observed at lower precipitant concentrations whereby a higher protein concentration than the average of the system was measured. Ammonium sulphate and sodium citrate in 50mM phosphate buffer pH 7.0 were dispensed with 50mM phosphate buffer pH 7.0 diluent followed by 30uL of 5mg/ml IgG₁, making a final concentration of 0.5mg/ml. 30 minutes of orbital shaking was followed by centrifugation at 4,000 rpm for 30 minutes. Six consecutive 30uL samples were aspirated to show the effects of protein concentration across each layer. The top 180ul was inspected, limited only in order to keep the number of micro-well plates used low. Liquid level tracking was used with tip aspirations to make sure minimal liquid disruption occurred. Each 30uL was dispensed into 270uL of 50mM phosphate buffer, for a 1_{in}10 dilution. The A280 of each supernatant 'layer' was taken, and protein solubility curves were displayed. Absorbance readings were equated to IgG₁ concentration based on a 6-point standard curve (triplicate of each condition, R² >0.99).

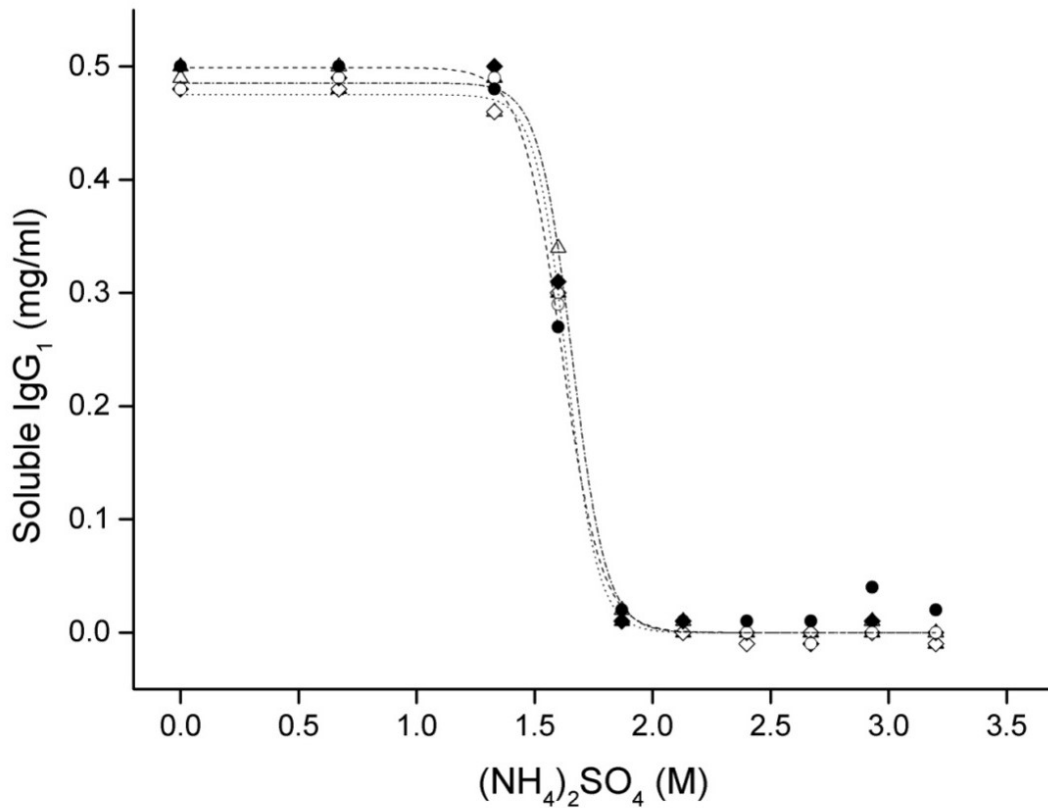


Figure 26. IgG₁ solubility profiles at different liquid heights.

The soluble IgG₁ measured in the 1st layer (△) 2nd layer (▲), 3rd layer (◇), 4th layer (◆), 5th layer (○) and 6th layer (●) of the supernatant at different ammonium sulphate concentrations. Sigmoidal lines were fitted to the 1st layer (dot-dash), 3rd layer (dotted) and 6th layer (dash) to demonstrate variance in protein solubility and hence precipitation curves.

In Figure 26 the soluble protein midpoints were calculated to change from the 1st layer (1.66M), 3rd layer (1.64M) and 6th layer (1.61M) which would indicate a slight overall decrease from the top layer to the bottom of -3%. On the transitional points at 1.6M (NH₄)₂SO₄ there would appear to be no significant trend of reduced soluble IgG₁ as the layer sampling goes down. The same lack of trend was observed with sodium citrate, with all points showing conformity, and precipitation midpoints recorded at layers 1 (0.85M), 3 (0.83M), and 6 (0.84M) all display very similar solubility midpoints. 30µL samples taken from the top layer of wells post centrifugation are a robust and representative techniques for assessing soluble protein and hence the extent of precipitation. What should be focussed on is consistency; if

the samples are aspirated under the same conditions each time, which comes with the territory with automation, this consistency allows good evaluation between tested variables.

3.3.8 Supernatant Removal

For the near complete removal of the supernatant post plate centrifugation a different approach was chosen. A consecutive set of commands with liquid level detection was run in order to remove as much detected liquid as possible whilst minimising the disturbance and loss of the solid protein precipitate. For the 300 μL scale, a system of 100, 80, 50, 20 then 10, 10 and 10 μL aspirate commands were set, adding up to only 280 μL , with the difference being the wet-solids. Each tiered aspirate command had liquid level detection, so the aspirations would halt once no more liquid was detected. To trace the exact volumes removed the software logs could be evaluated, but the removed supernatant was transferred to a new micro-well plate, enabling volumes and hence mass balances to be determined by A977nm.

3.3.9 Control of pH

The measurement of system pH in micro-wells proved to be challenging. The conventional approach for measuring with a pH probe was not possible due to the geometric constraints of micro-wells. Small pH probes were available, but aside from strapping one to the RoMa robotic arm and programming a system of measurements, washes and calibrations whilst recording the values there was no clear way of incorporating into an automated approach. There was capacity on the system to employ a real time pH sampling, whereby sample volumes typically 30-50 μL would be aspirated by the robotic tips and dispensed into pH sensor channels. However, the system required complex set up and calibration and was very time intensive to sample an entire micro-well plate. It was more suited for 8 sample chromatography systems in mind with lower throughput and hence would not be as much of an issue. For effective rapid screening of precipitants under different pH conditions the best approach was deemed to be preparing suitably adjusted stock solutions and feed material to the desired pH and blending the systems together. Buffered systems were used, and selected

conditions tested in larger (50mL) volumes. This allowed a conventional pH probe system to evaluate whether any deviation occurred during the mixing of different systems.

Future work could involve developing buffer blending using the Tecan-Excel spreadsheet, and by collecting the responses generated by different ratios of conjugate acids and bases. This would allow for precise pH systems to be created within a design space and allow for much greater resolution when exploring pH as a key experimental factor. The influence of neutral salts can markedly change the behaviour of buffered systems and coupled with the protein feed which can also buffer against small shifts in pH, this may prove to be too complicated a solution. Looking towards high throughput real-time measurement systems may be the solution; pH sensor micro-well plates are commercially available, typically associated with upstream processing operations where pH, dissolved oxygen tension, and temperature need to be meticulously logged for example 96-Well SensorPlates (PreSens, Regensburg, Germany).

3.3.10 Control of Temperature

The effect of temperature was not investigated in this thesis. Aside from alcohol precipitations which were discounted early on in screening for their non-ideal characteristics, little work in the literature suggested temperature control was an issue with precipitation of monoclonal antibodies. Since no issue with protein denaturation or propensity to irreversibly aggregate was seen with the monoclonal antibody under investigation, there was no obvious need to improve conditions by lowering or raising liquid temperature away from ambient conditions. The first issue would be that temperature would have to remain constant across each micro-well plate, so one temperature per plate could be explored. The source of heat transfer that is applied to the plate would need to be uniform, or at least fully characterised such that the influence of a temperature gradient could be defined. If temperature were to be evaluated, conditions could be controlled by creating the precipitant and buffer conditions, cooling or heating until at the desired level then adding the pre-heated/cooled protein feed to ensure conditions are at the correct temperature from the very start of initial mixing, and subsequently maintained throughout.

3.4 Mixing in Micro-wells

Identifying dynamic similarity between shaken micro-titre plates and stirred vessels presents some challenges, notably equating the different flow regimes [168]. Micro-well shape, the surface area to volume ratio, as well as the frequency and intensity of shaking all have been shown to affect the mixing performance [169]. Wall effects and liquid surface tensions are contributory factors, with well dimensions under 3.5mm shown to exhibit meniscus curvature with even low viscosity fluids as the surface tension forces are not overcome by centrifugal forces [170]. Typical effects of scale are characterised by mixing and oxygen transfer [171], with the latter more of interest for upstream operations than for a precipitation step.

Effective mixing was achieved via two mechanisms throughout the precipitation screening methodology; tip driven jet macro mixing initially to mix the system liquids, this was then sustained by orbital shaking at a controlled amplitude and frequency to maintain homogeneity and avoid particle settling.

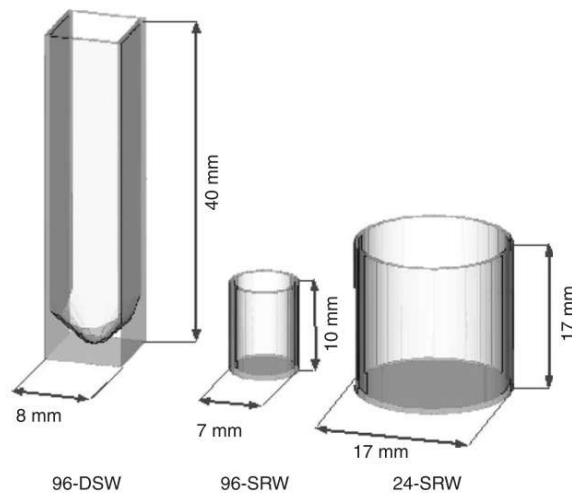


Figure 27. Schematic diagrams of individual micro-well formats.

Dimensions for 96-DSW deep square well, 96-SRW standard round well and 24-SRW standard round well [153].

Figure 27 reviews the main micro-well plate formats. For work carried out, V-shaped DSW (deep square wells) and flat-bottomed SRW (standard round wells) were the labware of choice. Larger 24 well plates were considered for precipitation experimentation, however with over

3mL working volumes multiple tip operations would be required to set-up and run reactions. The number of experimental conditions per plate is reduced whilst requiring the same material requirements.

3.4.1 Jet Macro Mixing

Jet mixing applies to micro-wells if the liquid system is viewed as a downward, vertical jet stream [172]. This can be used as an initial mixing stage, with the true ‘jet mixing’ only present during the dispense time span, which is a function of the volume and dispense speed in question. The objective is to achieve full macro-mixing of the liquid environment within this brief window. If micro-mixing is faster than macro-mixing then over-precipitation only becomes an effect at very high precipitant concentrations [173].

3.4.2 Calculating the Reynolds number through the tips

The starting objective was to achieve a minimum jet Reynolds number of 1,000 in order to reach conditions where effective jet macro mixing could be achieved within the time span of the dispense operation [172]. The Reynolds number describing the flow regime of the liquid passing through the liquid handling tips could be calculated as follows.

$$Re = \frac{Q_t \rho d_i}{A_t \mu}$$

Equation 3.1 The Reynolds number of tip mixing where Q_t is the volumetric flow rate through the tip (m^3s^{-1}), ρ is the liquid density (kgm^{-3}), d_i is the tip nozzle diameter (m), A_t is the nozzle aperture area (m^2) and μ is the liquid viscosity (Nm^{-2}s).

Calculations were based on assumptions of a liquid density of 1000kgm^{-3} , and viscosity of $0.001\text{Nm}^{-2}\text{s}$. The diameter of each tip /nozzle was 0.54mm. With a Reynolds value at 1×10^4 , $400\mu\text{Ls}^{-1}$ was found to be the minimum dispense speed, whilst liquid splashing and subsequent loss at dispense speeds in excess of $900\mu\text{Ls}^{-1}$ were regularly observed often irrespective of the solution characteristics, the best range would then be between these. The trade-off would therefore be between speed of operation and error due to even small liquid volume losses.

3.4.3 Calculating required mixing times with Jet Macro Mixing

$$t_{95} = \frac{4.48D^{1.5}h^{0.5}}{u_0d_i}$$

Equation 3.2 The estimation of mixing times in turbulent flow regimes, whereby t_{95} is the time in seconds for the system to be mixed to within 95% confidence limit (s), D is the diameter of the well or vessel (mm), h is the height of the liquid (mm), u_0 is the nozzle velocity (mms^{-1}) and d_i is the diameter of the nozzle (mm) [172][174].

By inputting the system characteristics it was clear that the t_{95} for conditions in both micro-well plates and deep-well plates was greater than the total jet time for both pure protein screening, whereby $\sim 50\mu\text{L}$ protein feed is added to $250\mu\text{L}$ precipitant and buffer, or for cell culture fluid where typically $215\mu\text{L}$ feed is added to $685\mu\text{L}$, since the jet stream had ended before the minimum time for complete mixing had occurred. This was also tested and observed with early studies using salt and PEG solutions in combination with blue food dye, where incomplete mixing could clearly be seen. The issue stemmed from the fact that the volume of feed added was too low. The option of dispensing precipitant, buffer and protein all at once in one tip operation was not desirable as the reaction times across the plate could vary as much as 30 minutes between wells and there was more risk of contaminating stock solutions by aspirating with an already loaded tip. A mix step was added after the feed addition to accommodate the earlier ineffective mixing. A “ $V_{80\%}$ rule” was implemented, with the tips mixing at both draw and dispense speeds of $600\mu\text{Ls}^{-1}$, of eighty percent of the well volume 3 times per well. 80% was the highest value which could be easily aspirated and dispensed in succession without creating bubbles which was suggesting formation of an unfavourable air-protein-liquid interface. A Reynolds number exceeding 1400 and a t_{95} was achieved in under 25% of each dispense (and if we consider mixing inside the tip, then aspirate too) operation time. This added only 5 minutes more to the overall process but ensured robust mixing. Fundamentally, these calculations were used to initially plan the mixing conditions tested and were a good benchmark to work with. Working with both 40% PEG and 4M Ammonium Sulphate, with the food dyes (red, yellow, green and blue, 25-50% v/v, Super Cook, Leeds)

similar to the studies by Nealon [172] modelling the protein feed, the conditions were finally chosen showed complete mixing by visual inspection. Since the most viscous conditions were tested, so there was additional confidence that these parameters would work universally.

3.4.4 Calculating the critical frequency of plate shaking for exceeding liquid surface tension

The critical frequency required to exceed a liquid's surface tension has been could be determined from the following equation [155]:

$$N_{crit} = \sqrt{\frac{\sigma d_w}{4\pi V_L \rho d_s}}$$

Equation 3.3 The critical shaking frequency, N_{crit} (rps) which can be calculated from the terms, σ the liquid surface tension of fluid (Nm^{-1}), d_w the diameter of the liquid system (m), V_L the total liquid volume (m^3), ρ the liquid density (kgm^{-3}) and d_s the amplitude or shaken diameter (m).

This equation allows for the calculation of the minimum shaking frequency required for the centrifugal forces to exceed liquid surface tension and achieve a more disruptive mixing regime. Above this critical frequency, liquid height will increase, along with the interstitial mass transfer area [180]. This does not necessarily imply turbulent mixing; this would need to be checked with Reynolds calculations; however, it is a useful tool for designing and controlling mixing conditions.

At small scale this equation does not take into account wall effects, which were found to increase the N_{crit} value by 2-fold based on experimental observations. For example, with 900 μL volume cell culture fluid precipitations in 96 deep square wells, operating at 600rpm 3mm magnitude was found to mix high salt solutions reliably with no excessive agitation (liquid loss through splashing). A coefficient could be added to the equation allowing for the input conditions to be successfully related to the N_{crit} value; and would probably be a function of V_L and d_w . This equation provided a good initial understanding of the impact of liquid characteristics had upon mixing regimes, however relying purely on these predictions resulted in non-turbulent mixing.

3.5 Micro-well centrifugation

The minimum centrifugation time was defined as the minimum time required for a precipitate particle to pass from the top of liquid layer in a micro-well to the base of the well, travelling at the speed through the liquid phase as calculated from Stoke's Law.

$$t_c = \frac{\ln\left(\frac{R}{R_0}\right) 18\mu}{(\rho_p - \rho_f) D_p^2 \omega^2}$$

Equation 3.4 Calculating the minimum centrifugation time required for effective particle separation.

With t_c the minimum centrifugation time for effective phase separation (s), R is the distance from the centre of rotation minus the liquid height (m), R_0 is the distance from the centre of rotation (m), μ is the liquid viscosity (Nm^{-2}s), ρ_p is the density of the particles (kgm^{-3}), ρ_f is the density of the liquid (kgm^{-3}), D_p is the average diameter of the precipitate particles (m) and ω is the angular velocity of the centrifuge (rad.s^{-1}) [25].

Equation 3.4 was derived from Stoke's law of settling, with the following assumptions; the acceleration and deceleration of the centrifuge is discounted, particles are spherical, a homogenous liquid density and viscosity is maintained throughout, a mean precipitate particle size is used and wall effects in the micro-wells are negligible. In the presence of gravity, the inertial acceleration is 9.81ms^{-2} , however if the particle is moving outward from the centre of rotation in a centrifuge then this g term is replaced by an angular velocity term and distance term. This takes into account the particles constantly moving outwards from the centre of rotation of the centrifuge. In principle, the greater the density disparity between precipitate particles and the liquid phase, the size of the particles and the centrifuge spin speed, the faster effective phase separation can be achieved.

This tool was initially used to understand the required centrifuge conditions to achieve good separation of the precipitate from the liquid phase. Precipitate particle average density was assumed to be 1300kgm^{-3} based on soya protein precipitate with an average particle diameter of $5\mu\text{m}$ [140], liquid density was assumed to be 1100kgm^{-3} , and a raised viscosity 0.01PaS . However, since no direct measurements of viscosities or densities were run during this work,

this remained a theoretical exercise. This predicted minimum centrifugation times of approximately 10 minutes for 300 μ L and 30 minutes for 900 μ L systems.

Practically for 300 μ L volume 96 well plate precipitations on pure protein, centrifuging the plates at 4000rpm for 30 minutes consistently achieved a greater than 99% clarification of the supernatant. For cell culture fluid, at typical well volumes of 900 μ L, plates were spun at 4000rpm for 60 minutes in order to achieve the same level of separation.

3.6 Micro-well dimensions and pathlength calculations

For Corning 96 well UV readable plates, there was a slight discrepancy between top and base radii, meaning non-cylindrical dimensions; it was worth checking the impact this could have upon experimental measurements:

$$V_{UV96wellplate} = \left(\frac{A_1 + A_2}{2} \right) h = 0.5h_b [(\pi r_b^2) + (\pi r_a^2)]$$

Equation 3.4 The volume of a flat bottomed micro-well (m^3) determined by A_1 the cross sectional area of top of well (m^2), A_2 the cross sectional area of base of well (m^2), r_b the upper radius of the well (m), r_a the base radius of the well (m), and h_b the height of well, (m)

For example, with a Flat Bottom well design, modelling wells as simple cylinders would result in a 7-8% inaccuracy in liquid heights or volumes for and in doing so would void the accuracy of pathlength calculations. All spectroscopy was carried out in 300 μ L volumes, mitigating error which could arise from variation from volumes and different well geometries. The same labware from the same manufacturer was used throughout.

3.7 Ionic Strength

Calculating the ionic strength of different precipitants allowed for direct comparison to be readily made across systems. The total ionic strength is the sum taken of all ions in solution, allowing for the direct comparison of different salts

$$I = \frac{1}{2} \sum_i z_i^2 C_i$$

Equation 3.5 Calculating total ionic strength, I (M) from the concentration of each ion (C_i) and its respective charge number (z_i).

The ionic strengths of the main salts under investigated have been plotted in Table 11, with the standard stock solutions and the corresponding stock ionic strengths shown as well. . For example, 1 molar ammonium sulphate has 3M ionic strength based on its constituent 2 NH_4^+ and 1 SO_4^{2-} ions. $I = 0.5 * ((1^2 * 2) + (2^2 * 1)) = 3\text{M}$ per 1 M ammonium sulphate. Or for lithium citrate, based on 3 Li^+ and 1 $\text{C}_6\text{H}_5\text{O}_7^{3-}$ ions; $I = 0.5 * ((1^2 * 3) + (3^2 * 1)) = 6\text{M}$ per 1M lithium citrate.

Table 11. Main salt precipitants investigated and their corresponding ionic strengths.

Salt	Cations	Anions	Ionic strength (M)	Stock solution (M)	Stock Ionic Strength (M)
Ammonium Citrate	3 x NH_4^+	1 x $\text{C}_6\text{H}_5\text{O}_7^{3-}$	6	4	24
Ammonium Phosphate	2 x NH_4^+	1 x PO_4^{2-}	6	4	24
Ammonium Sulphate	2 x NH_4^+	1 x SO_4^{2-}	3	4	12
Lithium Citrate	3 x Li^+	1 x $\text{C}_6\text{H}_5\text{O}_7^{3-}$	6	1.5	9
Lithium Phosphate	2 x Li^+	1 x PO_4^{2-}	3	1.5	4.5
Lithium Sulphate	2 x Li^+	1 x SO_4^{2-}	3	2.5	7.5
Potassium Citrate	3 x K^+	1 x $\text{C}_6\text{H}_5\text{O}_7^{3-}$	6	1	6
Potassium Phosphate	2 x K^+	1 x PO_4^{2-}	3	1	3
Potassium Sulphate	2 x K^+	1 x SO_4^{2-}	3	1	3
Sodium Acetate	2 x Na^+	1 x $\text{CH}_3\text{COO}^{2-}$	3	4	1
Sodium Chloride	1 x Na^+	1 x Cl^-	1	4	4
Sodium Citrate (tri)	3 x Na^+	1 x $\text{C}_6\text{H}_5\text{O}_7^{3-}$	6	2	12
Sodium phosphate (mono)	2 x Na^+	1 x PO_4^{2-}	3	4	12
Sodium Sulphate	2 x Na^+	1 x SO_4^{2-}	3	2	6

3.8 Volume measurement

A method to determine liquid volumes in micro-wells was required in order to effectively measure and perform a mass balance on the precipitation and the subsequent recovery by re-suspension of the precipitate in a new buffer system.

To measure the liquid volumes in each well, the absorbance readings of samples at 977nm were measured. Water is transparent from 200-900nm, yet has a distinctive absorbance peak at the near infrared end of the spectrum, with maximum absorbance at 977nm [176]. Hence absorbance values can be used as a base from which to equate liquid volumes. However, with high salt systems present there were two issues: firstly, path-length through the liquid in the well varied due to differences in surface tension [67] and secondly, highly saturated salt solutions could contain as little as 50mL water per 100mL solution. A set of calibrations were prepared to measure volumes of liquid with varying constituents:

$$\text{Volume in microwell } (\mu\text{L}) = \frac{\text{Absorbance at 977nm (AU)}}{\text{Specific solution correlation (AU} \cdot \mu\text{L}^{-1})}$$

Equation 3.7 The absorbance at 977nm (AU) can be equated to the volume of liquid in the micro-well (μL) by an experimentally determined specific solutions correlation of that solution ($\text{AU} \cdot \mu\text{L}^{-1}$).

300 μL total working volumes were throughout all experiments to standardise readings. Stock solutions were prepared, and pH adjusted by 0.1M NaOH/HCl to the conditions typically carried out in the main experiments, in order so as to be as representative as possible. Plates were designed using the Excel-Tecan design tool and prepared on the Tecan deck. Samples were mixed by 3x $V_{80\%}$ aspirate-dispense mix operations then maintained on the Te-Shake for 30 minutes before absorption readings were run on the plate reader. One issue to consider with 977nm measurements is that temperature can affect absorbance, but all measurements were taken with the same plate reader, in the same room with temperature control and no adverse results were seen which would necessitate a change in approach.

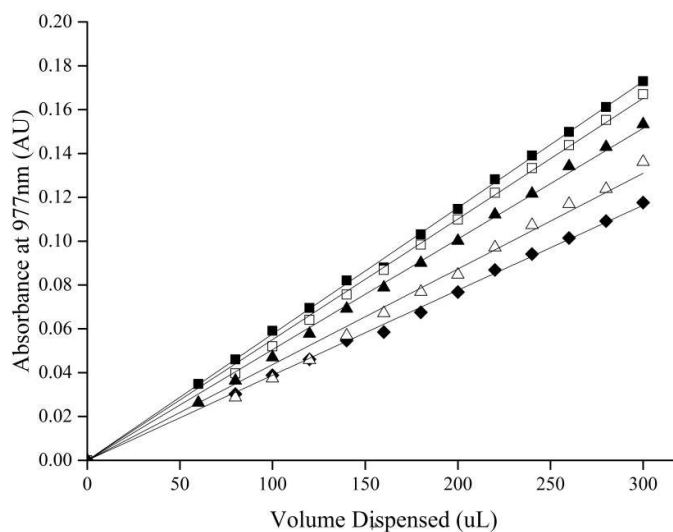


Figure 28. Solution absorbance at 977nm.

Water (■), 50mM phosphate buffer (□), 2.0M Sodium Sulphate (▲), 2.5M Lithium Sulphate (△) and 4.0M Ammonium Sulphate (◆). Volumes were dispensed through robotic liquid handling into 96 well Corning UV readable 96 well plates. All conditions were run in triplicate with the average value displayed, error bars not plotted for clarity.

Figure 28 and Table 12 show how solution properties affect the absorption of light at 977nm.

There is a significant level of variation in absorbance due to high salt saturations and meniscus curvature caused by the solute. For corning flat UV readable 96 well plates, volumes below 60µL could not accurately be measured as the liquid did not sufficiently cover the base of the micro-well and as such were unrepresentative.

This approach was mainly used to determine the volume of the re-suspended precipitate, since a fixed re-suspension buffer was added; there was variation in the residual liquid associated with the precipitate. For measuring volumes in the opaque 2ml V-shaped deep well plates, samples need to be transferred to UV readable plates to determine the liquid volume. The re-suspension buffer used throughout this thesis was a 50mM Phosphate buffer, so re-suspended protein solution volumes were calculated from that specific absorbance value (ϵ). This was based on the assumption that levels of residual salt in the precipitate did not adversely affect this value.

Table 12. A977nm specific absorption values for different solutions.

Liquid	ϵ_{977} (AU μL^{-1})
Water	5.76×10^{-4}
50mM Phosphate Buffer	5.51×10^{-4}
2.0M Sodium Sulphate	5.05×10^{-4}
2.5M Lithium Sulphate	4.37×10^{-4}
4.0M Ammonium Sulphate	3.88×10^{-4}
4.0M Ammonium Citrate	3.61×10^{-4}
1.0M Potassium Citrate	4.73×10^{-4}
4.0M Sodium Phosphate	4.14×10^{-4}
2.0M Sodium Citrate	4.36×10^{-4}
4.0M Ammonium Phosphate	3.60×10^{-4}

3.9 The impact of high salt solutions upon 280nm absorbance

Based on early observations that precipitants could interfere with measurements a set of experiments was run to understand the effect high salt concentrations had upon absorbance readings run in UV readable micro-well plates. UV absorbance at 280nm was used to determine protein concentration, so understanding the interference precipitant salt concentrations could have upon these absorption values was important for ensuring representative measurements. Absorbance at 977nm was run concomitantly to the 280nm readings to further understand the displacement of water by the dissolved salt and also to shed light upon absorption path-length; viscous liquids exhibit more meniscus curvature in micro-wells, reducing the distance light travels through the sample and thus reducing the overall absorption at the defined wavelength being tested.

300 μL total working volumes were run throughout all experiments to standardise readings. Stock solutions of 4M Ammonium Sulphate and 1.6M Tri-sodium citrate were prepared in 50mM phosphate buffer and adjusted to pH 7 with 0.1M HCl/0.1M NaOH, in keeping with standard precipitant preparation SOPs. A pH 7.0 50mM phosphate buffer was the diluent. Plates were designed using the Excel-Tecan design tool and prepared on the Tecan deck. Samples mixed by 3x $V_{80\%}$ aspirate-dispense mix operations then maintained on the Te-Shake for 30 minutes before absorption readings were run on the plate reader.

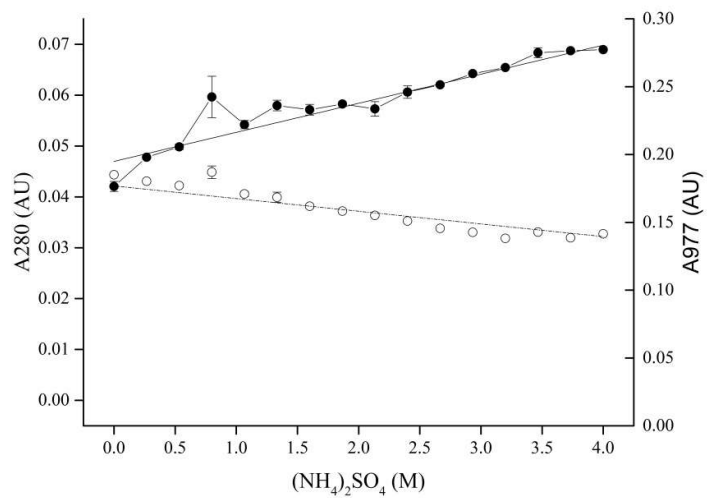


Figure 29. The effect of increasing Ammonium Sulphate concentration.

300 μ L total volume on 280nm absorbance (●) and 977nm absorbance (○). Points are the average of triplicate experiments with standard deviation plotted as error bars.

The ammonium sulphate concentration and 280nm linear relationship was calculated to be:

$$A_{280} = 0.00571[(NH_4)_2SO_4] + 0.04698, \text{ with an } R^2 \text{ value of } 0.986. \text{ Whilst the AS}$$

concentration and 977nm linear relationship was $A_{977} = -0.00934[(NH_4)_2SO_4] +$

0.17688 with an R^2 value of 0.925.

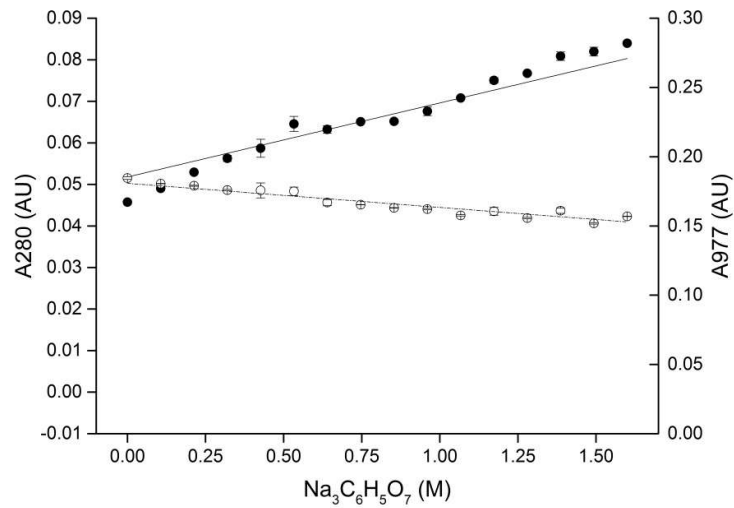


Figure 30. The effect of increasing Tri-Sodium Citrate concentration.

300 μ L total volume on 280nm absorbance (●) and 977nm absorbance (○). Points are the average of triplicate experiments with standard deviation plotted as error bars.

The Sodium Citrate concentration and 280nm linear relationship was: $A_{280} = 0.01782[\text{Na}_3\text{C}_6\text{H}_5\text{O}_7] + 0.0518$, $R^2 = 0.999$. The 977nm linear relationship for sodium citrate was: $A_{977} = -0.0174[\text{Na}_3\text{C}_6\text{H}_5\text{O}_7] + 0.1808$, $R^2 = 0.918$. A good linear fit was observed for both the absorbance at 280nm and 977nm with Ammonium Sulphate and Sodium Citrate. The 280nm results at 0.8M $(\text{NH}_4)_2\text{SO}_4$ are obvious outliers, possibly due to liquid handling or measurement errors. Looking at the same value for 977nm, the same outlier can be seen, so the change in 977 path-length indicates a liquid handling error.

For ammonium sulphate, the background absorption values at 280nm slightly increased. For example, at 2M $(\text{NH}_4)_2\text{SO}_4$ absorbance at 280nm increases by +25% from 0.047 to 0.058AU. Protein samples are normally read at between 0-1AU so this 10mAU increase could adversely affect readings depending on protein concentration. A similar trend can be observed for tri-sodium citrate, typical precipitations occur at 1M, so this would result in a background absorption increase from 0.0518AU to 0.0696 AU, a +35% increase. This issue only applies to samples measured from the high salt supernatants. The consequence of analysing protein concentration from the supernatant is that at higher salt concentrations there's typically a lower

protein present, so the potential error can be more significant. From the methodology, analysis of 1_{in}10 dilutions from the supernatant ensured the protein concentration kept within optimal range of the spectrophotometer. This has the combined benefit of reducing the salt concentrations by 90%, so a 2M Ammonium Sulphate precipitation would result in 200mM salt, which increasing background absorbance by +2.5%, and could be deemed to be insignificant to measurements, especially since other experimental errors could dwarf these small variances.

For re-solubilised precipitate samples, the salt concentration was already markedly reduced by removal of the supernatant, which was then compounded by 1_{in}10 sampling to hold protein concentrations within optimal absorption range. The higher salt concentrations are typically associated with higher re-solubilised protein concentrations, so the relative error would be further diminished.

When calculating protein concentration values from raw absorbance readings at 280nm, no additional calculations are deemed to be required to accommodate interfering agents. For new precipitants, it would be prudent to test if they interfere more strongly with testing techniques, but other than that no further action needs to be taken.

3.10 Precipitate recovery

To understand how the volume of buffer added to the solid precipitate at the base of the wells in the 96 well format affected its transition back into soluble form, a study looking at precipitate re-suspension was undertaken. Re-suspending protein in a smaller volume of liquid carries the advantage of reduced process volumes downstream; for salt-driven precipitate there will also be a higher residual salt concentration which may cause problems downstream of the process.

Recovery yields of greater than 95% can be achieved in micro-wells, provided only no more than 85% of the total volume is removed, however this leaves >15% of supernatant remaining with the precipitate resulting in greater impurities when applied to process feed-streams. Re-suspension in volumes of 50 μ L or greater are viable with a mixing regime of 3x V_{80%} tip mix

operations then orbital shaking at 900rpm for 30 minutes. For volumes of re-suspension buffer lower than 50 μ L, visible precipitates could still be observed following the re-suspension step. The maximum concentration of proteins would be 14.5 mg/ml in the 50 μ L re-suspension when considering the precipitate wet volume, so there is no question of protein solubility limits being exceeded. The conclusion to be drawn from this result set is that for protein recovery in small buffer volumes, a more comprehensive mixing and recovery regime needs to be instigated.

3.11 The Small Scale Precipitation Screening Methodology

This chapter has covered the modular steps taken to devise a micro-well format screening approach for precipitation, including suitable liquid class handling operations, and effective mixing. Suitable conditions for effective centrifugation, phase separation and precipitate re-solubilisation have all been identified. Utilising the Excel-Evoware Design Tool, conditions can not only be prepared rapidly with precision, but samples could be readily prepared for analysis including standards and controls. By combining this knowledge an automated high throughput screening methodology was devised.

Figure 31 shows the full methodology devised to characterise accurately precipitation. Liquid handling and robotic arm movements were carried out using a Freedom EVO® series platform (TECAN, Reading, UK). It details the systematic approach whereby precipitations are carried out, precipitate and supernatant are separated and subsequently analysed using a variety of techniques to assess performance.

For testing on pure protein, 300 μ L volumes in 96-well flat bottom Costar® UV Micro-well plates were run and for cell culture fluid investigations 900 μ L volumes in Corning 96 well 2mL, V-bottom deep well plates were selected. The Excel-Evoware design tool was used to control the conditions generated in each micro-well plate with different combinations of stock solutions. Different stock solutions were typically aspirated in one go and initially mixed

through the dispense operation followed by a $3 \times V_{80\%}$ mix operation. The diluent was always aspirated first, as this meant it could be used to flush out any viscous fluid subsequently aspirated and ensure accurate results. It was important to pre-mix the liquids before addition of the protein feed as this meant no localised areas of poor mixing were present which could have adverse effects upon the protein upon addition. Protein feed was then dispensed across the plate and the system was mixed through tip-mixing followed by sustained orbital plate shaking for 30 minutes at 3mm magnitude, 900rpm. Plates were then centrifuged at 4,000 rpm for 30 minutes with the 300 μ L volumes and for 60 minutes with the 900 μ L volumes.

Following phase separation, supernatant was analysed via A280nm or PrA HPLC to measure the soluble IgG₁. Clarification efficiency could also be determined at A600nm and samples could also be taken for analysis by SDS-PAGE or with the Bioanalyzer. Precipitates were re-suspended in a suitable volume of pH 7.0 50mM phosphate buffer and mixed through $3 \times V_{80\%}$ tip mixes and up to 30 minutes of sustained orbital plate shaking.

Re-suspended material could then be measured at A600nm to check the extent of re-solubilisation of the precipitate; this was constrained to UV readable plates, so not applicable for cell culture fluid evaluations in the 2mL, V-bottom deep well plates. Re-suspended samples were then transferred to new plates via gwl scripts to prepare plates including controls and standards for all relevant plate-based analysis. Two plates run in staggered operations including initial spectroscopic analysis could be run in under three hours. More detailed assays proved to be the rate limiting steps and were typically queued up and run overnight.

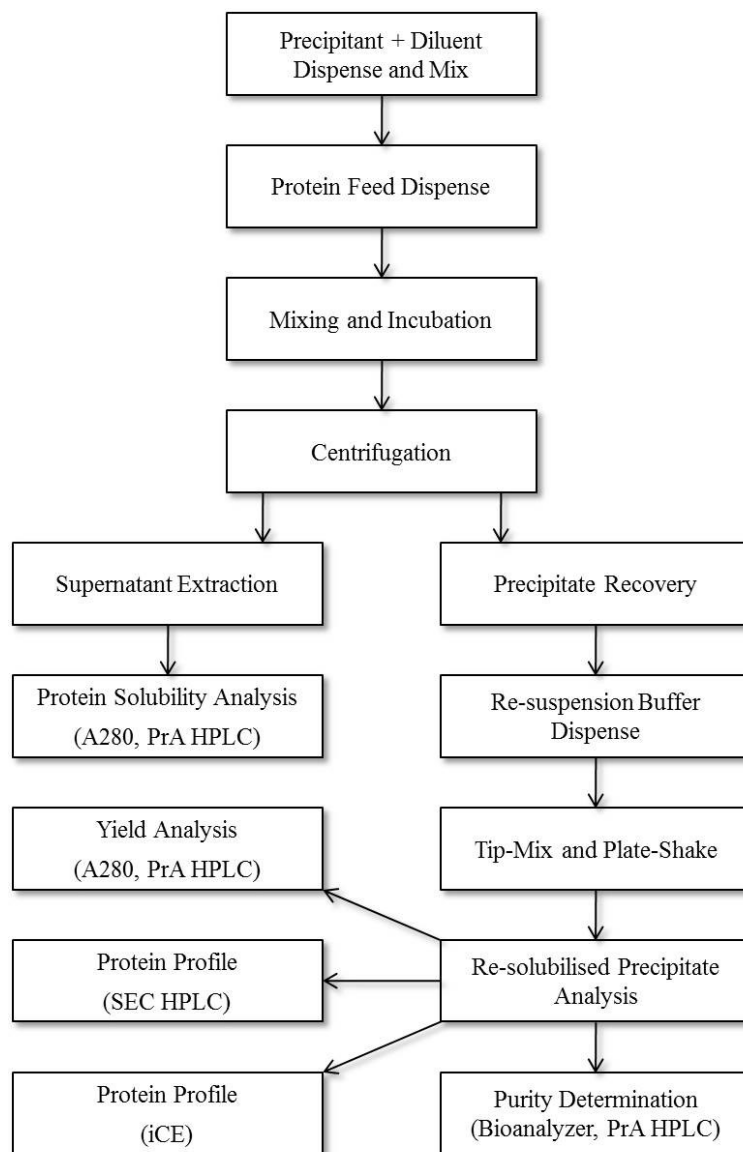


Figure 31. The high throughput screening methodology.

Precipitation, recovery, re-suspension, and analytics were all performed in a 96 well format.

3.12 Chapter Summary

Liquid handling systems require a sizeable investment, with basic systems costing in excess of £100k; this figure can be much higher with added modular components such as plate readers, mixing systems and centrifuges as a premium is charged to incorporate third party products through custom fittings and device driver software. The best way to assess the merits of automation may be to look at the relative throughputs of a system with an operator versus three or four laboratory workers running the same work.

The time taken firstly to build up expertise and then write scripts to operate liquid handling systems also needs to be considered. Software such as Tecan's Evoware is logical and intuitive to run, with training courses and expertise readily available, yet developing protocols can be time-consuming. The decrease in experimental runtime that automation offers should be countered with the time taken to program the system and validate the protocol. Therefore, automating experiments should really be focussed on high frequency runs where net time savings can be made, not for assays maybe run once or twice a year. This is rather simple to state, but with the shift towards more and more process automation, the quick test of "is this worth it?" should be held at the forefront of the mind during early process development, to avoid the temptation of overcomplicating experiments and actually slowing down progress. For new experimental approaches, comparing results to standard practice and ensuring alignment may not always be simple; incongruences between the two may actually highlight questions about the accuracy of the either test which may not be welcome!

With the methodology foundations built, this leads onto Chapter Four, where studies on the precipitation of purified IgG₁ are carried out.

Chapter Four: Precipitation Screening

“Science is composed of laws which were originally based on a small, carefully selected set of observations, often not very accurately measured originally; but the laws have later been found to apply over much wider ranges of observations and much more accurately than the original data justified.”

Richard Hamming- The Unreasonable Effectiveness of Mathematics,

4.1 Abstract

The work presented in this chapter investigates how precipitation could be applied to the purification of monoclonal antibodies. Screening and characterisation work was carried out on a pure IgG1 feedstock leading to selection of the best precipitants to bring forward for further evaluation. The impact of precipitant concentrations, system pH, ionic strength and protein concentration were studied and in doing so built up a good framework of understanding of how to control yield and recovery of precipitation. Protein function and activity were found to be unaffected under all conditions tested. Crucially, precipitation conditions were successfully linked to process relevant cell culture fluid meaning the knowledge built up on pure protein models could accelerate process development through simplifying assays and speed of experimentation.

4.2 Introduction

The first experimental stage of this project was to screen for precipitants in order to determine which performed best for the recovery and purification in downstream processing. Based on the review of precipitants in Chapter 1, select candidates from the following categories were considered: neutral salts, non-ionic polymers, acids, alcohols and polyelectrolytes. Affinity ligands were disregarded since ligands would require synthesising and designed to be pH or

thermo-responsive, which could be a whole project in itself. Screening was run on a fully purified IgG₁, which been through UCB's full platform purification of 3 chromatographic separations.

Pure protein studies were run so that basic information could be quickly acquired such as whether a material could induce precipitation and how effective was it, in terms of reducing protein solubility, precipitate formation, recovery and re-suspension of the starting material. Using a simplified, non-process feed-stream meant absorbance spectroscopy could reveal key information without complication from host cell proteins, media and DNA. The disadvantage being that the selectivity and purity afforded by precipitation wasn't clear, nor could the screening identify suitable negative precipitants. All screening results were carried out using the high throughput screening methodology detailed in Chapter 3. A hierarchical screening approach was undertaken, with quick and simple assays run on the largest sample set, with more expensive, time intensive assays assigned to the most relevant conditions, as shown in Figure 32. The first stage was to determine if the material tested precipitated and recovered the protein, this was done by looking for visible solid precipitate formation and measuring the solids absorbance at A600nm. Measurements were often also run at A340nm as a quick check for sub-visible aggregates.

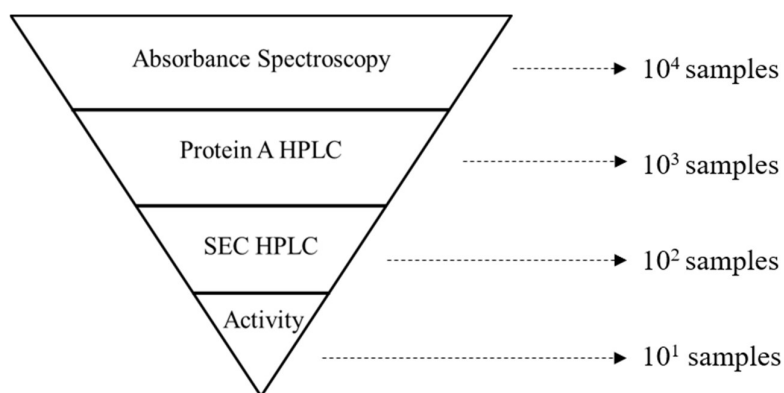


Figure 32. Analytical approaches used in a hierarchical screening approach, with number of conditions tested at each level shown.

Analysis by Protein A affinity HPLC could then be run on successful precipitation conditions as a crude check for retention of protein structure by measuring the bound IgG₁ and hence retention of the structure of Fc region of the immunoglobulin. Size exclusion chromatography could also quantitatively measure yields, but this technique was employed to check the monomer and aggregate profile of samples. Finally select conditions could be taken and checked to see if the activity of the protein was retained.

4.3 Initial Screening

A range of different potential precipitants were tested in a broad screening exercise. Near-saturated stock solutions were made up of each candidate, to as high a concentration as possible so that a full range of concentrations could be explored. Running experiments in micro-wells with automated liquid handling facilitated testing of a wide range of concentrations. This avoided the risk of missing conditions which could lead to precipitation, for example in the case of polyelectrolytes an excess concentration can reduce protein aggregation, with low concentrations optimal [102].

For systems with a pH between 4 & 6, a 50mM acetate buffer was used, for 6-8 it was a 50mM phosphate buffer, and alkaline conditions above pH 8 were buffered with 50mM Tris-HCl. In hindsight these buffers should have all been adjusted so that they have equal absolute ionic strengths, however this was realised later in the project and when taking into account the high molarities of neutral salts involved in most experiments the difference could be regarded as negligible. Since many new chemicals were screened with little starting knowledge it was likely a lot of non-ideal conditions were used. Stock solutions were buffered to pH 7 unless otherwise stated; this was in order to fix a reference point. The risk being that a candidate may not show any indication of precipitating at this neutral pH, and its potential may be missed. However, running every screening experiment under a larger range of parameters would have required a significant increase in time and materials. IgG₁ concentrations were also fixed; 0.5mg/mL was set as the concentration to screen candidates against, based on a starting

2mg/mL titre set to a maximum realistic precipitant to feed dilution of 3:1 v/v. Higher protein concentrations are expected to precipitate more readily, so again there was the issue of missing precipitants which may have worked at higher concentrations.

Table 13. Screening results table on pure protein

Precipitant	Stock	Range Explored	System pH	Precipitation	Precipitation Yield	Recovery Yield
Ammonium Citrate	2M	0-1.6M	7	+	100%	80%
Ammonium Formate	6M	0-5M	7	-	-	-
Ammonium Phosphate	4M	0-3.29M	7	+	100%	80%
Ammonium Sulphate	4M	0-2.67M	7	+	100%	80%
Calcium Sulphate	10mM	0-8mM	7	-	-	-
Copper Sulphate	1.2M	0-1M	5	-	-	-
Lithium Citrate	1.5M	0-1.2M	7	+	100%	80%
Lithium Phosphate	2M	0-1.6M	7	+	100%	80%
Lithium Sulphate	2.5M	0-2.1M	6.15	+	100%	80%
Magnesium Sulphate	1M	0-830mM	7	-	-	-
Nickel (II) Sulphate	4M	0-3.2M	4.45	-	-	-
Potassium Chloride	4M	0-3.2M	7	-	-	-
Potassium Citrate	1M	0-800mM	7	+	85%	70%
Potassium (di) phosphate	1M	0-800mM	9	-	-	-
Potassium (mono) phosphate	4M	0-3.5M	5	+	100%	80%
Potassium Sulphate	1M	0-850mM	7	-	-	-
Silver Nitrate	0.1M	0-83mM	4.8	+	100%	0%
Sodium Acetate	4M	0-2.67M	7	-	-	-
Sodium Chloride	4M	0-2.67M	7	-	-	-
Sodium Citrate	1.5M	0-1M	7	+	100%	80%
Sodium Formate	6M	0-5M	7	-	-	-
Sodium mono Phosphate	4M	0-3.5M	5	+	-	-
Sodium Sulphate	2M	0-1.6M	7	+	100%	80%
Zinc Iodide	1M	0-1M	4.45	+	100%	0%
Zinc (II) Sulphate	2M	0-1.6M	7	-	-	-

Table 13 summarise the screening results for different salts. The list was chosen based on a combination of salts already established in the literature to work and also combinations which were up to now untested. Stock solutions were made up based on expected solubility from material factsheets where available and by trial and error when not. A range of alcohols, non-ionic polymers and polyelectrolytes were screened in addition to salts.

Ethanol, methanol, N-butanol, and N-propanol were all tested up to ~35% v/v against 0.5mg/mL IgG₁. These systems were not buffered. There was no indication of protein aggregation by A600nm nor A280nm, however conditions were tested under ambient conditions, and typical alcohol precipitations are run at 0-4°C to mitigate against temperature linked denaturation [132]. This avenue of investigation was stopped early on since temperature control on the liquid handling platform wasn't available at the time and low operating temperatures were never ideal when considering large scale bioprocess applications.

Based on earlier work on both Fab' and HEWL, Polyethylene Glycol between molecular weights PEG 100 to PEG 20k was screened. PEG 3350, 4000, 6000 and 8000 all precipitated, and led to the successful re-solubilisation of IgG₁. Compared to salt-driven precipitation several difficulties became apparent. Firstly, the high viscosity of the PEG systems made liquid handling difficult, requiring longer and more complex transfer and mixing regimes. Secondly centrifugal separation between the solid and liquid phases required double the time to achieve effective separation (clarification >99%), due to the increase in ρ_l , the density of the liquid phase. Finally, the precipitate was much denser, possibly due to the increased centrifugation but more likely attributable to the mode of preferential dehydration through non-ionic polymer precipitation and hence compactness of the precipitate. Longer re-suspension times were required combined with more vigorous mixing regimes.

Screening plates investigating acid driven precipitation such as with trichloroacetic acid (TCA), perchloric acid, and citric acid on pure protein produced precipitation curves only at low pH values <pH 3 (between concentrations of 10-100mM) and this was irreversible

precipitation based on denaturation. This indicated that these were ineffective positive precipitants at least for the tested molecule, but there may be scope for impurity removal. HCPs and impurities such as DNA may be removed by an initial negative acid precipitation step, clearing up the feed-stream for a better performance positive precipitation step afterwards. Caprylic (octanoic) acid effectively precipitated and led to the recovery of IgG₁, however only provisional testing was carried out. Caprylic acid is an organic phase liquid and difficulties were had in successfully buffering small volume emulsions for micro-well work whilst maintaining homogeneity and accurate liquid handling. The decision was made not to investigate further as salt driven precipitation was a more interesting avenue to explore at the time.

Zinc Iodide was tested manually using pipettes and disposable plastic tips since the material safety data sheet (MSDS) stated it was corrosive to metals, including the robotic liquid handling tips. It was selected since zinc ions had been shown to precipitate some proteins, and the material was already available in the laboratory. The bright orange solution was acidic at pH 4.8 in 1M saturation, and instantly produced fluffy, dispersed precipitates upon mixing. This eluded to denaturation of the polypeptide, which was then backed up when the recovered precipitate did not re-suspend in a range of buffers tested. It gave little indication of being useful for negative precipitation of impurities given how readily it crashed soluble immunoglobulins out of solution, and poor material compatibility meant this candidate was discounted quickly.

Nickel Sulphate, NiSO₄ was screened based on the sulphate anion and its use in polyhistidine tagging of polypeptides. The green solution showed no indication of aggregation. Blue copper II sulphate, CuSO₄ and clear ZnSO₄ confirmed that transitional metal salts of sulphate don't precipitate proteins or at the least the IgG₁ under investigation. The identifying of chemicals which don't induce precipitation can still provide valuable information. Silver Nitrate was screened and found to form very fine cloudy white protein precipitates at concentrations above 5mM, much finer than observed with salt-driven approaches. Precipitates could be easily

recovered by centrifugation but could not be re-suspended into solution. This was expected since it is a toxic, oxidising agent but serves as a reminder that most precipitation has a negative connotation, leading to denaturing pathways.

4.4 Precipitation by salting-out

Fractions of IgG₁ removed from supernatants were calculated by sampling the supernatant concentration and subtracting this value from the starting concentration. Figures shown in this chapter should be considered as *apparent* fractions since the fraction of IgG₁ removed from the supernatant can sometimes be a negative value, this is due to measured protein concentration from the supernatant sampling (with a 1in10 dilution) exceeding that of the input. Attributable errors would be from sampling, dilution, and measurement. These negative values are often seen before the precipitation transitional curve and do not affect key calculations.

For all purified IgG₁ screening in UV microplates, recovery yields up to 80% are recorded. The protein loss was where a small disc of protein was removed in the final supernatant aspirate by the robotic tips. Manual removal in several experiments and full analysis of supernatant and precipitate fractions showed a complete mass balance, so this reduction in yield was merely an artefact of using robotic tips to remove liquid. The onus was to reliably generate material for analysis, which the automated methodology succeeded in doing.

Several precipitation curves are shown, typical of the results generated in Table 13.

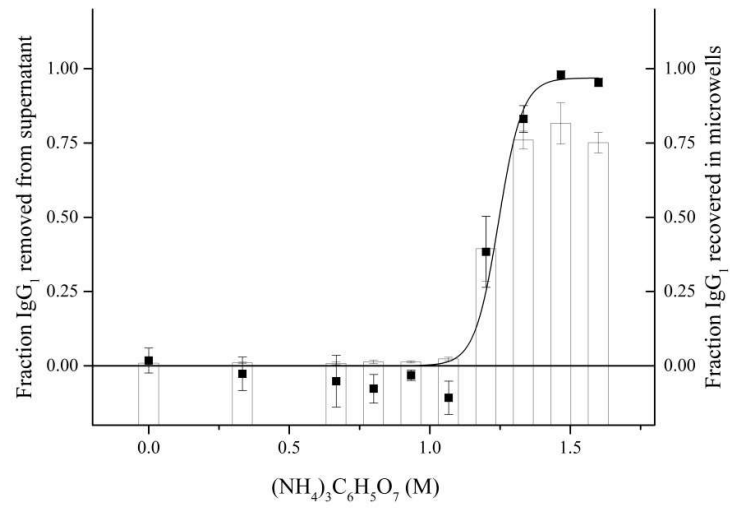


Figure 33. Ammonium Citrate profile for the precipitation of IgG₁.

Fraction IgG₁ precipitated out of solution (■) and the subsequent centrifugal recovery (bars). 0.5mg/mL IgG₁ at pH 7.0 under ambient conditions.

Large crystalline ammonium citrate salts readily dissolved into solution. As depicted in Figure 33, precipitation initiated at 1.1M and complete removal of protein was achieved at 1.4M. Complete re-suspension of the solid precipitate occurred within the first 5 minutes of addition of buffer.

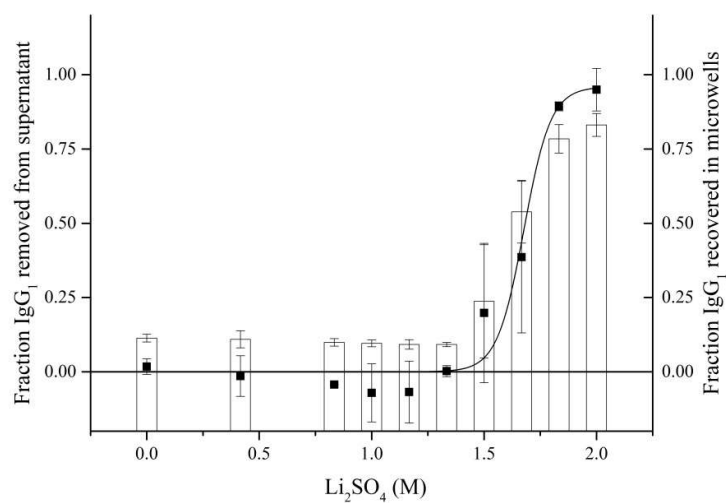


Figure 34. Lithium Sulphate profile for the precipitation of IgG₁.

Fraction IgG₁ precipitated out of solution (■) and the subsequent centrifugal recovery (bars). 0.5mg/mL IgG₁ at pH 6.25 in non-buffered conditions.

Lithium sulphate could be made up to 2.5M in solution, provided no buffer system was used. Any attempt to buffer the system caused the salt to crash out of solution and create a fine, white cloudy solution. This makes lithium sulphate non-ideal as a precipitant if pH control is important; it was measured to have a natural pH between 6.15-6.25 depending on concentration so within the 'kind' conditions spectrum. This incompatibility with buffer systems was also an occurrence with the citrate and phosphate anions of lithium cation.

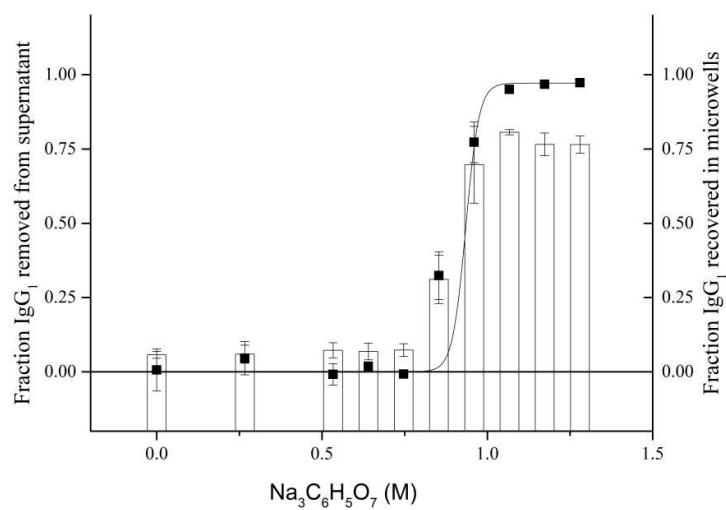


Figure 35. Tri-Sodium Citrate profile for the precipitation of IgG₁.

Fraction IgG₁ precipitated out of solution (■) and the subsequent centrifugal recovery (bars). 0.5mg/mL IgG₁ at pH 7.0 under ambient conditions.

Tri-sodium citrate was readily soluble up to 2 molar, in water creating systems between a pH of 8 to 8.15 and could be buffered. Completely soluble protein was achievable up to 0.9M, transitioning to completely insoluble protein at 1.1M as shown in Figure 35. Precipitates were recoverable dissolved readily into the re-suspension buffer.

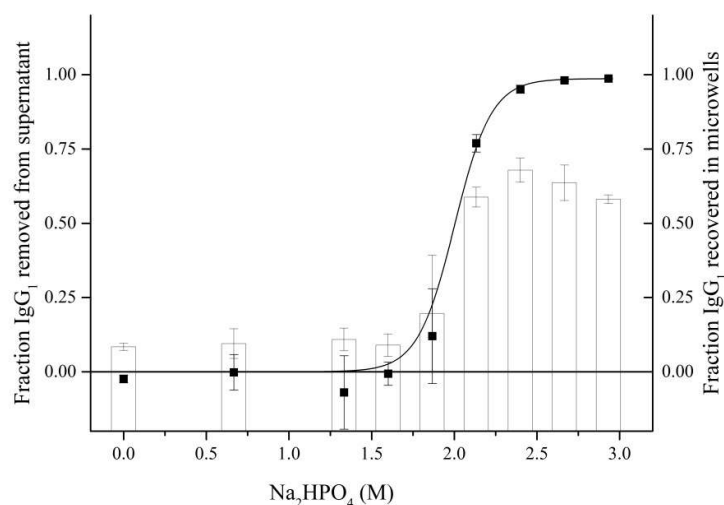


Figure 36. Sodium (mono) Phosphate profile for the precipitation of IgG₁.

IgG₁ precipitated out of solution (■) and the subsequent centrifugal recovery (bars). 0.5mg/mL IgG₁ at pH 7.0 under ambient conditions.

Typically used in phosphate buffer systems, Na₂HPO₄ was tested along sodium di-hydrogen phosphate NaH₂PO₄. Sodium di-hydrogen phosphate exhibits a markedly reduced solubility in water, around 1M and gave no indication of protein aggregation, however the monophosphate could be made up to 4M saturation and initiated precipitation above 1.75M.

4.5 The effect of protein concentration upon precipitation performance

One of the first parameters to understand is how the presence of different quantities of soluble protein affects its propensity to precipitate. There was an expectation for higher concentrations of proteins to exhibit reduced solubility in the presence of a precipitant based on previous work in the department [65][156]. A set of studies were undertaken to understand and quantify precipitation performance with varying protein concentrations for the IgG₁ under investigation and seeing how performance could be predicted based on the observations made.

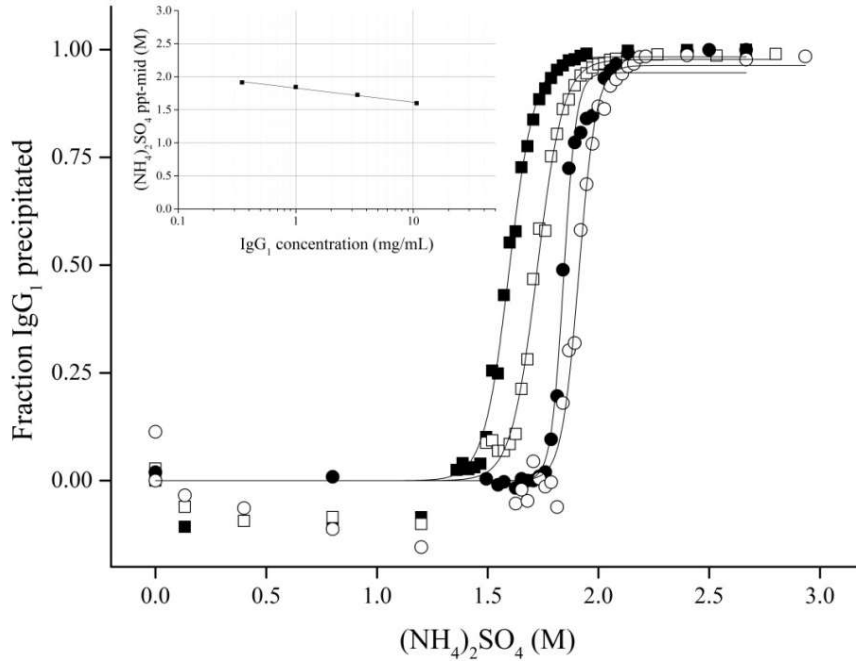


Figure 37. Ammonium sulphate precipitation profiles at different final concentrations of purified IgG1.
 IgG1 concentrations of 10.7mg/mL (■), 3.35mg/mL (□), 1.0 mg/mL (●), and 0.35 mg/mL (○) were all run under 32 incremental concentrations, in triplicate with the average values plotted.

The first study was run with 4 plates of 32 incrementally increasing ammonium sulphate (AS) concentrations run in triplicate. Two stock solutions of 4.0M and 0.8M ammonium sulphate were used allowing for a high-resolution experimental layout designed to capture the full curvature of the precipitation profiles. Early screening had already given an indication of where the precipitation curves for each concentration of protein may lie, so more data points were focused on the predicted regions, which as can be seen in Figure 37 was achieved very well. Again, the experimental artefact of ‘negative’ fractions precipitated between molarities of 0 and 1.5M AS, this was due to 5-10% more protein detected in the top 30µL sample taken post centrifugation, often observed with the much lower concentrations of protein studies, where experimental error can account for a much greater share of the A280nm absorbance values. Precipitation profiles were corroborated by A600nm measurements recording solids detected. There was a strong correlation between protein concentration and precipitation curves generated with ammonium sulphate. Across the concentrations tested, the ppt-mid

points change more than 300mM $(\text{NH}_4)_2\text{SO}_4$ across a 30x change in final protein concentration. The inserted graph in the top left of Figure 37 plots the log concentration of the starting IgG_1 against the calculated precipitation midpoints generated from the main dataset.

$$AS_Ppt_Mid = 1.83 - \log[\text{IgG}_1]^{0.214} \quad R^2 = 0.942$$

Equation 4.1 The relationship between the concentration of IgG_1 in solution and the precipitation mid-point, where 50% of protein is in both the soluble and insoluble state. Conditions were run under ambient temperatures, at pH 7.0.

The second experimental run was with tri-sodium citrate with 5 plates of 32 incrementally increasing concentrations run in triplicate; an additional plate was added to look at lower concentration for the cost of very additional little material and extra experimental time.

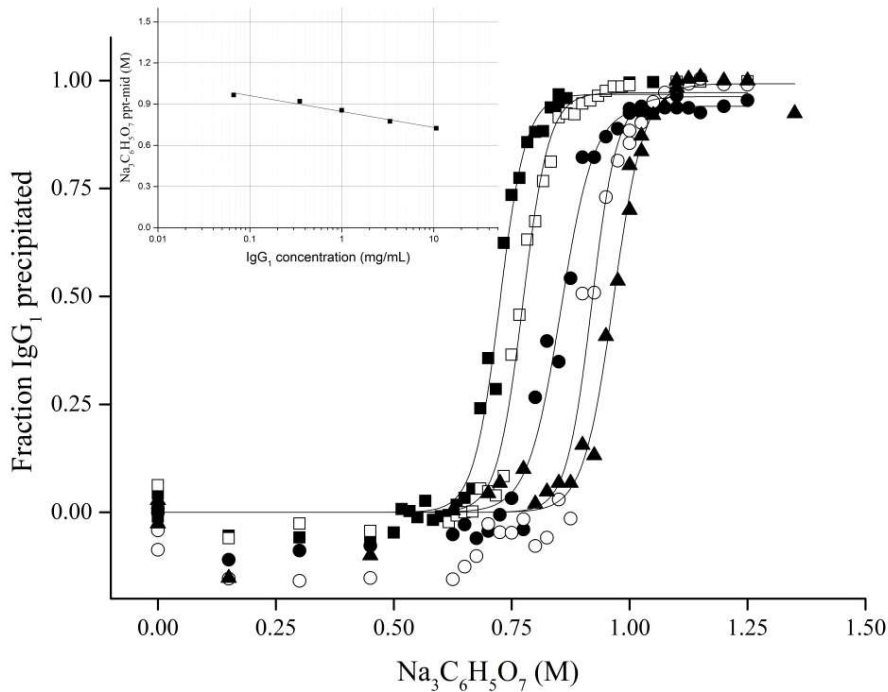


Figure 38. Tri-sodium citrate precipitation profiles at different final concentrations of purified IgG_1 .

IgG_1 concentrations of 10.7mg/mL (■), 3.35mg/mL (□), 1.0 mg/mL (●), 0.35 mg/mL (○), and 0.067 mg/mL (▲) were all run under 32 incremental concentrations, in triplicate with the average values plotted.

Across the concentrations tested, the ppt-mid points changed more than 250mM $\text{Na}_3\text{C}_6\text{H}_5\text{O}_7$ across a 150x change in final protein concentration. The inserted graph in the top left of Figure 38 plots the log concentration of the starting IgG_1 against the calculated precipitation midpoints generated from the main dataset.

$$\text{NaCit_Ppt_Mid} = 0.846 - \log[\text{IgG}_1]^{0.116} \quad R^2 = 0.970$$

Equation 4.2 The relationship between the concentration of IgG_1 in solution and the precipitation mid-point, where 50% of protein is in both the soluble and insoluble state. Conditions were run under ambient temperatures and at pH 7.0.

Again, for this second experimental set looking at a different precipitant salt, the same trends can be observed; the required precipitant concentration is inversely proportional to the log of the immunoglobulin concentration in solution. Developing a universal trend for salt driven precipitation does not seem possible however, since as the Hofmeister series predicts, the variation in each ion's salting out capability means that trends can only really apply to the specific entity under investigation.

The final experiment looking at protein concentration was carried out across 12 concentrations. This was determined by running 8-point precipitation titration curves in triplicate on 3 sets 96 well plates. This demonstrated that the same information could be acquired from fewer salt conditions, but more process change conditions, in this case the IgG_1 titre. Good fits for each sigmoidal precipitation curve were achieved and this ensured representative $[A]_{1/2}$, precipitation midpoints which could be plotted against protein concentration as depicted in Figure 39. Midpoints are solely plotted against concentration as displaying all the precipitation curves would impede brevity and clarity.

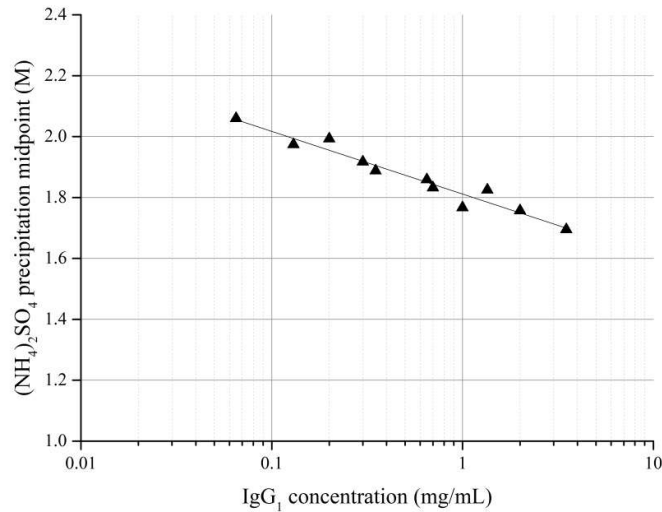


Figure 39. Ammonium sulphate precipitation mid-points against a log plot of IgG₁ concentration.

$$AS_Ppt_Mid = 1.81 - \log[IgG_1]^{0.206} \quad R^2 = 0.945$$

Equation 4.3 The relationship between the concentration of IgG₁ in solution and the precipitation mid-point, where 50% of protein is in both the soluble and insoluble state. Conditions were run under ambient temperatures.

Near identical fitting of the log plots relating ammonium sulphate precipitation midpoints and protein concentration between Figure 37 and Figure 39 indicates that as long as the precipitation curve is correctly captured by experimental points, the best approach to characterising changes in process conditions upon performance may be to run lower number titration curves on a greater number of variables. The range of concentrations studied was the expected range which a precipitation step may be expected to perform at. Concentrations above the 10.7mg/mL tested are expected to follow the model, considering future titres.

Precipitation performance can be predicted if the protein concentration is known. In Chapter 1 it was stated that amount of precipitant to achieve protein isolation and recovery is proportional to the volume of the system, and not linked to the mass of the product as with chromatographic separations. At higher titres, improved performance and throughput can be

expected, as the required volume of the system per mass unit of product effectively decreases whilst requiring reduced precipitant to achieve the same yield. How this will translate to complex protein feed conditions remains to be seen; protein-protein interactions (PPI) between the product and host cell proteins (HCPs) may not give as clear cut a trend as observed with pure protein systems, so it will be interesting to see how impurity fractions perform.

4.6 The effect of pH upon precipitation performance

How the pH of solution affected the solubility profiles of IgG₁ against a precipitant was the next key parameter to explore. As covered in Chapter 1, it is expected for there to be a reduction in protein solubility as conditions approach its isoelectric point (the pI of this IgG₁ was 8.7). Eight-point titrations of ammonium sulphate in triplicate were run for buffered conditions of pH 5, 6, 7, and 8. All feed, buffer and ammonium sulphate stocks were buffered in 50mM phosphate buffer with pH 5 maintained with a 50mM acetate buffer. Good curve fittings were achieved for each dataset and the midpoints were then plotted against pH.

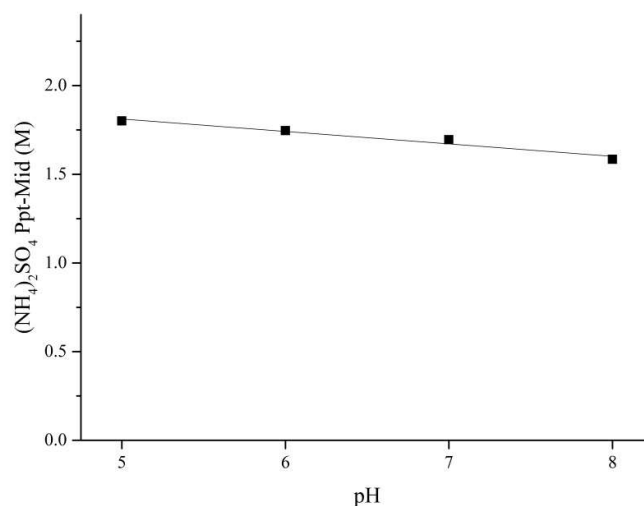


Figure 40. The impact of pH upon the precipitation performance of ammonium sulphate.

IgG₁ concentration at 0.5 mg/mL. Precipitation midpoints were determined to be 1.801 M for pH 5.0, 1.746 M for pH 6.0, 1.695M for pH 7.0 and 1.584M for pH 8.0. pH has a notable impact upon ammonium sulphate precipitation performance.

The results displayed in Figure 40 show a decrease in the precipitation midpoints as the pH of the system approached the pI of the protein. It would have been interesting to investigate more alkaline conditions; however ammonium sulphate is prone to releasing ammonia above pH 8 and this was an operational constraint. An alternative salt system should possibly have been used, but AS was selected since it was the well-characterised system available at the time.

A second experiment was carried out looking at higher pH conditions with sodium sulphate, a salt more suitable for alkaline conditions. A pH range between 7.0 & 8.5 was investigated in 0.25 pH unit increments. All feed, buffer and ammonium sulphate stocks were buffered in 50mM phosphate buffer.

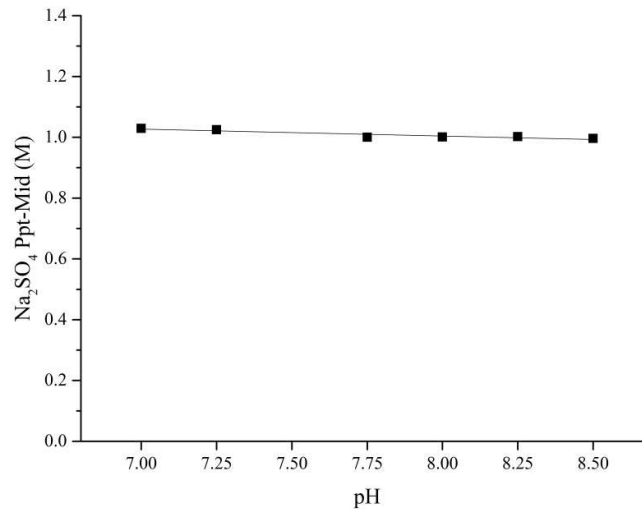


Figure 41. The impact of pH upon the precipitation performance of sodium sulphate.

IgG₁ was tested at 0.5 mg/mL. pH 7.5 is missing due to a liquid handling error, meaning an accurate precipitation transition curve could not be generated, the trend is clear and obvious. pH has no notable impact upon sodium sulphate precipitation performance.

In Figure 41, the pH of the system was found to have no effect upon performance of sodium sulphate precipitation. A 3% decrease in the precipitation midpoint between pH 7.0 and 8.5 can be disregarded as noise. The precipitation curve for pH 7.5 was a poor fit and so discounted from the results set. This result was unexpected, as it would appear sodium sulphate performance is unaffected by the pH conditions. Being pH independent makes the salt system more robust and reliable for process feed variability, however there is limited scope to reduce salt concentrations under optimised conditions. Either way additional work would need to be run to investigate further.

4.7 Assessing the impact of different sodium salts upon precipitation.

A study was run to understand how three different sodium salts impacted upon protein precipitation with respect to the ammonium sulphate salt. Previous work on Fab' and ADH has shown that the addition of sodium chloride decreased the observed transition midpoints for ammonium sulphate between 0.5-0.8M AS /M NaCl [65] inferring that sodium chloride displays 50-80% of the salting-out capacity of ammonium sulphate. This initially seemed quite high, as from early screening experiments sodium chloride was not found to promote protein aggregation in concentrations tested up to 3.2M (which, based on a 1.6M ammonium sulphate benchmark, a 50-80% capacity would predict this to occur between 2-3.2M NaCl). Work looking at acetate or citrate ions had not been previously undertaken. This study was run in order to greater understand both the standalone and potential synergistic effects sodium chloride, sodium acetate and tri-sodium citrate could exhibit.

The precipitation screening methodology was run on purified IgG₁ at a final concentration of 3.35mg/mL, with all systems buffered to pH 7.0. Eight point ammonium sulphate concentrations were run in triplicate for each specified sodium salt concentration. The sigmoidal fitting was applied and from this precipitation mid-points for ammonium sulphate were generated for each set. These were then plotted against the sodium salt concentration, in order to give an indication of trends and how the protein solubility characteristics changed.

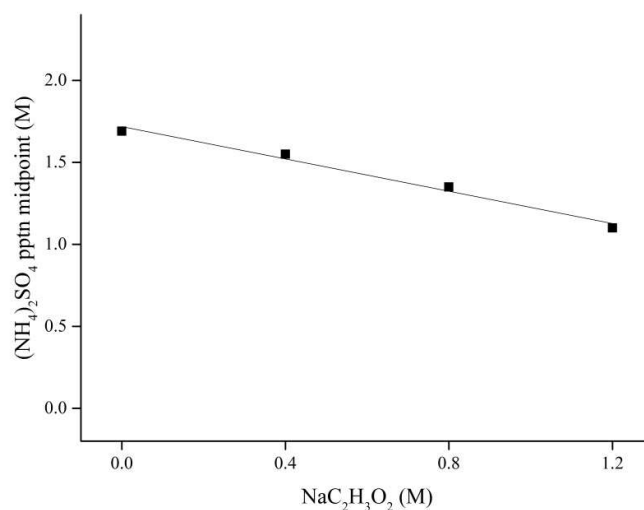


Figure 42. The impact of sodium acetate upon the precipitation performance of ammonium sulphate.

Under conditions of pH 7.0, IgG1 final concentration at 3.35 mg/mL. Ammonium Sulphate precipitation midpoints were found to decrease at $-0.493[\text{Sodium Acetate}]$, $R^2 = 0.977$. This was based upon 8-point triplicate precipitation curves run at 0, 0.4, 0.8 and 1.2M sodium acetate with precipitation midpoints generated from the sigmoidal fitting equation.

Using ammonium sulphate as the precipitation *gold standard* reference, sodium acetate could be described as exhibiting ~49% of the salting-out efficiency of ammonium sulphate under the experimental conditions tested. This would also explain why sodium acetate when was screened gave there was only a slight indication of precipitation; firstly typical screening was run at 0.5mg/mL to be conservative with material where lower protein concentrations require higher precipitant concentrations. This was then compounded by a typical precipitation midpoint for 0.5mg/mL IgG₁ with ammonium sulphate under standard conditions of 1.8M. If sodium acetate is only ~50% as efficient a precipitant then we could expect a midpoint of 3.6M, and from early screening the only indication of precipitation had been seen at 3.2M which would correspond to a broad transition curve. It is clear that under the conditions tested sodium acetate is a poor choice as a precipitant; very high concentrations would be required, reaching 80-90% saturation under pH 7.0 conditions. Under alkaline conditions sodium acetate is expected to perform better and possibly is a good example of the limitations of the

screening methodology when only one pH is properly explored. Previously sodium acetate at 80% saturation had been reported to precipitate an IgG at pH 8 only [32].

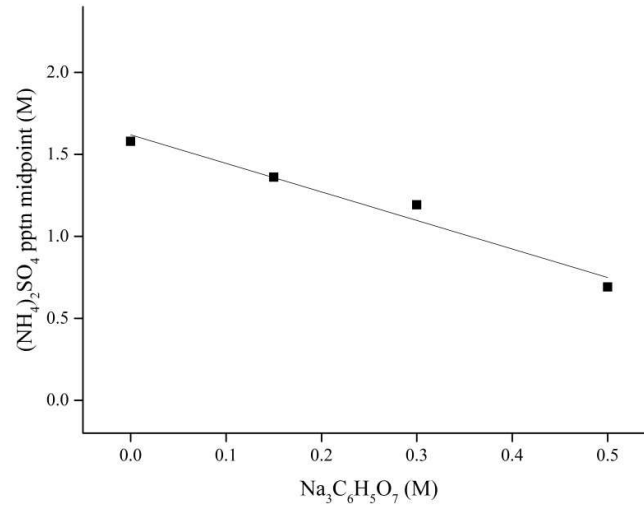


Figure 43. The impact of tri-sodium citrate upon the precipitation performance of ammonium sulphate.

Under conditions of pH 7.0, IgG₁ final concentration at 3.35 mg/mL. Ammonium Sulphate precipitation midpoints were found to decrease at $-1.74[\text{Sodium Citrate}]$, $R^2 = 0.951$. This was based upon 8-point triplicate precipitation curves run at 0, 0.15, 0.3 and 0.5M sodium citrate with precipitation midpoints generated from the sigmoidal fitting equation.

Figure 43 captures the reduction in AS concentration required to precipitate IgG₁ with the addition of $\text{Na}_3\text{C}_6\text{H}_5\text{O}_7$. In direct molarity, sodium citrate much more readily precipitates IgG₁ than AS, as can be seen by the 1.74[NaCit]:1[AS] ratio. Sodium citrate has an ionic strength of 6M/M sodium citrate. If compared to absolute ionic strengths (6M to 3M), then tri-sodium citrate could be described as 87% as effective a precipitant as $(\text{NH}_4)_2\text{SO}_4$.

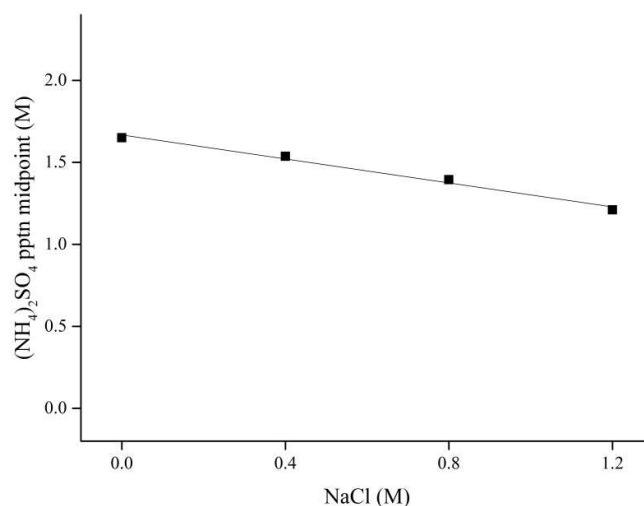


Figure 44. The impact of sodium chloride upon the precipitation performance of ammonium sulphate.

Under conditions of pH 7.0, IgG₁ final concentration at 3.35 mg/mL. Ammonium Sulphate precipitation midpoints were found to decrease at $-0.366[\text{Sodium Chloride}]$, $R^2 = 0.982$. This was based upon 8-point triplicate precipitation curves run at 0, 0.4, 0.8 and 1.2M sodium chloride with precipitation midpoints generated from the sigmoidal fitting equation.

Here sodium chloride was measured as ~35% as efficient a precipitant as ammonium sulphate, under the fixed conditions tested. From this the predicted precipitation midpoint for 0.5mg/mL IgG₁ could be as high as 4.9M. Saturated solutions can be made up to 6M, so this *is* achievable; however, by this prediction 80% saturation would be required and would not be ideal.

These studies have shown no obvious synergistic effects between the salt system combinations. Combinations of different acidic/basic salts may be advantageous, and so could running 1st and 2nd cuts using different salts, however this will only become apparent when testing on process relevant feed-streams where impurity fractions can be considered.

4.8 Size exclusion chromatography results

Re-solubilised precipitate samples were run through SEC HPLC measure any discernible change following the disruptive process of precipitation. Materials and methods are detailed in Chapter 2.

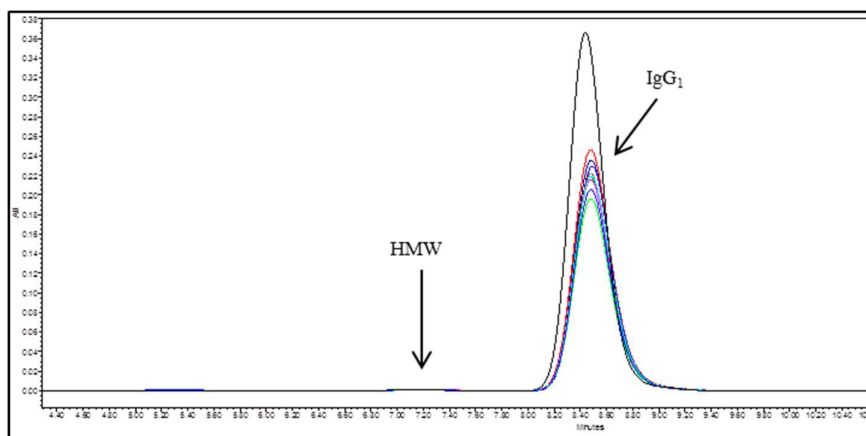


Figure 45. SEC Chromatogram for re-solubilised precipitates.

The black line plot was a purified IgG₁ standard, with all coloured plots depicting re-solubilised precipitants from different precipitants. The disparity in peak heights was due to variance in protein loading onto the column. The Y axis could be normalised for direct comparisons.

Upon re-suspension of the solid IgG₁ precipitate, not one sample showed a profile with a change from that of the starting material. 99.5% monomer and 0.5% aggregates were detected in purified protein samples with a variance of only $\pm 0.2\%$ across assays. This applied to all salting-out precipitants. This may have been due to the fact that only precipitations between pH 5-9 were only tested and that greater shifts acid or alkali conditions may have forced the formation of irreversible low or high molecular weight species (LMW, HMW). The longest period solid precipitates were held for before re-suspension into solution was 24 hours and it is possible that longer periods of solid stasis could also be detrimental to product integrity. This was not investigated further however and hold-time studies may be an interesting future avenue of research.

4.9 Activity ELISA results

A dual binding activity ELISA was run on re-solubilised IgG₁ following precipitation with the four main precipitants studied. 2.0M Ammonium Sulphate, 1.8M Lithium Sulphate, 1.1M Sodium Citrate and 1.2M Sodium Sulphate precipitations were run at pH 7.0 on purified IgG₁ at a final concentration of 1mg/mL and re-suspended in 50mM phosphate buffer pH 7.0 to

2mg/mL. The four different conditions were directly compared to the IgG₁ product standard calibration curve.

Samples were buffer-exchanged with 2-3 volumes in Amicon™ Ultra 30K membrane 0.5mL centrifugal filters (Millipore, Hertfordshire, UK) to remove residual salts and then analysed.

The assay is detailed in Chapter 2, with names substituted for confidentiality.

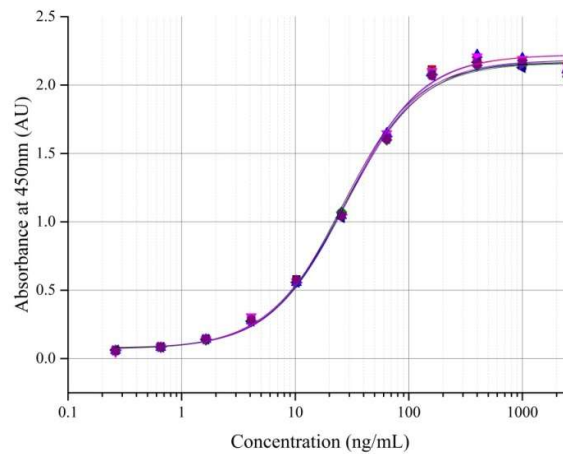


Figure 46. Activity ELISA for binding site 1.

Plot of absorbance at 450nm versus concentration of IgG₁. Details are covered in Table 14, good geometric alignment seen across 3 controls and the 4 the samples.

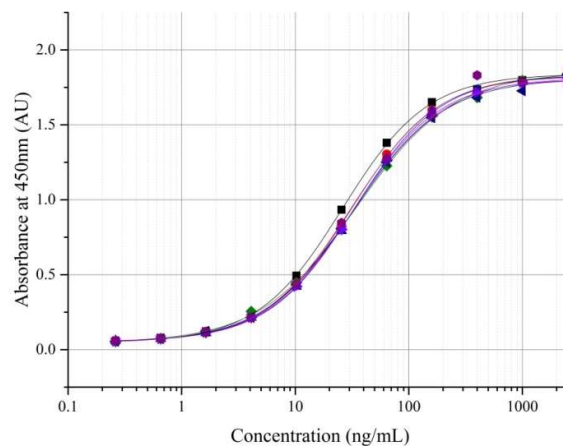


Figure 47. Activity ELISA for binding site 2.

Plot of absorbance at 450nm versus concentration of IgG₁. Details are covered in Table 14, good geometric alignment seen across 2 controls and the 4 the samples, standard 1 (■) slightly misaligned, possibly due to liquid handling error or assay variation.

Table 14. Results for both the *binding site 1* and *binding site 2* activity assays.

Summarising Figure 46 and Figure 47.

Plate 1		C-parm	ratio STD1	ratio STD2	ratio STD3	Geo mean
BS 1	STD1	26.4	NA	NA	NA	NA
AS	Sample A	28.1	94.3	98.3	98.1	96.8
LIS	Sample B	28.3	93.4	97.4	97.2	96.0
NaC	Sample C	28.2	93.8	97.8	97.6	96.4
NaS	Sample D	26.9	98.4	102.6	102.4	101.1
Start IgG	Sample D2	28.0	94.4	98.4	98.2	96.9
	STD2	27.6	NA	NA	NA	NA
	STD3	27.5	NA	NA	NA	NA
Plate 2		C-parm	ratio STD1	ratio STD2	ratio STD3	Geo mean
BS 2	STD1	26.2	NA	NA	NA	NA
AS	Sample A	31.1	84.3	104.6	100.8	96.2
LIS	Sample B	33.4	78.4	97.4	93.8	89.5
NaC	Sample C	32.9	79.7	98.9	95.3	90.9
NaS	Sample D	34.4	76.1	94.5	91.0	86.8
Start IgG	Sample D2	32.5	80.5	100.0	96.3	91.9
	STD2	32.5	NA	NA	NA	NA
	STD3	31.4	NA	NA	NA	NA

For the *binding site 1*, it can be concluded that the percentage activity of the samples are highly comparable to the reference standard, with a geometric overall mean close to 100%. For the *binding site 2*, the overall the geometric mean was a bit lower in comparison to the reference material. However, on the *binding site 2* plate the C value of STD1 was a bit lower in comparison to STD2 – 3. This could be linked to the variability in the method or to a small pipetting error. Due to the lower C-parameter for this curve, the calculated ratios in comparison to this STD1 are also lower. Therefore, taking into consideration just the 2nd and 3rd standards (C-parm of 32.5, 31.4) it can be acknowledged that near 100% similarity to the reference standard has also been maintained. These were all compared directly to the IgG₁ standard.

The indication that complete retention of protein function / activity following what is a disruptive precipitation process was expected. Work cited in the literature gave no indication that immunoglobulins were adversely affected by salt precipitation under kind processing conditions, and size exclusion chromatography indicated no change in the size profile or increase in aggregates which could be an early indicator of activity degrading conditions.

Only four different salts have been tested under one fixed condition each, since the activity assay is time intensive and expensive to run. It makes sense to run more generic high-throughput analytics first and test just the key points which seem to deviate from the norm and indicate loss of structure/activity. As it stands precipitation by salting-out remains a suitable step for the early clarification of IgG₁. If activity loss was seen, then the direction of the project could have focused on negative precipitation. This would have involved the targeting of impurity fractions, where the recovery and retention of function would have been irrelevant.

4.10 Linking precipitation on pure protein to cell culture fluid

Crucially for work carried out in this chapter was the need for a real link between studies on purified protein and that of process relevant cell culture fluid. A set of studies on salts were carried out on both feed-streams under that same precipitant conditions, in order to understand how salt-driven precipitation behaved in more complex systems.

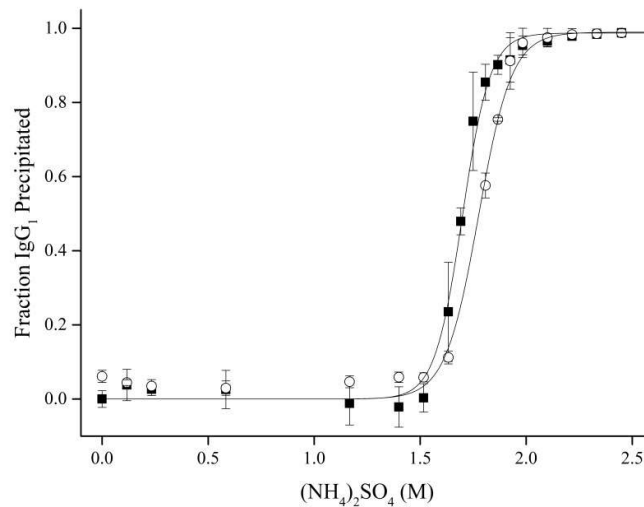


Figure 48. Comparing precipitation of pure and CCCF IgG₁ based material.

Precipitation curves for ammonium sulphate at a final IgG₁ concentration of 0.5mg/mL, at pH 7.0 for both pure protein (■) and cell culture fluid (○).

Figure 48 displays the precipitation curves for purified IgG₁ feed and clarified cell culture fluid feeds using ammonium sulphate. Performance was comparable between the two, meaning initial screening translates well into process conditions. Pure feed precipitations were carried out at 300 µL volumes in Corning UV plates and mammalian cell culture fluid precipitations were run at 900 µL volumes in 2mL deep well plates. Experimental work connecting the two scales in both pure and cell culture fluid precipitations showed no discernible change. The ammonium sulphate precipitation midpoint for the purified IgG₁ was measured at 1.69 M, whilst the IgG₁ in the cell culture fluid was 50% precipitated at the slightly higher concentration of 1.78M. This increased precipitant concentration requirement was seen across the board and indicates it may be stabilising compounds within the cell culture broth that increase the IgG₁ solubility profile and/or decrease protein aggregation tendencies [134]. The 7% difference in required precipitant concentration between pure protein and process fluids was observed for all salts tested (4±3%), except for Potassium Citrate which required a concentration exceeding its solubility in solution.

4.11 Chapter Summary

Table 15 summarises the screening of salt precipitants on purified monoclonal antibody. Ammonium, sodium, and lithium cations were the best cation choices and dictated salt solubility. The trend of ammonium > sodium > lithium > potassium for achieving precipitation from the lowest volume of saturated salt stock was seen.

Table 15. Effectiveness of different cation-anion combinations for precipitating IgG₁.

Cations are ranked from most kosmotropic (ammonium) to most chaotropic (magnesium) whilst Anions are ranked from most kosmotropic (citrate) to neutral (acetate). The table shows how different combinations of key Hofmeister ions perform as precipitation candidates for the IgG₁ investigated. (+) indicates successful precipitation and recovery of soluble IgG₁ from the precipitate, (-) represents no precipitation properties observed, (nt) means that the candidate was not tested.

		Anions			
		Citrate	Sulphate	Phosphate	Acetate
Cations	Ammonium	+	+	+	NT
	Potassium	+	-	-	NT
	Sodium	+	+	+	-
	Lithium	+	+	+	NT
	Magnesium	NT	-	NT	NT

Potassium showed limited precipitation potential, for example potassium citrate at around 90% saturation of a near saturated solution of 1.00M was found to precipitate 0.5mg/mL IgG₁ incompletely, however it is believed that process condition optimisation could improve upon this. The issue being potassium ions weren't as soluble, limiting solutions to lower ionic strengths of alternative cation counterparts. Citrate, sulphate and phosphate were all shown to be the best anion choices for salting-out. Regarding acetate anion salts, ammonium acetate was quickly tested up to 3M but gave no indication of precipitation under the conditions tested, but this was not an exhaustive test. Sodium acetate has been predicted to precipitate at high

levels of saturation or under more alkaline conditions, so future experiments looking at acetate more thoroughly would be wise.

In this work precipitation by salt-driven precipitation has shown good promise with a range of different salts available, a range of candidates each offering alternative attributes.

Screening has shown how pH, concentration and ionic strength all affect performance.

Sigmoidal fits and quantifiable midpoints have characterised performance well for a range of variables tested and provide a means to predict and control process conditions. Further studies could include particle size analysis; different precipitants formed visibly different protein precipitates and being able to characterise these variances in terms of size and distribution may aid in the selection of better choices. Similarly, microscopy would have been a helpful addition to assessing precipitates. More in depth analysis of protein structure and function would improve understanding as would testing greater extremes of conditions, such as pH and temperature in order to understand and place the possible edges of failure.

Chapter Five: Precipitation as a primary purification step

“Science, my boy, is made up of mistakes, but they are mistakes which it is useful to make,
because they lead little by little to the truth.”

Jules Verne, Journey to the Centre of the Earth

5.1 Abstract

In this chapter a series of precipitations were carried out on process cell culture fluid containing the target IgG₁ molecule to be recovered and purified. Precipitation performance and trends were shown to translate well from pure protein studies to the case of process relevant material. Recovery yields were found to be equivalent, and selectivity could be evaluated by a range of techniques including Bradford total protein assay, chip-based electrophoresis, SDS-PAGE, and Protein A HPLC. The best salting-out precipitants were identified as ammonium sulphate, lithium sulphate, sodium citrate, and sodium sulphate based upon the stated performance criteria.

The influence of pH, fermentation titre, and ionic strength were evaluated through a series of ammonium sulphate driven precipitations. Process variation was shown to be controllable.

Two full factorial design of experiment (DoE) runs were carried out. The first tested the performance of ammonium sulphate precipitations, since this was well-characterised and the trends re-enforced previous findings. The second DoE investigated the performance of sodium citrate, sodium sulphate and lithium sulphate, looking at any synergistic effects which could lead to improved yield or selectivity.

5.2 Introduction

Identifying precipitation conditions on pure protein models through rapid, high throughput screening was achieved with primarily spectroscopic analytical techniques to define performance. This was an efficient and effective approach to build up understanding on a range of variables, with low material consumption. The next step was to transfer this knowledge gleaned from model systems and apply it to process relevant conditions, whilst taking into account factors such as specificity, product purity, material handling, and process robustness.

5.3 Screening of precipitants on cell culture fluid

Analysing the performance of precipitation on cell culture fluid is more complex. This is due to the mix of different HCPs alongside the target protein in conjunction with media components which all dominantly absorb at 280nm, obfuscating UV spectroscopy techniques to directly quantify IgG precipitation and recovery yields upon re-suspension of the protein pellet. Absorbance at 600nm still proved effective for semi-quantitatively monitoring precipitation progression as solids created; however more dedicated assays such as SDS-PAGE, Bioanalyzer, Protein A HPLC and Bradford Total Protein (detailed in chapter 2) were employed as the main tests for work presented in this chapter.

A screening campaign, akin to that seen with the pure protein studies, albeit more refined, was undertaken on clarified cell culture fluid. In accordance with the high throughput screening methodology laid out in Chapter Three, precipitations were carried out in 2mL 96 V-shaped deep-well plates, with pellets isolated through centrifugation and recovered in the re-suspension buffer, followed by analysis. Results from the primary screening on pure protein models corresponded rather seamlessly to complex feed-stream precipitations, with the same recovery yields achievable at slightly elevated precipitant ionic strengths of approximately +5% of what was achieved in Chapter Four. IgG₁ purity was found to be consistent throughout at about 80% of total protein by chip-based electrophoresis. Total

impurity removal, as measured by the flow-through peak by Protein A HPLC was more sensitive, with purity shown to be directly dependent on the extent of supernatant removed / dewatering of the precipitate pellet.

Table 16 summarises the screening results, displaying only the key successful precipitants for clarity, whilst summarising the metrics of dozens of precipitation salting-out graphs for brevity. The automated screening methodology allowed for hundreds of conditions to be tested with relative ease; experiments could be easily programmed into the Excel-Evoware design tool and executed on the robotic platform deck. Following precipitation, recovery, and re-suspension of the precipitate, samples could then be prepared by dilution for any subsequent assays just as easily through the same route. The accessible plate format meant that plates could be sealed and stored for future use, with data tracking and future material handling stored electronically through the Excel code.

Table 16. Performance of various precipitants tested with the screening methodology on pure IgG₁ and cell culture fluid.

Precipitation Candidate	Stock	Pure IgG ₁ Evaluation						Cell Culture Fluid Evaluation				
		IgG ₁ pptd	C _{min}	C _{mid}	C _{max}	Recovery Yield	Monomer Profile	IgG ₁ precipitated	Optimal concentration	Recovery Yield	Protein Purity	Total Purity
Ammonium Citrate (tribasic)	4.0M pH 7.0	>95%	1.41M	1.69M	1.94M	>90%	99.5%	>95%	2.0M	>95%	NT	NT
Ammonium Phosphate	4.0M pH 7.0	>95%	1.80M	1.84M	1.88M	80%*	99.5%	>95%	1.95M	>95%	75%	85%
Ammonium Sulphate	4.0M pH 7.0	>95%	1.42M	1.60M	1.77M	>95%	99.5%	>95%	1.80M	>95%	80%	85%
Lithium Sulphate	2.5M pH 6.25	>95%	1.41M	1.69M	1.94M	>95%	99.5%	>95%	2.0M	>95%	85%	85%
Potassium Citrate	1.0M pH 7.0	75%	0.85M	-	-	70%	99.5%	50%	0.85M	50%	NT	NT
Sodium Citrate (tribasic)	2.0M pH 7.0	>95%	0.77M	0.89M	1.02M	>95%	99.5%	>95%	1.1M	>95%	80%	85%
Sodium Phosphate	4.0M pH 5.0	>95%	1.78M	2.02M	2.26M	80%*	99.5%	>95%	2.3M	80%	NT	NT
Sodium Sulphate	2.0M pH 7.0	>95%	1.00M	1.05M	1.10M	>95%	99.5%	>95%	1.2M	>95%	80%	85%

All salts were investigated at a final concentration IgG₁ of 0.5mg/mL in cell culture fluid, pH 7.0 in 50mM phosphate buffer, with the exception of sodium phosphate and lithium sulphate, with saturation concentrations and percentages subject to change with different protein concentrations, buffer strengths and pH. The stock displays the concentration and pH precipitating salts were prepared at. C_{\min} is the concentration of precipitant calculated where precipitation initiates (5% precipitation), C_{mid} is the mid-point concentration where the protein is in equilibrium with soluble and insoluble state in equal abundance, C_{\max} is the concentration of precipitant where 95% of protein has precipitated. These values were calculated from the sigmoidal fitting of precipitation curves. Recovery yield shows the IgG₁ percentage recovered following precipitation, centrifugation, separation and re-solubilisation. The monomer yield depicts the structure profile based on the starting IgG₁ at 99.5%. For cell culture fluid evaluations, the optimal concentration was found by optimising yield and purity profiles whilst minimising precipitant concentration. Protein purity was determined by chip-based electrophoresis, with total impurities measured by protein A HPLC. Potassium citrate could not achieve C_{mid} and C_{\max} values since the solubility of the salt was reached at 1M, and precipitation only started to occur at 0.85M. NT indicates not tested. The best salting-out candidates were ammonium sulphate, sodium citrate, sodium sulphate, and lithium sulphate, with the two sodium salts offering the best performance at the lowest salt saturations.

5.5 How pH control influences precipitation performance

With results generated from pure and complex feed streams bearing a strong resemblance, a series of more in depth precipitation studies were then undertaken, looking to characterise the effect of key processing constraints upon not just recovery yields, but also upon selectivity of the step. The first parameter to explore was the pH of the reaction. In Chapter 4, pH had been shown to strongly affect precipitation performance, with IgG₁ solubility profiles reduced at closer to the pI of the protein or alternatively with the same recovery yield achievable from a

lower precipitant concentration. Seeing how this reduced solubility would impact selectivity was well worth investigating.

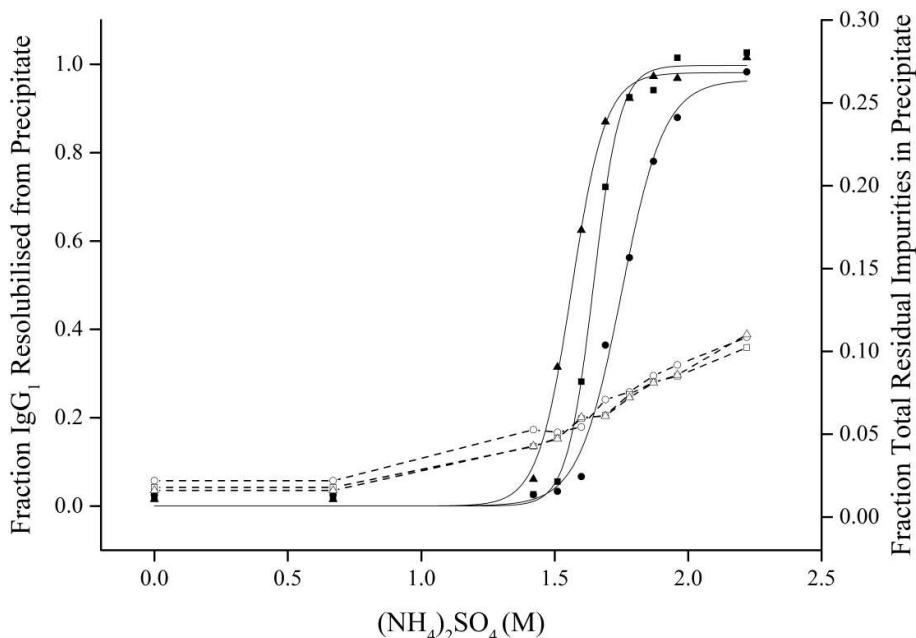


Figure 49. The effect of pH on the precipitation profiles with ammonium sulphate.

Precipitations were run in 2mL v-shaped 96 well plates on cell culture fluid, 900 μ L total well volume, with final IgG₁ concentrations of pH 6.0 (●), pH 7.0 (■), pH 8.0 (▲), with residual impurities recovered in the precipitate at 6.0 (○), pH 7.0 (□), pH 8.0 (△). All points are an average of triplicate repeat conditions.

Cell culture fluid of a known IgG₁ titre was pH adjusted with 0.1M HCl/NaOH, then blended with the corresponding 50mM phosphate buffer and buffered ammonium sulphate stock solution, all in accordance with the methodology described in Chapter 3. Re-suspended precipitates were then analysed by Protein A HPLC to determine both IgG₁ recovery and also a measure of total residual impurities by integrating the reduction in flow-through peak versus the starting material.

Figure 49 demonstrates how operating closer to the pI of the IgG₁ (pI = 8.7) enables the use of a lower precipitant concentration whilst achieving full recovery of the target protein.

Precipitation midpoints from the sigmoidal fitting were measured as 1.75M, 1.64M and 1.56M (NH₄)₂SO₄ for precipitation carried out at pH 6.0, 7.0 and 8.0 respectively. This is likely due to a reduction in net protein charge as the solution pH approaches the pI leading to

reduced protein-protein repulsion and in turn decreasing the protein solubility. No apparent improvement in impurity removal was observed, when running precipitations at a higher pH. This strategy confers the advantage of requiring less salt, and hence reducing overall process volumes. Understanding the effect of pH on precipitation is important in order to define appropriate precipitation process conditions. Excess salt leads to a reduction in material purity whilst an insufficient level leads to reduced yields. Unlike the sigmoidal relationship between salt concentration and IgG₁ precipitation, impurities are removed in a linear fashion with salt concentration. This is likely due to the amalgamation of different impurities which, if individually analysed, are expected to display similar, but offset solubility profiles to the IgG₁. A Bradford total protein assay was also performed on all samples. Total protein minus IgG₁ was also plotted, showing remaining HCPs in precipitate, however the plot displaying around 90% removal of process fluid impurities measured from the PrA HPLC flow-through peak captured the precipitation performance in a more informative way, since it isn't just proteins which are being removed from this primary purification step, but also non-proteinaceous media components.

5.6 Precipitation on future feed-streams

The next variable investigated was the effect of titre upon salt driven precipitation. As stated in Chapter 1, with advances made in upstream processing, higher titres of product are placing a burden upon downstream processing unit operations as they struggle to match throughput [7]. As established in Chapter 4, increased protein concentrations exhibit reduced solubilities when a precipitating agent is added, so salt-driven precipitation would appear to offer better performance per unit volume with increasing titres, as less precipitant needs to be added to purify and recover a greater mass of product.

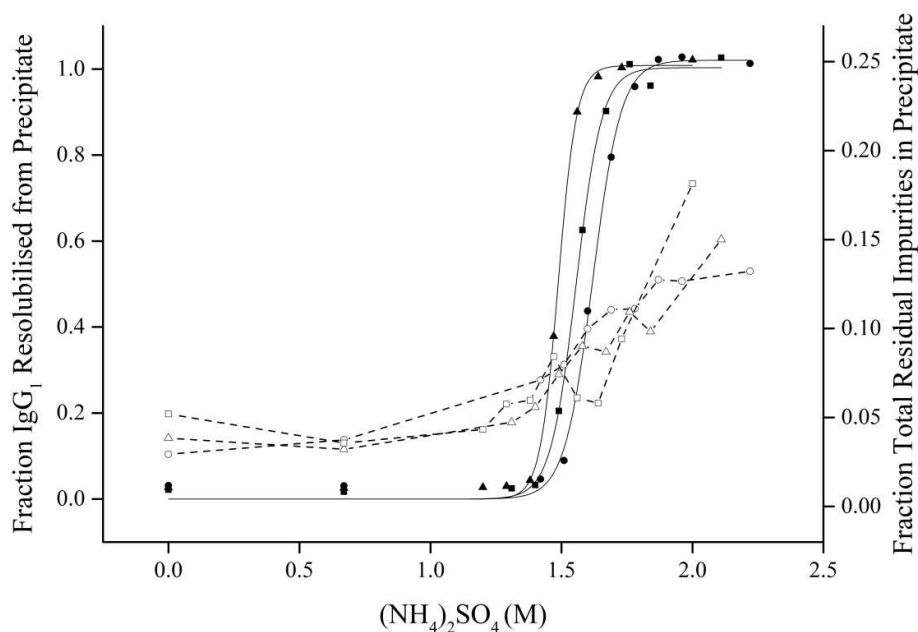


Figure 50. Effect of antibody titre has upon the precipitation profiles with Ammonium Sulphate.

Precipitations were run in 2mL v-shaped 96 well plates on cell culture fluid, 900 μ L total well volume, pH 7.0 with final IgG1 concentrations of 0.5mg/mL IgG1 (●), 1.2mg/mL IgG1 (■), 2.4mg/mL IgG1 (▲), with residual impurities recovered in the precipitate at 0.5mg/mL IgG1 (○), 1.2mg/mL IgG1 (□), 2.4mg/mL IgG1 (△). All points are an average of triplicate repeat conditions.

To emulate a higher titre feed-stream, whilst maintaining the same impurity profiles in the cell culture fluid, IgG₁ was spiked in from a concentrated 80.1mg/mL stock to create three feed-stocks of 2.1 mg/mL, 5.0 mg/mL and 10.0 mg/mL. These were selected to be effectively current, near-future, and future cell culture titres. Minimal dilution of the material occurred due to the small volumes involved. These feed-streams were then blended with corresponding 50mM phosphate buffer and buffered ammonium sulphate stock solution, again accordance with the methodology described in Chapter 3. Protein A HPLC and Bradford total protein assays were performed on the recovered precipitate.

Figure 50 shows a very clear trend with the influence of feed-stream titre. Increasing the protein concentration in cell culture fluid showed a marked reduction in the precipitant concentration required to achieve a desirable level of recovery. Precipitation midpoints for 0.5mg/mL, 1.2 mg/mL and 2.4 mg/mL IgG₁ at pH 7.0 were seen to decrease from 1.62M,

1.56M and 1.49M $(\text{NH}_4)_2\text{SO}_4$ respectively. Salt-driven precipitation was shown to offer better performance at higher titres, as a higher fraction of IgG₁ can be precipitated at lower salt concentrations, meaning that a greater level of removal of impurities from the step can be realised from the procedure, whilst also requiring less precipitant per unit volume of material processed.

5.7 The impact of feed-stream ionic strength upon precipitation

The final detailed study looked at how ionic strength of the process fluid impacted upon protein solubility when a precipitant is applied. Ionic strength is still an important determinant of precipitation effectiveness that needs to be measured in process feeds in order to enable better control of the precipitation process. For example, if a recipe change in the upstream processing stages led to the cell culture fluid containing 150mM more salts, then the conditions of the precipitation stage could be adjusted to accommodate this change whilst maintaining step performance. Sodium chloride was varied to achieve this. Previously to 4.0M NaCl was shown to precipitate this IgG₁. In Chapter 4 different sodium salts were investigated for synergy with ammonium sulphate precipitation, with 1M NaCl shown to offset the ammonium sulphate performance by 350mM.

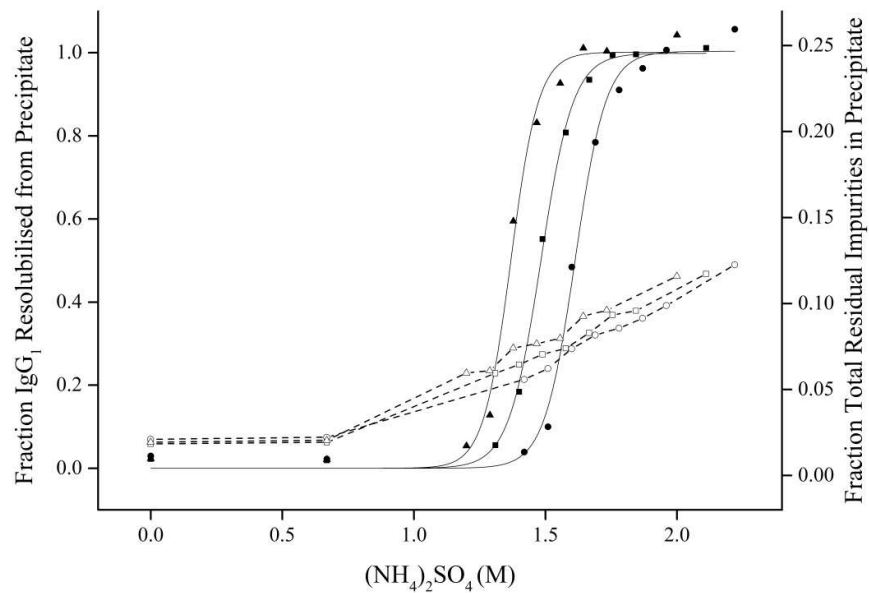


Figure 51. Effect of NaCl on the precipitation profiles with ammonium sulphate.

Precipitations were run in 2mL v-shaped 96 well plates on cell culture fluid, 900 μ L total well volume, pH 7.0 with final IgG₁ concentrations of 0.5mg/mL IgG₁ at 0mM NaCl (●), 400mM NaCl (■), 800mM NaCl (▲), with residual impurities recovered in the precipitate at 0mM NaCl (○), 400mM NaCl (□), 800mM NaCl (△). All points are an average of triplicate repeat conditions.

Increasing the overall ionic strength of ammonium sulphate precipitations through NaCl supplementation reduced the concentration requirements of the primary precipitant. Precipitation midpoints decreased by 130mM and 240mM ammonium sulphate when the sodium chloride concentration was increased by 400mM and 800mM, respectively. This could be construed as sodium chloride exhibiting a 30-33% salting out efficiency, which matched up well with the 35% value seen with pure protein studies. When compared to absolute ionic strengths, sodium chloride is a less effective precipitant, which is to be expected from the positioning of the ions in the Hofmeister series.

As a supplement to the results generated from Figure 50 and Figure 51, several samples were analysed for overall protein purity through the Bioanalyser assay and directly compared to the more all-encompassing purity measurement through the Protein A HPLC assay.

Table 17. Comparison of purity values.

Determined through the Bioanalyzer and Protein A HPLC assays. Bioanalyzer purity values are from single samples, whilst Protein A HPLC purity values are the average of triplicate conditions.

Material	Protein Purity (Bioanalyzer)	Total Purity (Protein A HPLC)
Purified IgG Standard	96.1	98
Clarified Cell Culture Fluid (CCCF)	66.3	28
1.96M (NH ₄) ₂ SO ₄ , 0mM NaCl, pH 7.0 Precipitation	78.5	74.8
1.84M (NH ₄) ₂ SO ₄ , 400mM NaCl, pH 7.0 Precipitation	82	75.2
1.73M (NH ₄) ₂ SO ₄ 800mM NaCl, pH 7.0 Precipitation	82.8	75.3
1.96M (NH ₄) ₂ SO ₄ , pH 6.0 Precipitation	76.4	72.6
1.96M (NH ₄) ₂ SO ₄ , pH 7.0 Precipitation	81.4	76.9
1.96M (NH ₄) ₂ SO ₄ , pH 8.0 Precipitation	79.4	75.8

Table 17 distinguishes between the recovered IgG purity with respect to total protein versus the overall purity of the recovered precipitate as determined by measuring the flow-through on the PrA HPLC assay. The experimental conditions selected can be identified on the

precipitation curves in Figure 50 and Figure 51. The total overall purity of the recovered precipitate takes into account any impurity species which absorbs at 280nm, hence the leap from ~28% purity in the CCCF to ~75% upon purification.

5.8 Investigating precipitation performance with Design of Experiments

5.8.1 Design

A full factorial 3 level DoE was run with 2 set of replicates, resulting in 81 experimental runs performed in a plate, as depicted in Figure 9. Three levels per factor (low, middle, high) enables quadratic response surface models to be employed, which are more flexible and allow better understanding of trends and interactions [165]. Precipitations were carried out in 2mL V-shaped deep-well plates, with each condition tested in a working volume of 900 μ L, in accordance with the screening methodology in Chapter 3. Micro-well automation allowed for a robust design space was chosen since experimentation and analysis could be readily programmed and executed rapidly. The three factors investigated were: 1) the concentration of ammonium sulphate as the primary precipitant 2) the sodium chloride concentration as a secondary precipitant and 3) the sum pH of the system.

Table 18. The design constraints set out for the DoE for the first experimental run, and then the additional conditions for the second run.

		1 st Run			2 nd Run		
		Low	Mid	High	Low2	Mid2	High2
Factor 1	Ammonium Sulphate	1.5M	1.75M	2.0M	1.8M	1.85M	1.9M
Factor 2	Sodium Chloride	0M	0.5M	1.0M	0.4M	0.45M	0.50M
Factor 3	pH	6	7	8	6	7	8

The range of ammonium sulphate was chosen between 1.5-2M, looking at Figure 16 as the example, this is the clutch concentration range where zero to complete salting out occurs (albeit this figure was tested on 3.35mg/mL IgG), hence it was expected to observe notable changes in process performance across these values with changes in factors 2 and 3. Sodium chloride concentrations were ranged between 0-1M, to cover ranges similar to previous studies on cell culture fluid, whilst the pH range was kept within the well characterised range of pH 6-8. Using ammonium sulphate, pH 8 is the limit as it prone to releasing ammonia at higher

pHs. The responses to this study were set as the percentage yield of recoverable IgG from the precipitate, and the subsequent purity of this recovered protein. Both analyses were measured through the HPLC PrA methods for yield and purity.

5.8.2 Results & Analysis

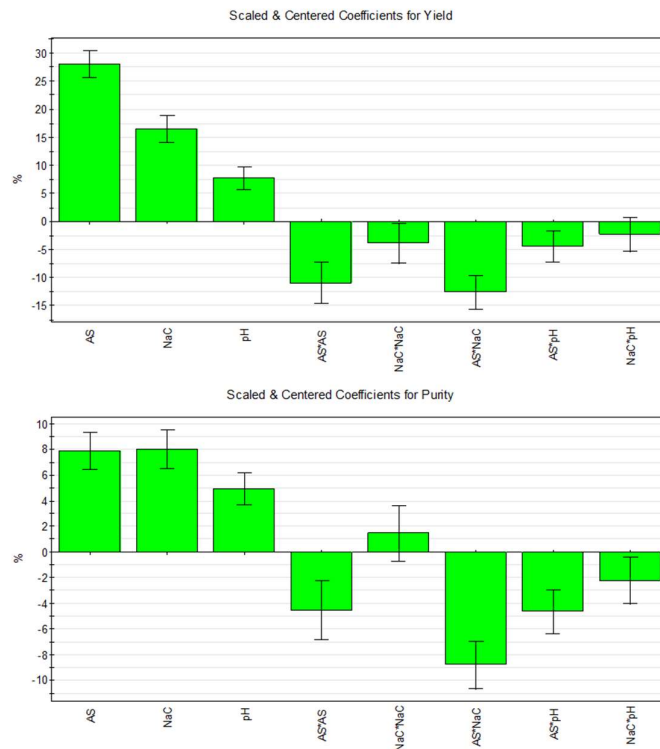


Figure 52. Coefficients for DoE model.

The pH*pH term was removed to improve model strength since it was shown to be ineffective. The model expressed an R^2 of 0.93, and Q^2 of 0.91, with the model showing both excellent fitting and prediction qualities.

The quadratic fitting model applied excellently to the data generated, testament to the precipitation screening methodology and time spent optimising robotic liquid classes and liquid handling approaches to minimise sources of error. As shown in Figure 52, the key coefficient for yield was the main salt precipitant followed by the supplementary NaCl salt, then pH, however the impact of each is attributable to the scale the parameters are varied by, since the upper and lower ranges for each differed markedly. For purity, again we see each factor affecting the purity of the recovered protein, with the combination of ammonium

sulphate and sodium chloride leading to undesirable co-precipitation of additional impurities, verified through earlier work.

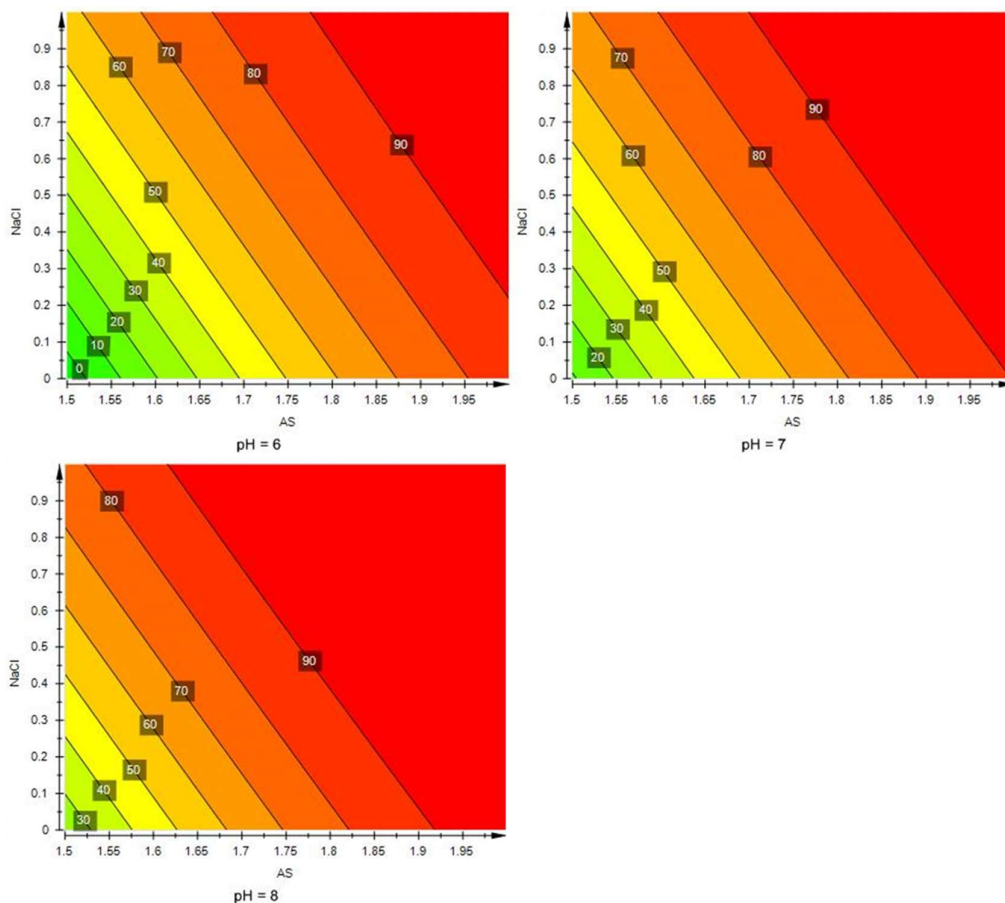


Figure 53. 4D contour plots showing the recovery yield of IgG1.

As a function of ammonium sulphate (M) and sodium chloride (M) at pH 6, 7 and 8. The response plots were fitted with a quadratic model, with all data fitting performed with Umetrics Modde 9.1 (Umetrics, Malmö, Sweden).

Figure 53 shows the response plot for yield for all the variables tested, predicting that targeting maximum yield requires either a higher pH (a pH closer to the pI of the protein) or higher precipitating salts to compensate otherwise. Relatively ammonium sulphate concentration dominates precipitation, enabled primarily by the pH of the system and supplemented by sodium chloride. The results are congruent with the study on NaCl in Figure 51, where increasing sodium chloride concentration shows a reduced ammonium sulphate concentration

required to achieve the same level of precipitation, and pH in Figure 49 showing better performance at conditions closer to the pI of the protein, with precipitation conditions at pH 8.0 creating a larger window of conditions which can achieve high recovery yields.

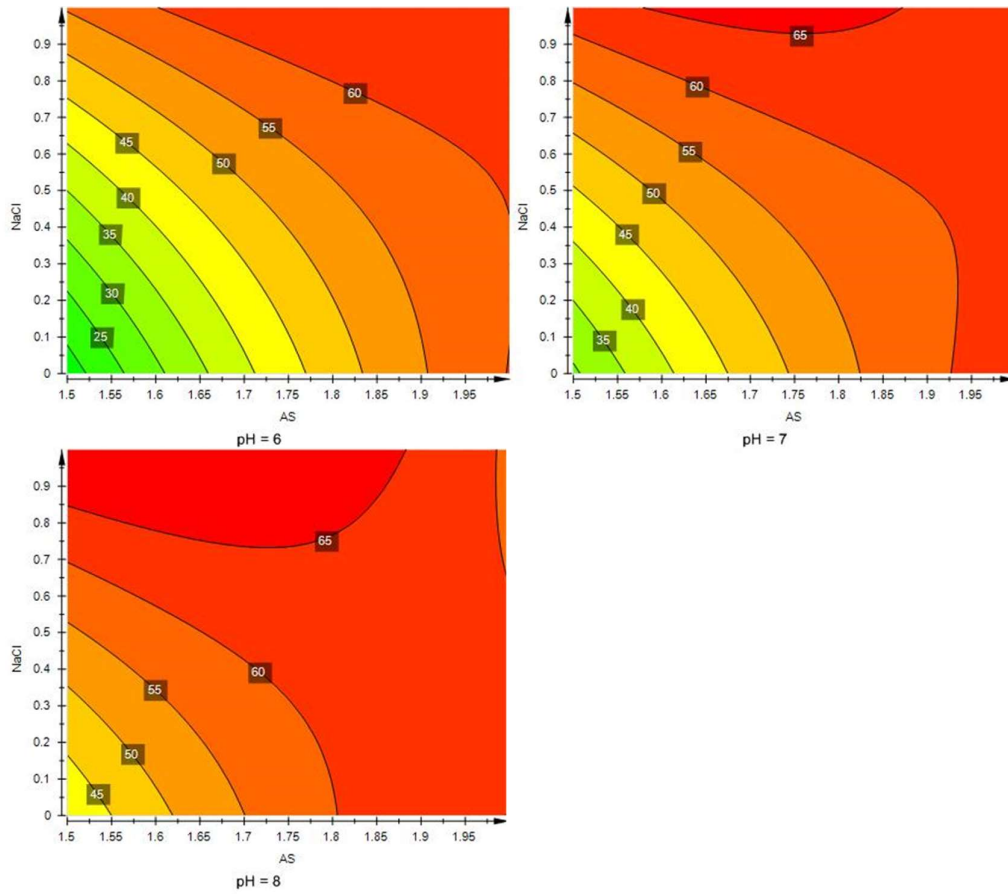


Figure 54. 4D contour plots showing the recovered purity of IgG₁.

As a function of ammonium sulphate (M) and sodium chloride (M) at pH 6,7 and 8. The response plots were fitted with a quadratic model, with all data fitting performed with Umetrics Modde 9.1 (Umetrics, Malmö, Sweden).

The response surface plot (Figure 54) for purity draws parallels with the yield plot; better results are achievable when the pH of the precipitation reaction is aligned with the pI of the protein, and following that improved IgG purity tracks with increasing the ammonium sulphate precipitant concentration. What was unexpected from this study is the indication that NaCl, at concentrations exceeding 800mM in pH 7 and pH 8 environments, allows for IgG selectivity to be boosted.

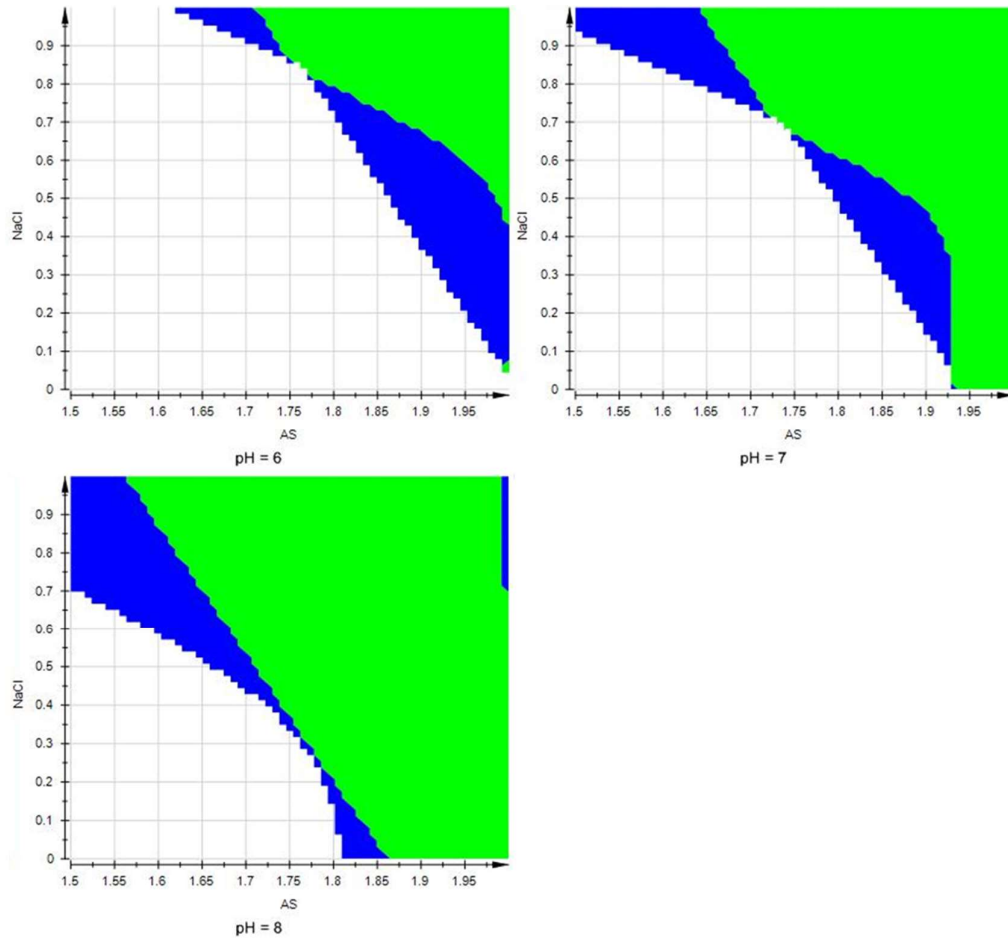


Figure 55. Sweet spot prediction plots for design space tested.

Green areas indicate both criteria of a precipitation yield greater than 80% with a final IgG₁ purity of greater than 60%, with blue areas displaying conditions where only one criterion has been met, typically the yield only. The sweet spot plot was generated with Umetrics Modde 9.1 (Umetrics, Malmö, Sweden).

Figure 55 shows the results of the *sweet spot* predictive tool generated by Umetrics Modde. As corroborated by earlier experiments, operating precipitation conditions at a higher pH and/or closer to the target molecule pI reduces the precipitant required to successfully bring mAb out of solution. The design space shown includes experimental upper limits; 2M ammonium sulphate and 1M sodium chloride combined push the solution to near saturation when added to cell culture fluid and hence the experimental design cannot be explored at higher concentrations for both factors.

An argument can be made that sodium chloride does not add value to the precipitation performance, and that increasing the ammonium sulphate concentration instead would achieve

the same result, but at a lower overall ionic strength, thus increasing experimental flexibility and opportunity to expand the design space. The initial rationale to investigate sodium chloride, which did not precipitate mAb at concentrations up to the 4.0M tested, was to see if it could contribute to the ammonium sulphate driven precipitation by improving purity. Investigating the effect of alternative precipitants through the DoE format would be worthwhile, to understand their influence upon yield and purity and to identify any synergistic effects not currently identified.

The pH therefore remains the most flexible factor investigated for controlling precipitation performance, reducing the required precipitation concentrations, and a consequence creating a larger window of operation where both yield and purity criteria for the recovered precipitate are met. Future experiments should look at pH in greater detail, across a wider range and through smaller increments. Ammonium sulphate is the limitation in this regard, with solutions exceeding pH 8 prone to releasing ammonia gas and therefore changing in composition. An alternative more pH-flexible precipitant, such as sodium citrate or sodium sulphate, should be employed for a more detailed and controlled pH study.

The robustness of precipitation as an early purification step has been demonstrated. Yields of greater than 80% can easily be obtained from recovery of the precipitate with overall IgG₁ purities in excess of 60%. As seen from large *sweet spot* plots, notably at higher pHs of 7 and 8, there is a good range of conditions which can be run to achieve the same target outputs. The step is adaptable and robust to potential variation in incoming feed material.

If the constraints are tightened, to identify conditions exceeding a recovery yield of 95% and a recoverable purity of 65% then the conditions required to achieve this are constricted to pH 8.0, ammonium sulphate concentrations between 1.65-1.8M with 800mM-1M NaCl. If purity is only required to be 60%, then NaCl requirements can drop by as much as 400mM.

The main target on this step should be recovery yield, where a higher precipitant concentration has a marked improvement to product recovery following re-solubilisation of the precipitated pellet. The trade-off here would be an increased conductivity in the re-suspended protein solution, which may then require a buffer exchange step prior to the next downstream unit

operation, especially if we are considering an anion exchange flowthrough using a salt sensitive quaternary ammonium ligand. Since purity levels can be optimised by ~5% after reaching the 60% threshold, there may be no need to finesse that aspect since the next purification stage may comfortably take up the slack in removing those impurities.

5.9 The evaluation of precipitants through Design of Experiments

5.9.1 Introduction

In Chapter 4, precipitations combining ammonium sulphate and different sodium salts inferred no potential synergy with respect to yield. These studies were carried out on purified protein; hence selectivity could not be evaluated. Guided by the principles of Design of Experiments, an analysis on the performance of different salts on clarified cell culture fluid was carried out. Sodium citrate, sodium sulphate and lithium sulphate were selected for this study as they were all proven effective individual precipitants, the objective was to see how combining Hofmeister series salts could impact upon protein salting-out performance.

5.9.2 Design

A full factorial 3 level quadratic DoE was run with 1 set of replicates, resulting in 54 experimental runs performed in a plate, again as shown in Figure 9. The three factors are detailed in Table 19.

Table 19. The design constraints for the DoE first experimental run.

		Low	Mid	High
Factor 1	Sodium Citrate	0.36M	0.45M	0.54M
Factor 2	Sodium Sulphate	0.36M	0.45M	0.54M
Factor 3	Lithium Sulphate	0.28M	0.36M	0.44M

The study was performed in 2mL V-shaped deep-well plates on clarified cell culture fluid, 900 μ L working volume in each well as detailed in the methodology in Chapter 3. pH was controlled at a fixed pH 7, in 50mM phosphate buffer. The upper limit concentrations of each factor are noticeably lower than individual starting concentrations which have been shown to initiate IgG salting out for each salt, this was to accommodate the blending of each salt stock with the cell culture fluid and buffer diluent in total working volume in each well the plate.

The responses to this study were again set as the percentage yield of recoverable IgG₁ from the precipitate, and the subsequent purity of this recovered protein. Increasing total salt concentrations leading to higher precipitation recovery yields was expected, but the question remained over how overall selectivity could be affected.

5.9.3 Results & Analysis

Precipitations were carried out and the recovered precipitate was analysed with Protein A HPLC to assess both the recovery yield and purity of the product. Data was input into Umetrics Modde 9.1. The model expressed an R² of 0.97, Q² of 0.95, and reproducibility of 0.98 indicating excellent fitting and prediction attributes. From this the predictive contour plots for yield and purity values could be analysed with a high degree of confidence.

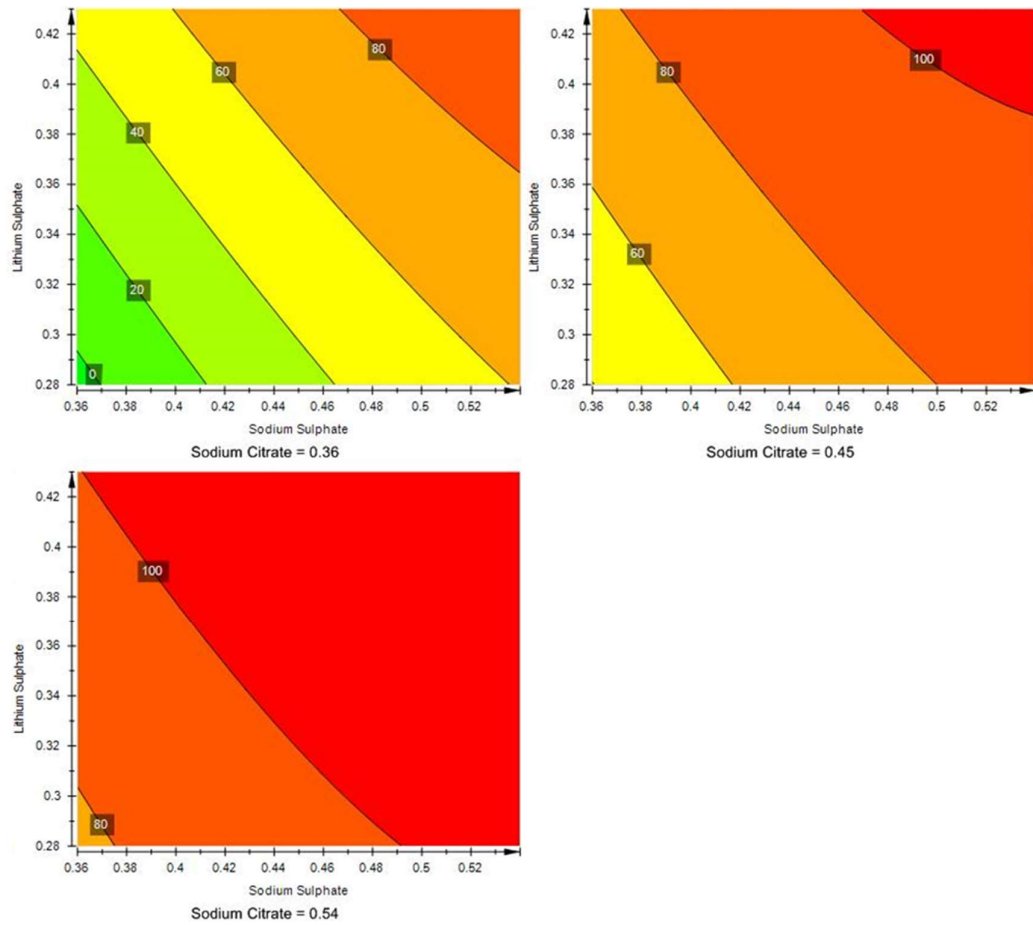


Figure 56. 4D contour plots showing the recovery yield of IgG₁.

From precipitation reactions comprising differing concentrations of sodium citrate, sodium sulphate and lithium sulphate salts. Precipitations were carried buffered at pH 7.0 in 50mM phosphate, on clarified cell culture fluid following the screening methodology described in Chapter Four. The response plots were fitted with a quadratic model, with all data fitting performed with Umetrics Modde 9.1 (Umetrics, Malmö, Sweden).

The predictive yield contour plot (Figure 56) displays a clear trend; increasing the solution concentration of any individual precipitant salt, or a combination of these three components lead to an increase in the overall salting-out of the target IgG from solution, and subsequently its isolation and recovery from the starting clarified cell culture fluid. There is no indication that combining different salts culminated in any coactive improvement, nor was this expected; no references in the literature indicated combining Hofmeister salts could aid in effectiveness. The second response, purity was the main investigative target.

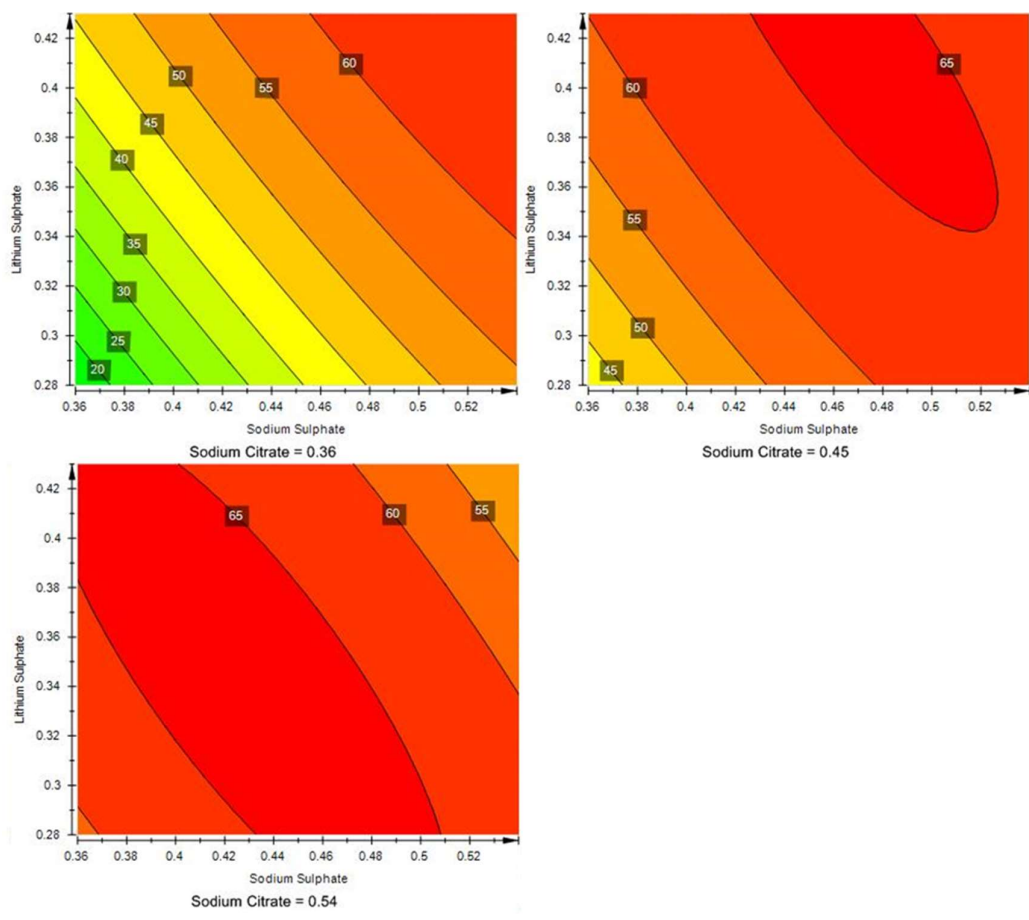


Figure 57. 4D contour plots showing the purity of IgG₁.

From the recovered pellet following precipitation reactions comprising differing concentrations of sodium citrate, sodium sulphate and lithium sulphate salts. Precipitations were carried buffered at pH 7.0 in 50mM phosphate, on clarified cell culture fluid following the screening methodology described in Chapter Four. The response plots were fitted with a quadratic model, with all data fitting performed with Umetrics Modde 9.1 (Umetrics, Malmö, Sweden).

The predictive purity contour plot (Figure 57), when reviewed in conjunction with the yield response, follows a very clear trend; increasing salt concentration leads to an improved purity as more IgG is recovered from solution. Upon reaching 100% recovery, excessive salt then leads to a decrease in re-solubilised precipitate, a more impurities are captured; a trend covered comprehensively by Figure 49 through to Figure 51. In conclusion, when pH is controlled, combining different precipitants confers no obvious advantage to the quality of the recovered product.

5.10 Chapter Summary

Precipitations carried out on clarified cell culture fluid matched the performances predicted from the pure protein scouting experiments. Specifically, the solubility curves and precipitation mid-point values have been shown to align meaning that rapid screening on purified material can provide insightful information, reducing the need to scout conditions as broadly when testing on process relevant feed-streams which are more reliant on more resource heavy assays. Screening on a range of precipitants identified the best precipitants, these being ammonium sulphate, sodium citrate, sodium sulphate and lithium sulphate. We have seen how the key process constraints ionic strength, feed titre, and pH affect yields and selectivity of precipitation performance using ammonium sulphate as the model precipitant. Design of Experiments (DoE) was then used to investigate how these parameters influenced each other, whilst building a better overall understanding. The study was performed in 96 2mL V-shaped deep-well plates on clarified cell culture fluid, 900 μ L working volume in each well as detailed in the methodology in Chapter 3.

In conjunction to host cell protein removal offered by salting-out was the improvement in feed clarity. With greater than 95% removal of the supernatant, subject to the efficiency of the solid/liquid separation effect came with the removal of colour and odour attributable to the media and other impurities. Future work could implement buffer exchange / desalting 96 well plate formats to allow for high throughput automated material prep.

Following on from developing precipitation steps, the next chapter will investigate how readily precipitation can be linked into conventional chromatography.

Chapter Six: Process Integration

“A good scientist is a person with original ideas. A good engineer is a person who makes a design that works with as few original ideas as possible. There are no prima donnas in engineering.”

Freeman Dyson

6.1 Abstract

An anion exchange (AEX) chromatography was linked to several different precipitation steps to evaluate potential integration into a full bioprocess. Ammonium sulphate, sodium citrate, lithium sulphate, and two sodium sulphate precipitations, one with a prior low pH step, were carried out to capture IgG₁ from clarified cell culture fluid at 160mL scale, with the re-solubilised precipitates subsequently concentrated and buffer exchanged, then further purified with an anion exchange chromatography step. Precipitation conditions were selected from screening results based in Chapter Five.

Yield and purity performance were tracked throughout the process with protein A HPLC, size exclusion chromatography, lab-on-a-chip electrophoresis and non-reduced SDS-PAGE. Precipitation yields were found to exceed 95% with a 60% yield on the buffer exchange step and 70% on the AEX chromatography. At larger scale the cumulative yield is expected to be in excess of 80% for all three complete steps. The performance of different salt precipitants with respect to product purity carried across to the AEX step, with sodium sulphate the best performing precipitant, and the early work on the low pH step indicating even better process performance. Therefore, the selection and optimisation of salt-driven precipitants demonstrated the importance of impurity removal early on in downstream processing in order to reduce the burden on following purification steps.

6.2 Introduction

The main focus in this module of work was to understand how compatible salt-driven precipitation could be with fixed bed chromatography.

Prior art linking precipitation to ion exchange chromatography includes the purification of F(ab')₂ antibodies with caprylic acid precipitation and cation exchange chromatography [177], blood plasma protein fractionation with ethanol and cation exchange chromatography [132], and IgG precipitation with PEG followed by an anion and then a cation exchange chromatography step [98].

Knowing how the performance of different salt systems can impact the process would add clarity to the precipitant selection process. For example, if we saw the same yield and purity levels for all samples post chromatography, then the improved performance of different salts could be argued to be irrelevant if the subsequent step can *take up the slack*. Alternatively, *over-designing* the purification regime may still be advantageous, adding a greater level of robustness to in-process variation.

6.3 Precipitation conditions

Five precipitation conditions were brought forward to investigate. Four were selected based on performance and process understanding, whilst a bonus condition was tested which was based on promising early work on low pH conditions removing notable amounts of impurities. The conditions and results are covered in Table 20. 50mL of cell culture fluid was brought up to a working volume of 160mL with the addition of precipitants and diluents. Reactions were mixed in 500mL glass vessels using a magnetic stirrer set to 300rpm for 1 hour – the stirrer speed was calibrated with a light meter. Material was then transferred to sets of 50mL Falcon tubes and centrifuged for 45 minutes at 4,000rpm. Supernatant was removed by pipetting manually with minimal disruption of the precipitate and the net precipitate was res-suspended in 15mL of standard re-suspension buffer. The final volume was higher taking into account

the volume of the wet precipitate. All precipitates visibly re-solubilised in under a minute through a set of aspirate / dispense liquid manipulations by a pipette, as predicted from the micro-well experiments.

The low pH system was achieved by addition of 50mM acetic acid to the cell culture fluid to achieve a pH of 4.5. Instantaneous precipitation was observed, so a short hold time of five minutes was selected to mitigate against any possible product loss. Material was then 0.22µm filtered to remove precipitates, with the permeate then subjected to a 1.1M sodium sulphate precipitation, adjusted back up to pH 7.0 with 50mM NaOH under well mixed conditions (referenced as pHNaS for simplicity). Precipitated material from the low pH system could not be re-suspended into solution, indicating an irreversible precipitation pathway attributable to denaturation of the proteins from acidic conditions.

Table 20. Performance of precipitation steps on cell culture fluid.

160mL working volumes, IgG₁ concentration at 0.66mg/mL following addition of precipitants. IgG₁ yields and purity were measured through protein A HPLC.

Precipitant	Conditions (M, pH)	Re-suspended precipitate (mL)	IgG ₁ Concentration (mg/mL)	IgG ₁ recovered (mg)	Step yield (mg)	Total Purity (%)
Ammonium Sulphate	2.0M pH 7.0	16.87	6.22	118.35	112.7%	38.6%
Sodium Citrate	0.9M pH 7.0	16.92	6.21	122.41	116.6%	44.1%
Lithium Sulphate	1.6M pH 7.0	15.57	6.74	108.87	103.7%	49.9%
Sodium Sulphate	1.1M pH 7.0	15.95	6.58	115.39	109.9%	49.8%
Low pH + Sodium Sulphate	pH 4.0 then 1.1M pH 7.0	18.89	5.46	105.55	100.5%	58.2%

The step yields were based on an expected 105mg of IgG₁ in the starting feed, based on 50mL of 2.1mg/mL cell culture fluid. Yields exceeding 100% are most likely attributable to inaccuracy in the PrA HPLC method used to measure either the starting material or the recovered samples. The re-suspended precipitate volume was measured by determining the mass of the liquid and converted against a liquid density of 1000kgm⁻³, which could have

inflated the recovery yield if the material was denser. All supernatants were sampled and found to contain less than 1% of starting IgG through Protein A HPLC, so fundamentally the precipitation steps showed complete product precipitation, and with absence of residual solids, complete recovery. Absolute purity values, measured from the flow-through peaks differed between systems employed with the ammonium sulphate reaction performing the worst, and as expected the low pH followed by sodium sulphate reaction was the best. Protein A HPLC analysis on the five re-solubilised precipitates saw a variety in purification performance from the flow-through peaks at 0.6 minutes, attributable to selectivity differences of the purification performances. Purity can be said to follow the trend of pHNaS>NaS=LiS>NaCit>AS.

Table 21. pH and conductivity tracking throughout precipitation steps.

Precipitant	Stock		Mixed system		Re-solubilised material		Buffer exchange 1		Buffer exchange 2	
	pH	Ω mS/cm	pH	Ω mS/cm	pH	Ω mS/cm	pH	Ω mS/cm	pH	Ω mS/cm
Ammonium Sulphate 3.5M	7	253.9	7.05	210.6	7.67	95.5	8.07	4.9	8.02	3.3
Sodium Citrate 1.6M	7	59.1	7.11	65.3	7.58	40.2	7.74	5.7	8.01	3.2
Lithium Sulphate 2.5M	7.25	82.4	-	-	8.29	39.2	8.16	4.8	8.03	3.3
Sodium Sulphate 1.6M	7	115.3	7.23	100	8.24	34.3	8.26	5.3	8.06	3.3
pH pre-Sodium Sulphate n/a	n/a	n/a	4	12.3	-	-	-	-	-	=
post pH Sodium Sulphate 1.6M	7	115.3	6.95	98.8	7.43	30.6	8.18	3.34	8.06	3.3

Table 21 tracks the pH and conductivity of the systems as they went through the precipitation, recovery and buffer exchange steps. Stock represents the measured characteristics of the starting salt stock solutions, with the mixed system being the feed upon addition of diluent/precipitant. Each precipitant was buffered to pH 7.0 in 50mM phosphate buffer, with the exception of lithium sulphate, which was controlled slightly with a 10mM phosphate buffer, which avoided clouding the LiS. The criteria for the material to be suitable for anion exchange was set at <4mS/cm and at pH 8.0±0.1. Two buffer exchange steps were run until material met the specifications. The measurements for lithium sulphate upon precipitation

were mislaid, however are expected to be similar to the other precipitation systems and crucially the re-solubilised protein was within spec and readily buffer exchanged for the AEX steps.

6.4 Buffer exchange step

The re-solubilised material, at ~15mL in volume, were spun at 4,000 rpm for 15 minutes in 30kDa molecular weight cut-off spin tubes where typically 14-14.5mL of liquid had passed into the permeate. The retentate was then brought back to 15mL in pH 8.0 30mM Tris-HCl-10mM NaCl buffer with the action repeated for a second time. This was 15² to 30² in dilution ranging from 225 to an upper limit of 900 times, which in retrospect may have been a bit excessive. As displayed in Table 21, a second buffer exchange step was needed; however it would have been more sensible to set a retentate volume of 2mL each time, aiming for a combined buffer exchange factor of approximately 55.

Table 22. Buffer exchange step performance

Precipitant	Buffer Exchange step yield (%)	Total Purity (%)
Ammonium Sulphate	60.1%	48.2%
Sodium Citrate	49.8%	55.3%
Lithium Sulphate	62.1%	59.7%
Sodium Sulphate	57.4%	61.4%
Low pH + Sodium Sulphate	69.8%	70.7%

By over-concentrating the protein material significant IgG₁ was lost to the membrane, reducing the yield. Between thirty to fifty percent of IgG₁ product was lost on the membranes as detailed in Table 22. A280nm measurements on the permeate using a Nanodrop 2000 (Thermo Scientific, location) UV reader confirmed that material hadn't passed through the membrane. Carrying out this operation at larger scale, a step yield from a UF/DF step would be expected to be greater than 95%, and for the purposes of this study there was enough material for continuation with the anion exchange chromatography was generated. The buffer exchange step added a small degree of purification to the material, with the IgG₁ molecule ending up on average +10% purer (based on FT peak analysis). Molecules less than 10kDa in size passed

through the membrane and were discarded in the permeate, which can be seen in the following SDS-PAGE analysis.

6.5 Anion exchange chromatography step

An anion exchange chromatography step was selected. This process was selected since it separates proteins, and other substances such as DNA, by binding to negatively charged molecules, with positively charged components allowed to flow-through unimpaired. The tightness of the binding is associated with the strength of the negative charge of the molecule. An industry standard quaternary anion exchange resin was selected for the purification. It is a strong anion exchange resin, composed of rigid, high agarose matrix with dextran surface extenders and a quaternary ammonium anion exchanger. This resin was selected for the treatment of post-precipitation samples based on its current usage as the subsequent chromatography step following the primary protein A affinity capture step in UCB's platform. It offers high dynamic binding capacities at high flow rates, although these were not needed for the early stage process incorporation. The material was run through at pH 8.0, <4mS/cm, enabling for the amphoteric IgG₁ with a pI of 8.7 to exhibit a net positive charge. Hence the process was designed for impurities to bind to the resin whilst the product flows through the column and is collected. Bound impurities could then be removed from the column by using a high-salt strip buffer, leading to column regeneration and re-use.

Precipitates were re-suspended in pH 8.0 30mM Tris-HCl, 10mM NaCl, and subsequently exchanged again with this buffer twice, where the conductivity was measured to be less than 5mS/cm; suitable for the flow-through step. Buffer exchange was carried out with Amicon™ Ultra 30K membrane 0.5mL centrifugal filters (Millipore, Hertfordshire, UK). A 1 cm diameter, 10 cm bed height column packed with 7.8mL AEX resin column run with an Akta Explorer (GE Healthcare) chromatography system. A 1.3mL/min flowrate equated to a representative 300cmh⁻¹. The sequence of operations in Table 23 detail the clean, charge, equilibrate, material load, flush and strip operations, as can be seen in the chromatogram in Figure 58.

Table 23. AEX column operation regime.

Step	Buffer	Details	CVs
Clean	NaOH	0.5M	3
Charge	NaCl	1M + 30mM Tris pH 8	3
Equilibrate	Tris-HCl	30mM Tris, 10mM NaCl, pH 8.0	5
Load	IgG Feed	IgG in 30mM Tris, 10mM NaCl, pH 8.0	~3-4
Flush	Tris-HCl	30mM Tris, 10mM NaCl, pH 8.0	2
Strip	NaCl	1M + 30mM Tris pH 8	3

The anion exchange resin has a dynamic binding capacity of up to 160mg/mL BSA, based on manufacturer's figures, with the 7.8mL column selected capable of impurity clearance of up to 1250mg of proteins. With a maximum load of 68mg of IgG, the highest expected impurity load would be 70mg requiring capture and removal; no more than 5% of the column capacity. It would be better in future experiments to either use a smaller resin volume or increase the material loaded to ensure the chromatography step is working efficiently. However, this was a primary study to connect precipitation with chromatographic separations and not on chromatography optimisation. As with the case of reduced recovery yields in the automated micro-well plate methods, the focus was always to generate material for analysis, and understand trends.

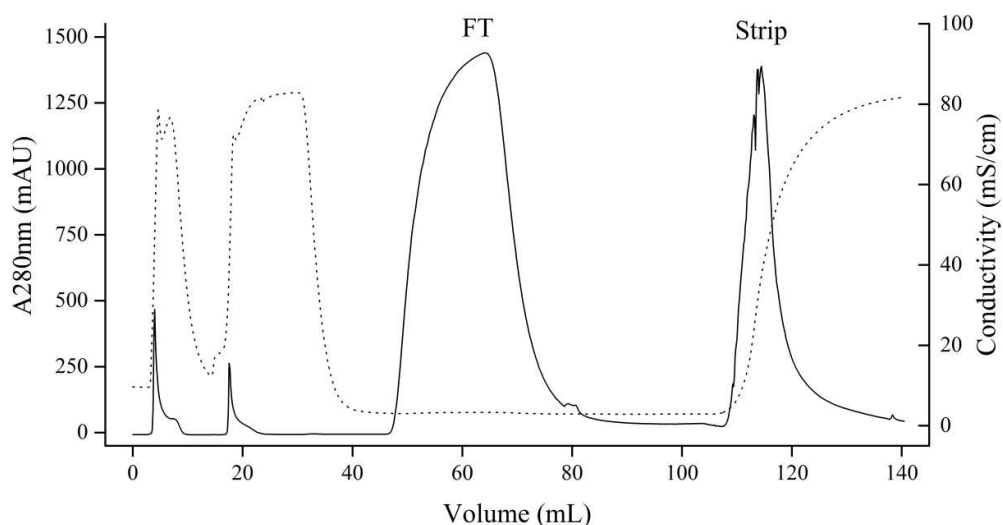


Figure 58. Anion exchange chromatogram for the purification of ammonium sulphate precipitated material.

Product was collected from the flow-through, with the AKTA system set up to collect flow-through once the absorbance exceeded 50mAU and end when it fell below. Impurities bound to the resin were collected in the 1M NaCl strip, in order to measure what had been removed in the step. Samples were then analysed.

Table 24. Anion exchange step performance.

Table covering the load, flow-through and strip volumes in the process. Bd denotes below detection limits of the method.

Starting Precipitant	IgG ₁ Loaded (mg/ml)	Loaded Volume (mL)	IgG ₁ Loaded (mg)	IgG ₁ Recovered (mg)	Step Yield	IgG ₁ in strip fraction (mg)	IgG ₁ in strip
AS	5.75	11.5	66.10	47.28	71.5%	0.91	1.4%
NaCit	5.73	9.84	56.35	28.80	51.1%	0.88	1.6%
LiS	4.76	12.74	60.70	46.34	76.3%	bd	0%*
NaS	5.55	11.05	61.34	37.56	61.2%	0.75	1.22%
pH-NaS	7.93	8.54	67.76	49.00	72.3%	0.62	0.89%

Through PrA HPLC analysis, displayed in Table 24, we can see low yields for the AEX step. The loss did not seem to be attributable to tightly bound product on the column as only a fraction was measured in the collected flow through. Assuming product was not denatured to an extent which would not bind to the Protein A ligand, the loss most likely resides from the volumes of material being run, with material lost in the pump wash steps. An injection loop would be the best option to minimise these losses.

6.6 Process flow SDS PAGE & Bioanalyzer

Non-reduced SDS-PAGE were run tracking the performance of each precipitant through the steps. Channels were loaded to 10 μg IgG₁ to display HCP bands more clearly.

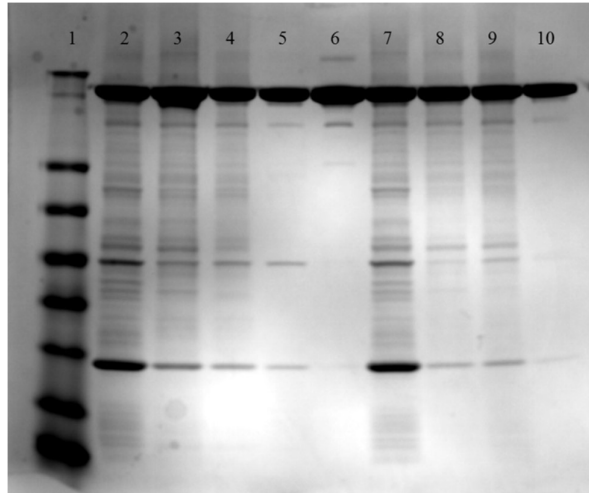


Figure 59. SDS PAGE process flow for ammonium sulphate and sodium citrate driven precipitations.

Lanes 1) protein ladder, 2) starting cell culture fluid 3) post ammonium sulphate precipitation 4) AS post buffer exchange 5) AS post AEX 6) IgG₁ standard 7) starting cell culture fluid 8) post sodium citrate precipitation 9) NaCit post buffer exchange 10) NaCit post AEX.

The non-reduced SDS-PAGE gel (Figure 59) shows the process flow for ammonium sulphate and sodium citrate. Immunoglobulin purity increases across the stages, with the buffer exchange step removing smaller proteins with the 10kDa molecular weight cut-off. Recovered material following the sodium citrate precipitation is the cleaner of the two, which was to be expected based on its superior selectivity. Each precipitation was carried out at pH 7.0 to standardise the salts.

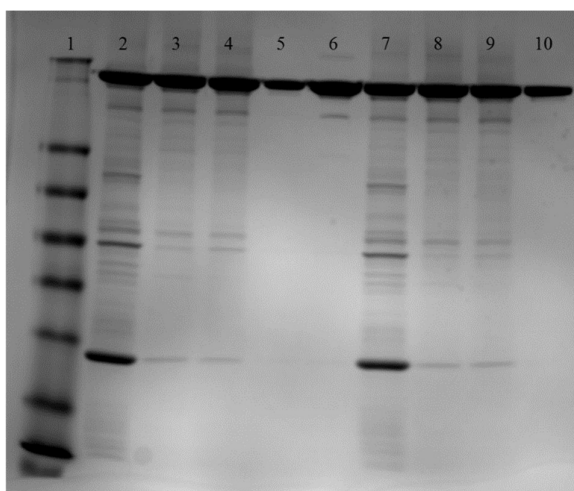


Figure 60. SDS PAGE process flow for lithium sulphate and sodium sulphate.

Lanes 1) protein ladder, 2) starting cell culture fluid 3) post lithium sulphate precipitation 4) LiS post buffer exchange, 5) LiS post AEX, 6) IgG₁ standard, 7) starting cell culture fluid 8) post sodium sulphate precipitation, 9) NaS post buffer exchange, 10) NaS post AEX.

Lithium and sodium sulphate salts (Figure 60) showed very similar performance, which was again expected. The final material in lanes 5 and 10 was under-loaded compared to the other samples so low concentration HCPs will be hard to see.

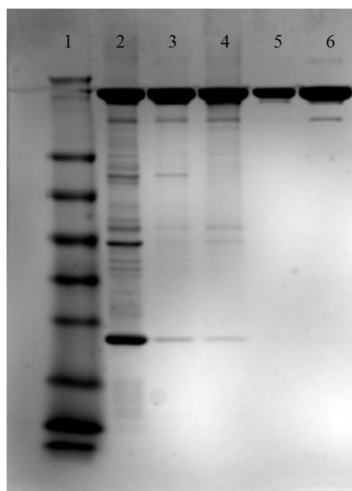


Figure 61. SDS PAGE process flow for the low pH plus sodium sulphate precipitation.

Lanes 1) protein ladder, 2) starting cell culture fluid, 3) post pH and sodium sulphate precipitation, 4) pH-NaS post buffer exchange, 5) pH-NaS post AEX 6) IgG₁ standard.

Finally, the low pH and sodium sulphate wildcard shows the cleanest feed, with a stark contrast between the starting process feed in lane 2 and the re-suspended material in lane 3. The

material post low pH only was omitted, which is a shame as seeing the HCP clearance by the acid addition could have added more insight. Nonetheless the purest material was generated from this approach, and this was without optimising the low pH hold step which offers an interesting avenue to explore in the future.

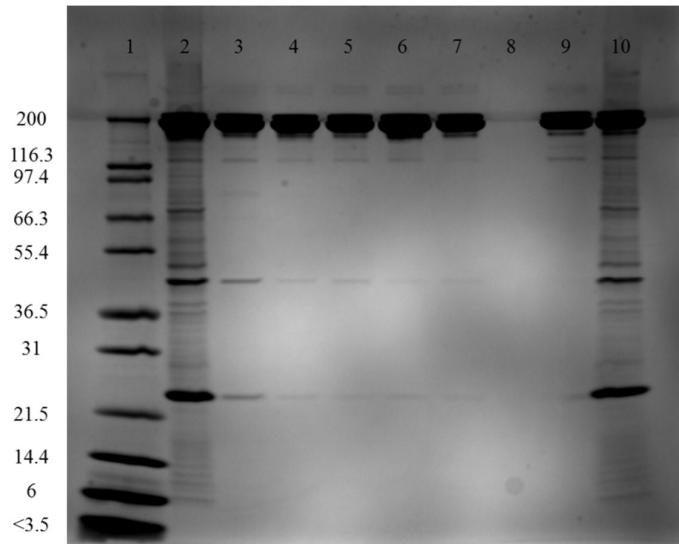


Figure 62. SDS PAGE displaying final feed compositions.

Lanes 1) protein ladder, 2) cell culture fluid sample, 3) ammonium sulphate driven precipitation, 4) sodium citrate, 5) lithium sulphate, 6) sodium sulphate, 7) sodium sulphate with a pre-pH step, 8) blank, 9) IgG₁ standard, 10) cell culture fluid sample.

Figure 62 shows non-reduced SDS-PAGE of the five purified IgG₁ materials having been put through their respective precipitation and anion exchange chromatography steps. All samples were loaded at 10µg of IgG₁ and by direct comparison the performance of different precipitants is clear. The least effective performing salt was ammonium sulphate with several clear HCP bands still present (between 55.4 - 36.5kDa and 31 - 1.5kDa), the purity increases from left to right, with the cleanest material being the low pH and sodium sulphate step. Although a qualitative assay, when compared to the IgG₁ standard in lane 9 which has been through a full purification process, precipitation plus anion exchange chromatography seems to closely match the purity. A further polishing chromatography step would be typically required to reduce HCP levels to a suitable ppm, e.g. 20ppm or less, and to ensure there is a step in the process to remove product related fragments/aggregates.

As an aside, with strong HCP bands still observable at around 25 and 45kDa, if a larger molecular weight cut-off membrane with utilised for the buffer exchange, such as a 50kDa average pore size, this may prove to add an extra level purification to the step whose primary objective is to prepare material for the anion exchange.

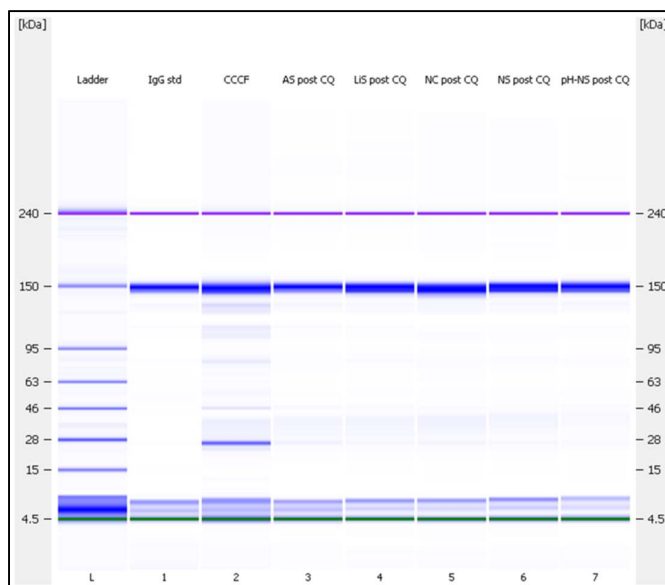


Figure 63. Non-reduced Bioanalyzer analysis of samples post AEX chromatography false gel image

Samples were then through a Bioanalyzer method to quantify the protein purity, Figure 63 displays the false gel image of the same samples run in Figure 62, whilst allowing for relative quantification of each protein band, hence allowing for an IgG₁ purity to be calculated. Table 25 records the protein purities of samples measured with the Bioanalyzer system. Greater than 10% of proteins were detected below 50kDa, confirming SDS-PAGE analysis.

Table 25. Bioanalyzer IgG₁ purity post anion exchange chromatography.

Standard purity was determined by the PrA HPLC flow-through method.

Sample	IgG standard	CCCF	AS	LiS	NaCit	NaS	pHNaS
Protein Purity	94.3%	50.5%	78.6%	83.3%	84.2%	83.7%	87.4%
Standard Purity	100%	53.6%	83.4%	88.3%	89.3%	88.8%	92.7%

6.7 iCE analysis

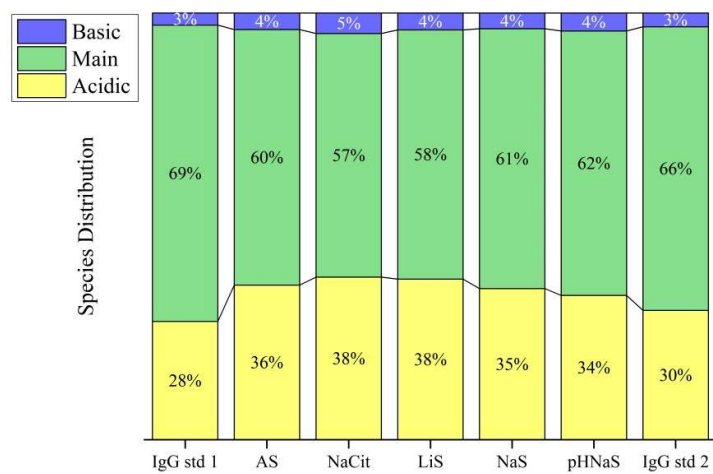


Figure 64. Isoelectric capillary electrophoresis of samples post precipitation and anion exchange chromatography.

The distributions of acidic, main and basic species of samples were then assessed through isoelectric capillary electrophoresis. Figure 64 shows the breakdown for each sample tested. The first observation is that for the five purified samples there's a $\pm 2.5\%$ variance between main and acidic species, which indicates little change of the IgG₁ (and remaining impurities in the sample). However, comparisons to the IgG₁ standard cannot be drawn with a greater than 5% decrease in main species observed. The first reason for poor comparison is that the purified IgG₁ and that from the cell culture fluid originated from different fermentation batches; secondly the purified immunoglobulin has been through a full purification process and may have been altered during this. Ideally a cell culture fluid sample purified by protein A chromatography should have been tested in parallel, in order to compare material from the same batches.

6.8 Process Integration Considerations

This initial work linking precipitation into a bioprocess regime has highlighted several challenges which are covered below.

6.8.1 Residual conductivity

The main challenge with linking salt-driven precipitation to anion exchange chromatography is that the residual salts, still native to the solid precipitate, raise the re-suspended solution to incompatible conductivities for the subsequent step. This makes a buffer exchange step essential to link the two processes together, adding an additional level of complexity to the process. However, as suggested earlier, if a higher molecular weight membrane, such as 50kD, then we could expect to see improved performance by removal of considerable low molecular weight HCPs. There are high salt-tolerant resins available commercially, for example, Capto MMC (GE Healthcare) offers dynamic binding capacities of 30-50mg/mL for up to 45mS/cm conductivities which could eliminate the need for a buffer exchange step, possibly only requiring only a 2-fold dilution on the re-solubilised precipitate – based on a sodium sulphate precipitate producing re-suspended conductivities of less than 35mS/cm.

6.8.2 Hydrophobic Interaction Chromatography

A different mode of chromatographic separation may avoid residual salt issues altogether. Hydrophobic interaction chromatography (HIC) works by manipulating the different hydrophobic properties of proteins by promoting separation based on hydrophobic interactions with immobilised ligands and non-polar regions on proteins [178]. The adsorption is most dominant under a high salt mobile phase (provided conditions conducive to precipitation are avoided) – which means that the precipitate could be simply re-suspended in this new salt system, and loaded onto the column, although we should expect much longer re-suspension times for the product. Selective elution is then achieved through a gradient dilution of the mobile phase eluent. The only foreseeable issue is that HIC works through a similar

mechanism akin to salting-out, by manipulating the hydrophobicity of soluble proteins (and other components) with similar Hofmeister trends observed for both precipitation and HIC [60], so the combination of these two steps may not offer a synergistic, orthogonal purification strategy.

Although not falling within the remit of this thesis, future experiments linking precipitation to chromatography could be readily integrated into the Tecan high throughput automated platform. Buffer exchange could be carried out on re-solubilised samples using a range of 96 well plate-based filter systems, such as MultiTrap 96-well plates (GE Healthcare) or AcroPrep 96 UF Filter Plates (Pall Life Sciences). Or through de-salting resins such as Zeba™ spin desalting plates (Thermo Scientific). Chromatography resins could then be screened in relatively high through-put of 8 columns on deck using MediaScout Robocolumns (Atoll). These are pre-packed small chromatography columns which can be packed with third party resins allowing for fully automated and parallel chromatographic separations through a liquid handling platform. Robocolumns would be the best option as they are compatible with the fixed tip robotic system employed, however for a disposable tip liquid handling platform, then PhyTip columns (PhyNexus) could be employed instead, these would require bi-directional liquid flow since these operate through resin-packed tips and it may be harder to equate to process relevant conditions.

The objective is to translate these small-scale findings to large scale application; adding chromatography screening to the high throughput precipitation screening platform could accelerate process development with potential for the whole process to be characterised and understood.

6.8.2 Pre-conditioning the process feed

One clear issue with salt-driven precipitation is the increase in process volumes required for the step. A 1:1- 1:2 dilution of feed to precipitant mix is typical so we can expect a 2 to 3-fold increase in volume of the cell culture fluid, which would require larger mixing and holding

vessels and increase purification process times. One option would be to pre-concentrate the cell culture fluid on a UF/DF rig to create a lower starting volume, allowing the precipitant solution to correct back up to the starting volume. The added advantage of this approach would be the creation of higher protein product concentrations which require lower concentrations of salt to precipitate, however it would be challenging to predict how purity would be affected since impurities would also be present in higher concentrations.

6.8.3 Mixing

Mixing conditions can dictate observed protein solubilities which have been shown to be the main contributing factor towards over-precipitation, followed then by the mode of precipitant addition and mixing shear rate [173]. This has been demonstrated in Figure 37 and Figure 38 in Chapter Four where the required precipitation mid-points were inversely proportional to the initial IgG₁ concentration.

Work in this thesis has solely focused on batch operations from varying micro-well volumes to lab scale mixing. As volumes scale up from the microlitre scale to large litre, mixing is expected to become less effective, as the mixing regime struggles to achieve homogenous conditions throughout the vessel. Poor mixing regimes will result in localised areas of non-homogeneity. For salt-driven precipitation the operating window is quite large, so higher or lower localised precipitant concentrations during initial mixing aren't expected to negatively impact performance, especially since the process has been shown to be freely reversible. This is an additional advantage salts hold over polyelectrolytes which are much more sensitive to small incremental pH and concentration changes. Over-precipitation, a consequence of high salt feed rates and low mixing conditions has been shown to lead to reduced protein activity upon re-suspension for the case of bovine liver catalase precipitation with ammonium sulphate [173].

Precipitation through salting out has been demonstrated to occur quickly; hence the contact time between feed and precipitant doesn't necessarily require a batch mix with a long incubation time. Continuous mixing may be an alternative option for process scale-up,

offering near-instantaneous mixing and theoretically uniform mixing. Precipitates can be rapidly formed in continuous reactors, however are most susceptible to shear breakup – whilst increasing the residence time hasn't been shown to significantly improve precipitate strength [148]. The mode of solid/liquid separation to recover the precipitates must be well characterised.

6.8.5 Centrifugal Recovery

Centrifugal recovery of precipitates has been run in batch mode, albeit in the micro-well format. When translating precipitate recovery to large scale, batch tubular bowl centrifugation appears to be the best option since it is designed for solid recovery and can offer high levels of dewatering. A high solids capacity means since protein precipitates may only amount to 3-4 g/L including product and HCPs, then it is protein mass and not system volume which is the rate limiting / equipment sizing determinant. High levels of equipment cycling won't be required nor exposure to high rates of shear.

Disk stack centrifuges are semi-continuous and can't be considered ideal for precipitate recovery since they generally offer lower dewatering and need to be re-configured for effective solids capture. However, if the equipment is already available, it would be worth considering instead of the need for increased capital investment. Disk stack centrifugation could be potentially easier to combine with a continuous precipitation mode of operation, however understanding particle sizing would be even more important since spin speeds cannot reach the levels of a tubular bowl, hence density disparity between precipitate and liquid phase needs to be maximised and well defined.

6.8.8 Recovery through filtration

An alternative approach for recovery and re-suspension of the protein precipitate could be to process the precipitated cell culture fluid on a UF/DF rig, where the solid precipitate is retained on the membrane, allowing for the liquid phase to be removed in the permeate. The precipitate

could then be re-suspended in a suitable buffer and flushed off the membrane. This could combine the separation, recovery and buffer exchange steps into a single unit operation, reducing time, material and equipment requirements. Limitations could include requiring a higher molecular weight cut-off, otherwise larger soluble HCPs could also be retained in the step, thus decreasing the purity of the recovered material. Membrane fouling could be an issue, along with a potential increase in levels of aggregation.

6.9 Chapter Summary

Early work linking precipitation to anion exchange chromatography indicates good synergy between the two steps. More detailed analysis will be required to verify these findings, such as activity testing and more sensitive purity analysis such through ELISA approaches. Running a direct comparison of a protein A chromatography step versus a precipitation and AEX step on starting cell culture fluid would provide the best benchmark to evaluate performance and allow for more informative results from the iCE, SDS-PAGE, and Bioanalyzer assays. A future experimental plan including an anion exchange step run directly on clarified cell culture fluid would help to understand how much value-added performance precipitation offers. Results have shown improved selectivity with different salts before, and after AEX so it is logical to conclude that the chromatography step is not simply picking up the slack. Resin re-use studies would also demonstrate the value of running a precipitation step. Precipitation allows for the near-complete removal of the liquid phase, so the expectation is for chromatography to exhibit better performance over time, assuming components leading to column fouling over time reside in the supernatant phase following precipitation.

Chapter Seven: Conclusions and Future Scope of Work

“Would you tell me, please, which way I ought to go from here?”
“That depends a good deal on where you want to get to,” said the Cat.
“I don’t much care where-” said Alice.
Then it doesn’t matter which way you go,” said the Cat.
“-so long as I get *somewhere*,” Alice added as an explanation.
“Oh, you’re sure to do that,” said the Cat, “if only you walk long enough.”

Lewis Carroll, Alice’s Adventures in Wonderland

7.1 Conclusions

An effective microwell format automated approach to isolating therapeutic proteins from cell broth through precipitation has been demonstrated, including the centrifugal recovery, re-suspension and analysis. The work was then used extensively to screen potential precipitants for an effective primary purification step. The focus has been upon salt driven precipitation and has shown how performance controlled by adjusting parameters such as pH, ionic strength and protein concentration. Sigmoidal precipitation curve fitting and midpoints were effective tools for quantifying the extent of precipitation, and for building an increased understanding of the effect of different Hofmeister salts. Notably the reproducibility of repeat experiments and quality of fitted data reflects well on the time invested in the method development and use of liquid handling robotics for precision experiments.

Aided with an improved control system for the Tecan liquid handling system, being able to readily run multi factor interactive experimental designs creates substantial process understanding in a short amount of time even with limited material available.

7.1.1 Alternative Applications

Techniques demonstrated in Chapter Three have a broader use beyond the scope of precipitation screening. During my time at UCB, the Excel VBA driven interface was introduced to scientists in both upstream and downstream processing sciences and from that *plug and play* protocols were built for fast, easy, and reliable total protein and DNA assays.

Using the Henderson-Hasselbach equation for pH, exact volumes of acid, base, and salt were calculated and then blended, creating individual well conditions with the Tecan systems. This enabled mini step gradients to be readily created in a 96 well plate and then applied to Atoll robocolumns to simulate gradient buffer profiles for more advanced chromatography scouting at microscale. Enhanced through Design of Experiments, more complex multicomponent screening of formulation buffers would also be simple to implement.

The screening methodology could readily be applied as an approach for identifying suitable buffer conditions for hydrophobic interaction chromatography, by actively avoiding precipitating conditions, whilst maximising the hydrophobicity of the target protein.

7.1.2 Scale-Up Considerations

One of the challenges with salt driven precipitation will be the material handling; large volumes of high molarity solution would require considerable time to create and blend before addition to the process fluid. Adding solid salt and dissolving it into the cell culture fluid may be one solution but achieving good homogeneity could be a challenge. Continuous mode of operation may be an option with precipitation, whereby mixing and precipitate aging could be controlled with a plug flow reactor. The solid/liquid separation and re-solubilisation steps may need to be performed semi-continuously from a practical perspective.

7.2 Future Expansion of Work

7.2.1 Key future work

Some important aspects of this project were not investigated and would need to be explored to expand the overall narrative and add credence to the impact of high throughput precipitation screening.

Running a parallel comparison with a default protein A then anion exchange chromatography would allow for the best direct comparison and highlight the strengths of each application. This could be done either with liquid handling robotics using scale down columns or run on conventional chromatography systems at lab scale.

An important bridging study should be done to test precipitation at increasing scales; microscale, 2 lab scales, and the pilot scale. This would establish the importance of mixing and processing time upon the process, which aren't covered in this body of work.

7.2.2 Acid pre-conditioning for precipitation

Although not presented, a series of experiments focused upon acidic / low pH precipitation conditions, which is what led to the low pH conditioning before sodium sulphate precipitation in Chapter Six. Adjusting the pH of the cell culture fluid to between pH 3 and 4.5 showed a near instantaneous cloudy solution, which could be removed either through 0.22 μ m filtration or conventional centrifugation. The precipitated material could not be re-suspended into a range of buffers tested and was assumed to be irreversibly precipitated / denatured. Following SDS-PAGE, Protein A HPLC, and Bioanalyzer assays, the precipitated material was shown to be a mixture of HCP impurities, and not the target IgG₁. This could include DNA and media impurities as well, though no tests were run to determine that.

Lowering the pH to even as low as 3 (0.2 increments up to pH 5 were tested) showed no loss of product. This may be due to the low pH being applied and mixed for 5 minutes before separating, but similarly low pH conditions are used on the IgG₁ in protein A affinity

chromatography for the elution step so this shouldn't be a surprise. CCCF was then pH adjusted back up to pH 7, 5 minutes showing itself to be a sufficient time to precipitate out a range of impurities from the process stream. Since a low pH hold operation is typically run post Protein A chromatography to act as a viral inactivation step, it could be advantageous for a precipitation driven purification regime to insert a low pH hold prior, and in doing so clean up the feed stream via a negative precipitation step.

This opens up an interesting future avenue of research, looking at the effect different precipitants could have upon this pre-low pH precipitation before the positive precipitation step is implemented. There may even be no need to remove the irreversible precipitates before adding the main precipitant, since the re-suspended material would likely be filtered before passing onto a subsequent downstream unit operation. Future investigations should focus on the use of polyelectrolytes, different acids, and processing times whilst tracking product structure and function throughout.

7.2.3 Analytical methods

Adding additional functionality to the automated screening protocol such as plate-based lipid and DNA assays would help build up a greater understanding of what impurities are removed and retained during precipitation. Sensitivity of these assays to residual salts would require de-salting / buffer exchange of samples before testing, which could be achieved on-deck with a range of plate-based solutions available commercially.

Host cell protein (HCP) ELISAs could also be incorporated into the methodology, however these are expensive assays and would be better suited for later stage development, especially considering the lower order of samples which can be assayed per plate when repeats and standards are included. Light Microscopy and Scanning Electron Microscopy (SEM) on both the suspended precipitates and on the recovered pellet would be informative. Precipitate pellets formed from different salts, PEG, and polyelectrolytes different in their physical appearance, ease of handling, and propensity to re-dissolve in solution. Visual inspection could aid in understanding how the appearance affects the physical properties, potentially identifying new combinations which could improve material handling. Particle size distribution on the precipitated solutions would add more quantitative information than microscopy data. Understanding precipitate sizes, and the effect time, shear caused by mixing, and precipitants have upon protein precipitates and their subsequent recovery and re-suspension would be important for scale up work.

Circular dichroism (CD) could be used to investigate the re-solubilisation / re-folding of precipitate pellets into a new buffer system. Throughout this work, the IgG₁ under investigation showed no issues with transitioning from a soluble to solid to soluble state, and loss of function was seen. Investigating the secondary structure of the protein in different states through CD could build a better understanding, especially for studies looking at the effect of precipitate hold/storage time and different, potentially more biologically aggressive precipitation strategies.

7.2.4 Screening on alternative proteins

Work throughout has focused on a specific monoclonal antibody. The high throughput methodology for precipitating, isolating, and recovering proteins could be readily applied to any number of new proteins requiring process development. This would be an interesting module of work, as it would identify suitable precipitants to build a purification step, but also determine how global the trends with protein concentration, pH, and ionic strength are, and whether a model could be built to predict future conditions based on starting information such as the pI of the protein and titre in the process fluid.

7.2.5 Recovery and re-suspension on a UF/DF rig

There is the option for using a UF/DF system for the separation and re-suspension of precipitates. The idea being that precipitated cell culture fluid could be passed onto the membrane, with the solids retained on the membrane in the precipitating solution, then flushed off and simultaneously recovered in the re-solubilisation buffer. The selection of a suitable molecular weight cut-off would be key when considering precipitates can lead to fouling and flow reduction. This would reduce the need for centrifugal separation and potentially increase the level of dewatering the protein pellet can achieve. Using established equipment would also decrease capital investment for integrating a precipitation step.

7.2.6 Alternative precipitants screening

Precipitation through salting-out has been the focus of investigations throughout this thesis. During the embryonic stages of this project a range of acids, high molecular weight polymers and polyelectrolytes were screened on early lysozyme model protein stocks and fab antibodies cultured from *Escherichia coli* fermentations. With the methodology established, future explorations of combinations of precipitants with differing modes of action would be an interesting avenue to explore. Polyelectrolyte precipitation has been shown to be very reliant on finessed pH and low conductivity conditions, so with the development of more accurate

high throughput probes for pH and conductivity measurement, screening becomes more viable.

7.2.7 The next step

Judging from the recent increase in publications on scale down chromatography using the Atoll robocolumn format, the expectation is for small scale automation to become a more dominant influencing factor in bioprocess research and development in the near future. Linking upstream and downstream unit operations together on a liquid handling deck, so that a seamless could be fully automated on the microscale will be the next big step. Following on from that, provided small scale data can be transformed to the manufacturing scale, we could well see the majority of future process development run at the microscale (or smaller), which can rapidly decrease development times and ultimately bring exciting new drugs to the market sooner. The loftier future goal would then be individually tailored medicines, all produced, purified, and formulated in micro or millilitre scale automated unit operations with in-line quality control.

Chapter Eight: References

References have been organised and formatted using Mendeley Reference Manager (Mendeley Inc, New York, US) and displayed in IEEE reference format. They are listed in the order they appear throughout the thesis.

- [1] R. P. Evens and K. I. Kaitin, "The Biotechnology Innovation Machine : A Source of Intelligent Biopharmaceuticals for the Pharma Industry Mapping Biotechnology's Success," *Nature*, vol. 95, no. 5, pp. 528-32, 2014.
- [2] J.A. DiMasi, et al., "Trends in risks associated with new drug development: success rates for investigational drugs." *Clin. Pharmacol. Ther.*, vol 87, no. 3, pp. 272-7, Mar. 2010.
- [3] D. W. Light and J. R. Lexchin, "Pharmaceutical research and development : what do we get for all that money ?," pp. 1–5, 2012.
- [4] S. Morgan, et al, "The cost of drug development: a systematic review.," *Health Policy*, vol. 100, no. 1, pp. 4–17, Apr. 2011.
- [5] M. Herper, "The cost of inventing a new drug," *Forbes*, 2013. [Online]. Available: <http://www.forbes.com/sites/matthewherper/2013/08/11/the-cost-of-inventing-a-new-drug-98-companies-ranked/>.
- [6] D. W. Light and R. Warburton, "Demythologizing the high costs of pharmaceutical research," *Biosocieties*, vol. 6, no. 1, pp. 34–50, Feb. 2011.
- [7] A. Shukla and J. Thömmes, "Recent advances in large-scale production of monoclonal antibodies and related proteins.," *Trends Biotechnol.*, vol. 28, no. 5, pp. 253–61, May 2010.
- [8] M. Micheletti and G. J. Lye, "Microscale bioprocess optimisation.," *Curr. Opin. Biotechnol.*, vol. 17, no. 6, pp. 611–8, Dec. 2006.
- [9] J. R. Birch and A. J. Racher, "Antibody production.," *Adv. Drug Deliv. Rev.*, vol. 58, no. 5–6, pp. 671–85, Aug. 2006.
- [10] P. Holmes and M. Al-Rubeai, "Improved cell line development by a high throughput affinity capture surface display technique to select for high secretors.," *J. Immunol. Methods*, vol. 230, no. 1–2, pp. 141–7, Nov. 1999.
- [11] F. M. Wurm, "Production of recombinant protein therapeutics in cultivated mammalian cells.," *Nat. Biotechnol.*, vol. 22, no. 11, pp. 1393–8, Nov. 2004.
- [12] D. Low, R. O'Leary, and N. S. Pujar, "Future of antibody purification.," *J. Chromatogr. B. Analyt. Technol. Biomed. Life Sci.*, vol. 848, no. 1, pp. 48–63, Mar. 2007.
- [13] B. Kelley, "Very large scale monoclonal antibody purification: the case for conventional unit operations.," *Biotechnol. Prog.*, vol. 23, no. 5, pp. 995–1008, 2007.
- [14] S. S. Farid, "Process economics of industrial monoclonal antibody manufacture.," *J. Chromatogr. B. Analyt. Technol. Biomed. Life Sci.*, vol. 848, no. 1, pp. 8–18, Mar. 2007.
- [15] K. M. Clark and C. E. Glatz, "Polymer Dosage Considerations in Polyelectrolyte Precipitation of Protein," *Biotechnol. Prog.*, vol. 3, no. 4, pp. 241–247, Dec. 1987.

- [16] A. Shukla, et al, "Downstream processing of monoclonal antibodies--application of platform approaches.," *J. Chromatogr. B. Analyt. Technol. Biomed. Life Sci.*, vol. 848, no. 1, pp. 28–39, Mar. 2007.
- [17] N. J. Titchener-Hooker, P. Dunnill, and M. Hoare, "Micro biochemical engineering to accelerate the design of industrial-scale downstream processes for biopharmaceutical proteins.," *Biotechnol. Bioeng.*, vol. 100, no. 3, pp. 473–87, Jun. 2008.
- [18] T. Yamada, "Therapeutic monoclonal antibodies.," *Keio J. Med.*, vol. 60, no. 2, pp. 37–46, Jan. 2011.
- [19] T. T. Hansel, H. Kropshofer, T. Singer, J. a Mitchell, and A. J. T. George, "The safety and side effects of monoclonal antibodies.," *Nat. Rev. Drug Discov.*, vol. 9, no. 4, pp. 325–38, Apr. 2010.
- [20] A. L. Nelson, E. Dhimolea, and J. M. Reichert, "Development trends for human monoclonal antibody therapeutics.," *Nat. Rev. Drug Discov.*, vol. 9, no. 10, pp. 767–74, Oct. 2010.
- [22] J. M. Reichert, C. J. Rosensweig, L. B. Faden, and M. C. Dewitz, "Monoclonal antibody successes in the clinic.," *Nat. Biotechnol.*, vol. 23, no. 9, pp. 1073–8, Sep. 2005.
- [23] P. McDonald, "Selective antibody precipitation using polyelectrolytes: a novel approach to the purification of monoclonal antibodies.," *Biotechnol. Bioeng.*, vol. 102, no. 4, pp. 1141–51, Mar. 2009.
- [24] F. Hilbrig and R. Freitag, "Protein purification by affinity precipitation," *J. Chromatogr. B*, vol. 790, no. 1–2, pp. 79–90, Jun. 2003.
- [25] R. G. Harrison, *Bioseparations Science and Engineering*. Oxford Univeristy Press, 2003.
- [26] H. F. Zoller, "Precipitation of Grain-Curd Casein from Pasteurized Milk, Including Sweet Cream Buttermilk.," *Ind. Eng. Chem.*, vol. 13, no. 6, pp. 510–514, Jun. 1921.
- [27] R. Aschaffenburg, "Preparation of β -casein by a modified urea fractionation method," *Reading*, no. 1003, pp. 259–261, 1963.
- [28] A.H. Palmer, "Crystalline Globulin from Cow's Milk," 1933.
- [29] M. Jeanpierre, "A rapid method for the purification of DNA from blood," *Nucleic Acids Res.*, vol. 15, no. 22, pp. 75014–75014, 1987.
- [30] E. Cohn, et al, "Preparation and Properties of Serum and Plasma Proteins. I. Size and Charge of Proteins Separating upon Equilibration across Membranes with Ammonium Sulfate Solutions of Controlled pH, Ionic Strength and Temperature," *J. Am. Chem. Soc.*, vol. 62, no. 12, pp. 3386–3393, Dec. 1940.
- [31] P. Kistler and H. Nitschmann, "Large scale production of human plasma fractions. Eight years experience with the alcohol fractionation procedure of Nitschmann, Kistler and Lergier.," *Vox Sang.*, vol. 7, pp. 414–24, 1962.
- [32] S. Matheus, W. Friess, D. Schwartz, and H. Mahler, "Liquid High Concentration IgG₁ Antibody Formulations by Precipitation," *J. Pharm. Sci.*, vol. 98, no. 9, pp. 3043–3057, 2009.
- [33] S. N. Timasheff, "The control of protein stability and association by weak interactions with water: How do solvents affect these processes?," *Control*, pp. 67–97, 1993.

- [34] T. Arakawa and S. N. Timasheff, "Mechanism of protein salting in and salting out by divalent cation salts: balance between hydration and salt binding.," *Biochemistry*, vol. 23, no. 25, pp. 5912–23, Dec. 1984.
- [35] S. Roe, *Protein Purification Techniques*, 2nd ed. Oxford Univeristy Press, 2000.
- [36] W. Melander and C. Horvath, "Chromatography on Hydrophobic Interactions of Proteins : An Interpretation in Precipitation and of the Lyotropic Series ' ,," *Biochem. Biophys.*, vol. 183, pp. 200–215, 1977.
- [37] J. J. Grigsby, H. W. Blanch, and J. M. Prausnitz, "Cloud-point temperatures for lysozyme in electrolyte solutions: effect of salt type, salt concentration and pH.," *Biophys. Chem.*, vol. 91, no. 3, pp. 231–43, Jul. 2001.
- [38] A. McPherson and J. a Gavira, "Introduction to protein crystallization.," *Acta Crystallogr. Sect. F, Struct. Biol. Commun.*, vol. 70, no. Pt 1, pp. 2–20, Jan. 2014.
- [39] F. Hofmeister, "Zur Lehre von der Wirkung der Salze," *Arch. Exp. Path. Pharm.*, vol. 24, p. 247, 1887.
- [40] Y. Zhang and P. S. Cremer, "Interactions between macromolecules and ions: The Hofmeister series.," *Curr. Opin. Chem. Biol.*, vol. 10, no. 6, pp. 658–63, Dec. 2006.
- [41] C. J. Coen, H. W. Blanch, and J. M. Prausnitz, "Salting out of aqueous proteins: Phase equilibria and intermolecular potentials," *AIChE J.*, vol. 41, no. 4, pp. 996–1004, Apr. 1995.
- [42] J. Lyklema, "Simple Hofmeister series," *Chem. Phys. Lett.*, vol. 467, no. 4–6, pp. 217–222, Jan. 2009.
- [43] Z. Yang, "Hofmeister effects: an explanation for the impact of ionic liquids on biocatalysis.," *J. Biotechnol.*, vol. 144, no. 1, pp. 12–22, Oct. 2009.
- [44] R. L. Baldwin, "How Hofmeister ion interactions affect protein stability.," *Biophys. J.*, vol. 71, no. 4, pp. 2056–63, Oct. 1996.
- [45] R. Curtis and L. Lue, "A molecular approach to bioseparations: Protein–protein and protein–salt interactions," *Chem. Eng. Sci.*, vol. 61, no. 3, pp. 907–923, Feb. 2006.
- [46] K. D. Collins, "Ions from the Hofmeister series and osmolytes: effects on proteins in solution and in the crystallization process.," *Methods*, vol. 34, no. 3, pp. 300–11, Nov. 2004.
- [47] R. Curtis, J. Ulrich, A. Montaser, J. M. Prausnitz, and H. W. Blanch, "Protein-protein interactions in concentrated electrolyte solutions.," *Biotechnol. Bioeng.*, vol. 79, no. 4, pp. 367–80, Aug. 2002.
- [48] R. Curtis, C. Steinbrecher, M. Heinemann, H. W. Blanch, and J. M. Prausnitz, "Hydrophobic forces between protein molecules in aqueous solutions of concentrated electrolyte.," *Biophys. Chem.*, vol. 98, no. 3, pp. 249–65, Aug. 2002.
- [49] M. M. Ries-kautts and A. F. Ducruix, "Relative Effectiveness of Various Ions on the Solubility and Crystal Growth of Lysozyme *," vol. 264, no. 2, pp. 745–748, 1989.
- [50] M. Boström, F. W. Tavares, S. Finet, F. Skouri-Panet, a Tardieu, and B. W. Ninham, "Why forces between proteins follow different Hofmeister series for pH above and below pI.," *Biophys. Chem.*, vol. 117, no. 3, pp. 217–24, Oct. 2005.

- [51] Y. C. Shih, J. M. Prausnitz, and H. W. Blanch, "Some characteristics of protein precipitation by salts.," *Biotechnol. Bioeng.*, vol. 40, no. 10, pp. 1155–64, Dec. 1992.
- [52] P. Foster, P. Dunnill, and M. Lilly, "The kinetics of protein salting-out: precipitation of yeast enzymes by ammonium sulfate.," *Biotechnol. Bioeng.*, vol. 18, no. 4, pp. 545–80, Apr. 1976.
- [53] P.R.Foster, P.Dunnill, and M.D.Lilly, "Salting-Out of Enzymes with Ammonium Sulphate.," *Biotechnol. Bioeng.*, vol. XI, pp. 713–718, 1971.
- [54] D. Atha and K. Ingham, "Mechanism of precipitation of proteins by polyethylene glycols. Analysis in terms of excluded volume.," *J. Biol. Chem.*, vol. 256, no. 23, pp. 12108–12117, Dec. 1981.
- [55] W. Kunz, J. Henle, and B. W. Ninham, "'Zur Lehre von der Wirkung der Salze' (about the science of the effect of salts): Franz Hofmeister's historical papers," *Curr. Opin. Colloid Interface Sci.*, vol. 9, no. 1–2, pp. 19–37, Aug. 2004.
- [56] A. McPherson and J. Gavira, "Introduction to protein crystallization.," *Acta Crystallogr. Sect. F, Struct. Biol. Commun.*, vol. 70, no. Pt 1, pp. 2–20, Jan. 2014.
- [57] I. Russo Krauss, A. Merlino, A. Vergara, and F. Sica, "An overview of biological macromolecule crystallization.," *Int. J. Mol. Sci.*, vol. 14, no. 6, pp. 11643–91, Jan. 2013.
- [58] A. Arunakumari and M. G. Ferreira, "Protein purification by citrate precipitation," US8063189 B22011.
- [59] E. Wenzig, S. Lingg, P. Kerzel, G. Zeh, and A. Mersmann, "Comparision of selected methods for downstream processing in the production of bacterial lipase," *Chem. Eng. Technol.*, vol. 16, pp. 405–412, 1993.
- [60] B. K. Nfor, et al, "High-throughput protein precipitation and hydrophobic interaction chromatography: salt effects and thermodynamic interrelation.," *J. Chromatogr. A*, vol. 1218, no. 49, pp. 8958–73, Dec. 2011.
- [61] F. Perosa, R. Carbone, S. Ferrone, and F. Dammacco, "Purification of human immunoglobulins by sequential precipitation with caprylic acid and ammonium sulphate.," *J. Immunol. Methods*, vol. 128, no. 1, pp. 9–16, Mar. 1990.
- [62] M. N. Gupta, R. Kaul, D. Guoqiang, U. Dissing, and B. Mattiasson, "Affinity precipitation of proteins.," *J. Mol. Recognit.*, vol. 9, no. 5–6, pp. 356–9.
- [63] F. Hilbrig and R. Freitag, "Protein purification by affinity precipitation," *J. Chromatogr. B*, vol. 790, no. 1–2, pp. 79–90, Jun. 2003.
- [64] Y. Cheng, R. F. Lobo, S. I. Sandler, and A. M. Lenhoff, "Kinetics and Equilibria of Lysozyme Precipitation and Crystallization in Concentrated Ammonium Sulfate Solutions," *Biotechnology*, no. Rie 1989, 2006.
- [65] S. S. Ahmad and P. Dalby, "Thermodynamic parameters for salt-induced reversible protein precipitation from automated microscale experiments.," *Biotechnol. Bioeng.*, vol. 108, no. 2, pp. 322–32, Feb. 2011.
- [66] S. Branston, E. Stanley, E. Keshavarz-Moore, and J. Ward, "Precipitation of filamentous bacteriophages for their selective recovery in primary purification.," *Biotechnol. Prog.*, vol. 28, no. 1, pp. 129–36, 2011.

- [67] M. A. H. Capelle, R. Gurny, and T. Arvinte, "High throughput screening of protein formulation stability: practical considerations.," *Eur. J. Pharm. Biopharm.*, vol. 65, no. 2, pp. 131–48, Feb. 2007.
- [68] S. Tobler, N. E. Sherman, and E. J. Fernandez, "Tracking lysozyme unfolding during salt-induced precipitation with hydrogen exchange and mass spectrometry.," *Biotechnol. Bioeng.*, vol. 71, no. 3, pp. 194–207, 2001.
- [69] D. E. Kuehner, H. W. Blanch, and J. M. Prausnitz, "Salt-Induced Protein Precipitation: Phase Equilibria from an Equation of State," *Science (80-.)*, vol. 116, pp. 140–147, 1996.
- [70] M. M. McKinney and A. Parkinson, "A simple, non-chromatographic procedure to purify immunoglobulins from serum and ascites fluid.," *J. Immunol. Methods*, vol. 96, no. 2, pp. 271–8, Feb. 1987.
- [71] A. Polson, G. Potgieter, J. Largier, G. Mears, and F. Joubert, "The fractionation of protein mixtures by linear polymers of high molecular weight," *Virus Res.*, vol. 82, no. 1964, pp. 463–475, 1963.
- [72] P. F. Schubert and R. K. Finn, "Alcohol precipitation of proteins: The relationship of denaturation and precipitation for catalase," *Biotechnol. Bioeng.*, vol. 23, no. 11, pp. 2569–2590, Nov. 1981.
- [73] "Method for the extraction of one or several proteins present in milk," CN101501059 A2009.
- [74] R. W. Maurer, S. I. Sandler, and A. M. Lenhoff, "Salting-in characteristics of globular proteins.," *Biophys. Chem.*, vol. 156, no. 1, pp. 72–8, Jun. 2011.
- [75] A. K. Balls and H. Lineweaver, "Isolation and properties of crystalline papain," *J. Biol. Chem.*, vol. 130, pp. 669–686, 1939.
- [76] G. Bizhanov, I. Jonauskienė, and J. Hau, "A novel method, based on lithium sulfate precipitation for purification of chicken egg yolk immunoglobulin Y, applied to immunospecific antibodies against Sendai virus.," *Scand. J. Lab. Anim. Sci.*, vol. 31, no. 3, pp. 121–130, 2004.
- [77] E. M. Akita and S. Nakai, "Comparison of four purification methods for the production of immunoglobulins from eggs laid by hens immunized with an enterotoxigenic E. coli strain.," *J. Immunol. Methods*, vol. 160, no. 2, pp. 207–14, Apr. 1993.
- [78] M. J. Surendar, "Fractionation of protein mixtures by salt addition followed by dialysis treatment," CA 1142175A11982.
- [79] R. Tran and N. J. Titchener-hooker, "Aqueous two phase extraction augmented precipitation process for purification of therapeutic proteins," EP2350113 A12014.
- [80] A. M. Azevedo, G. Gomes, P. J. Rosa, I. F. Ferreira, A. M. M. O. Pisco, and M. R. Aires-Barros, "Partitioning of human antibodies in polyethylene glycol–sodium citrate aqueous two-phase systems," *Sep. Purif. Technol.*, vol. 65, no. 1, pp. 14–21, Feb. 2009.
- [81] J. C. H. R. Jensenius, I. Andersen, J. Hau, and C. Koch, "Conveniently packaged antibodies. Methods for purification of yolk IgG," *J. Immunol. Methods*, vol. 46, pp. 63–68, 1981.
- [82] P. E. Howe, "The determination of fibrinogen by precipitation with sodium sulfate compared with the precipitation of fibrin by the addition of calcium chloride," *J. Biol. Chem.*, vol. 57, pp. 235–240, 1923.

- [83] G. Neal, J. Christie, E. Keshavarz-Moore, and P. A. Shamlou, "Ultra scale-down approach for the prediction of full-scale recovery of ovine polyclonal immunoglobulins used in the manufacture of snake venom-specific Fab fragment.," *Biotechnol. Bioeng.*, vol. 81, no. 2, pp. 149–57, Jan. 2003.
- [84] A. Deutsch, M. Eggleton, and P. Eggleton, "The use of sodium sulphate for the preparation of concentrated protein-free tissue extracts," 1937.
- [85] C. Fargeot, C. Bebon, D. Colson, J. P. Klein, A. F. Blandin, and M. Bossoutrot, J, "A simple and efficient method to characterize bonded water molecules in aqueous solutions of electrolytes: Application to sodium sulphate decahydrate," *J. Cryst. Growth*, pp. 97–103, 2007.
- [86] B. Balasundaram, S. Sachdeva, and D. G. Bracewell, "Dual salt precipitation for the recovery of a recombinant protein from *Escherichia coli*," *Biotechnol. Prog.*, vol. 27, no. 5, pp. 1306–14, 2011.
- [87] A. Senczuk and R. Klinke, "Process for purifying proteins," US8273707 B22004.
- [88] C. Polson, P. Sarkar, B. Incledon, V. Raguvaran, and R. Grant, "Optimization of protein precipitation based upon effectiveness of protein removal and ionization effect in liquid chromatography-tandem mass spectrometry.," *J. Chromatogr. B. Analyt. Technol. Biomed. Life Sci.*, vol. 785, no. 2, pp. 263–75, Mar. 2003.
- [89] A. Lali, A. N. R. John, and D. Thakrar, "Reversible precipitation of proteins on carboxymethyl cellulose," *Process Biochem.*, vol. 35, no. 8, pp. 777–785, Mar. 2000.
- [90] P. Zaworksi and G. Gill, "Precipitation and Recovery Supernatants of Proteins from Culture Using Zinc Plasminogen activator activity assay . PA," *Anal. Biochem.*, vol. 173, pp. 440–444, 1988.
- [91] P. Foster, P. Dunnill, and M. Lilly, "The precipitation of enzymes from cell extracts of *Saccharomyces cerevisiae* by polyethyleneglycol," *Biochim. Biophys. Acta - Protein Struct.*, vol. 317, no. 2, pp. 505–516, Aug. 1973.
- [92] T. Arakawa and S. N. Timasheff, "Mechanism of poly(ethylene glycol) interaction with proteins.," *Biochemistry*, vol. 24, no. 24, pp. 6756–62, Nov. 1985.
- [93] V. Kumar, V. K. Sharma, and D. S. Kalonia, "Effect of polyols on polyethylene glycol (PEG)-induced precipitation of proteins: Impact on solubility, stability and conformation.," *Int. J. Pharm.*, vol. 366, no. 1–2, pp. 38–43, Jan. 2009.
- [94] H. Mahadevan, "Experimental analysis of protein precipitation by polyethylene glycol and comparison with theory," *Fluid Phase Equilib.*, vol. 78, no. 2, pp. 297–321, Oct. 1992.
- [95] W. Hönig and M. R. Kula, "Selectivity of protein precipitation with polyethylene glycol fractions of various molecular weights.," *Anal. Biochem.*, vol. 72, pp. 502–12, May 1976.
- [96] T. J. Gibson, K. Mccarty, I. J. Mccadyen, E. Cash, P. Dalmonte, K. D. Hinds, A. A. Dinerman, J. C. Alvarez, and D. B. Volkin, "Application of a High-Throughput Screening Procedure with PEG-Induced Precipitation to Compare Relative Protein Solubility During Formulation Development with IgG1 Monoclonal Antibodies," vol. 100, no. 3, pp. 1009–1021, 2011.
- [97] C. Knevelman, J. Davies, L. Allen, and N. J. Titchener-Hooker, "High-throughput screening techniques for rapid PEG-based precipitation of IgG4 mAb from clarified cell culture supernatant.," *Biotechnol. Prog.*, vol. 26, no. 3, pp. 697–705, 2009.

- [98] G. Giese, A. Myrold, J. Gorrell, and J. Persson, "Purification of antibodies by precipitating impurities using Polyethylene Glycol to enable a two chromatography step process.," *J. Chromatogr. B. Analyt. Technol. Biomed. Life Sci.*, vol. 938, pp. 14–21, Nov. 2013.
- [99] S.-L. Sim, T. He, A. Tscheliessnig, M. Mueller, R. B. H. Tan, and A. Jungbauer, "Branched polyethylene glycol for protein precipitation.," *Biotechnol. Bioeng.*, vol. 109, no. 3, pp. 736–46, Mar. 2012.
- [100] A. Petenate and C. Glatz, "Isoelectric precipitation of soy protein. II. Kinetics of protein aggregate growth and breakage.," *Biotechnol. Bioeng.*, vol. 25, no. 12, pp. 3059–78, Dec. 1983.
- [101] F. Steindl, "Isoelectric precipitation and gel chromatography for purification of monoclonal IgM," *Enzyme Microb. Technol.*, vol. 9, no. 6, pp. 361–364, Jun. 1987.
- [102] J. Sieberz, B. Stanislawski, K. Wohlgenuth, and G. Schembecker, "Identification of parameter interactions influencing the precipitation of a monoclonal antibody with anionic polyelectrolytes," *Sep. Purif. Technol.*, vol. 127, pp. 165–173, Apr. 2014.
- [103] M. B. Dainiak, "Production of Fab fragments of monoclonal antibodies using polyelectrolyte complexes.," *Anal. Biochem.*, vol. 277, no. 1, pp. 58–66, Jan. 2000.
- [104] W. E. N. Chen, "The Effect of Polyelectrolyte Dosage on Floc Formation in Protein Precipitation by Polyelectrolytes," *Chem. Eng. Sci.*, vol. 48, no. 10, pp. 1775–1784, 1993.
- [105] V. Izumrudov, Galaev Yu, and B. Mattiasson, "Polycomplexes--potential for bioseparation.," *Bioseparation*, vol. 7, no. 4–5, pp. 207–20, 1999.
- [106] H. Morawetz and W. Highes, "The interaction of proteins with synthetic polyelectrolytes. The complexing of bovine serum albumin.," *Proteins*, vol. 56, no. 15, pp. 64–69, 1952.
- [107] M. Temponi, T. Kageshita, F. Perosa, R. Ono, H. Okada, and S. Ferrone, "Purification of murine IgG monoclonal antibodies by precipitation with caprylic acid: comparison with other methods of purification.," *Hybridoma*, vol. 8, no. 1, pp. 85–95, Feb. 1989.
- [108] V. Boeris, B. Farruggia, and G. Picó, "Chitosan-bovine serum albumin complex formation: a model to design an enzyme isolation method by polyelectrolyte precipitation.," *J. Chromatogr. B. Analyt. Technol. Biomed. Life Sci.*, vol. 878, no. 19, pp. 1543–8, Jun. 2010.
- [109] J. Ma, H. Hoang, T. Myint, T. Peram, R. Fahrner, and J. H. Chou, "Using precipitation by polyamines as an alternative to chromatographic separation in antibody purification processes.," *J. Chromatogr. B. Analyt. Technol. Biomed. Life Sci.*, vol. 878, no. 9–10, pp. 798–806, Mar. 2010.
- [110] A. G. Bozzano and C. E. Glatz, "Separation of proteins from polyelectrolytes by ultrafiltration," *J. Memb. Sci.*, vol. 55, no. 1–2, pp. 181–198, Jan. 1991.
- [111] R. R. Fisher and C. E. Glatz, "Polyelectrolyte precipitation of proteins: I. The effect of reactor conditions.," *Biotechnol. Bioeng.*, vol. 32, no. 6, pp. 777–85, Sep. 1988.
- [112] Y. Wang, J. Gao, and P. Dubin, "Protein Separation via Polyelectrolyte Coacervation: Selectivity and Efficiency," *Biotechnol. Prog.*, vol. 12, no. 3, pp. 356–362, Jun. 1996.
- [113] J. Xia, P. L. Dubin, Y. Kim, B. B. Muhoberac, and V. J. Klimkowski, "Electrophoretic and quasi-elastic light scattering of soluble protein-polyelectrolyte complexes," *J. Phys. Chem.*, vol. 97, no. 17, pp. 4528–4534, Apr. 1993.

- [114] S. I. Cheng and D. C. Stuckey, "Protein precipitation using an anionic surfactant," *Process Biochem.*, vol. 47, no. 5, pp. 712–719, May 2012.
- [115] J. Ma, H. Hoang, T. Myint, T. Peram, R. Fahrner, and J. H. Chou, "Using precipitation by polyamines as an alternative to chromatographic separation in antibody purification processes.," *J. Chromatogr. B. Analyt. Technol. Biomed. Life Sci.*, vol. 878, no. 9–10, pp. 798–806, Mar. 2010.
- [116] K. Kogej, "Association and structure formation in oppositely charged polyelectrolyte-surfactant mixtures.," *Adv. Colloid Interface Sci.*, vol. 158, no. 1–2, pp. 68–83, Jul. 2010.
- [117] C. D. Bain, P. M. Claesson, D. Langevin, R. Meszaros, T. Nylander, C. Stubenrauch, S. Titmuss, and R. von Klitzing, "Complexes of surfactants with oppositely charged polymers at surfaces and in bulk.," *Adv. Colloid Interface Sci.*, vol. 155, no. 1–2, pp. 32–49, Mar. 2010.
- [118] H. Shu, D. Guoqiang, R. Kaul, and B. Mattiasson, "Purification of the d-lactate dehydrogenase from *Leuconostoc mesenteroides* ssp. *cremoris* using a sequential precipitation procedure," *J. Biotechnol.*, vol. 34, no. 1, pp. 1–11, Apr. 1994.
- [119] C. Schneider, M. Guillot, and B. Lamy, "The Affinity Precipitation Technique. Application to the Isolation and Purification of Trypsin from Bovine Pancreas," *Biochem. Eng. II*, vol. 369, no. 12, pp. 257–264, 1981.
- [120] A. Kumar, I. Y. Galaev, and B. Mattiasson, "Affinity Precipitation of α -Amylase Inhibitor from Wheat Meal by Metal Chelate Affinity Binding Using Cu (II) -Loaded Copolymers of with N-Isopropylacrylamide," *Biotechnology*, no. II, 1998.
- [121] J. Chen, "Novel affinity-based processes for protein purification," *J. Ferment. Bioeng.*, vol. 70, no. 3, pp. 199–209, 1990.
- [122] K. Mosbach, H. Guilford, P. Larsson, R. Ohlsson, and M. Scott, "Purification of nicotinamide-adenine dinucleotide-dependent dehydrogenases by affinity chromatography.," *Biochem. J.*, vol. 125, no. 2, p. 20P, 1971.
- [123] J. C. Pearson, S. J. Burton, and C. R. Lowe, "Affinity precipitation of lactate dehydrogenase with a triazine dye derivative: selective precipitation of rabbit muscle lactate dehydrogenase with a procion blue H-B analog.," *Anal. Biochem.*, vol. 158, no. 2, pp. 382–9, Nov. 1986.
- [124] J.-P. Chen, "Novel affinity-based processes for protein purification," *J. Ferment. Bioeng.*, vol. 70, no. 3, pp. 199–209, Jan. 1990.
- [125] N. Labrou and Y. D. Clonis, "The affinity technology in downstream processing.," *J. Biotechnol.*, vol. 36, no. 2, pp. 95–119, Aug. 1994.
- [126] K. Flygare, S. Tadhg, G. Larsson, P-O. Mosbach, "Affinity precipitation of Dehydrogenases," vol. 6, 1983.
- [127] A. Kumar, I. Y. Galaev, and B. Mattiasson, "Isolation and separation of α -amylase inhibitors I-1 and I-2 from seeds of ragi (Indian finger millet , *Eleusine coracana*) by metal chelate affinity precipitation," *Enzyme*, no. Ii, pp. 129–136, 1998.
- [128] J. C. Pearson, Y. D. Clonis, and C. R. Lowe, "Preparative affinity precipitation of L-lactate dehydrogenase," *Structure*, vol. 11, pp. 267–274, 1989.
- [129] M. Hayet and M. Vijayalakshmi, "Affinity precipitation of proteins using bis-dyes. Synthesis of the bis-dye," *Science (80-)*, vol. 376, pp. 157–161, 1986.

- [130] I. Y. Galaev and B. Mattiasson, "Affinity thermoprecipitation: Contribution of the efficiency of ligand-protein interaction and access of the ligand.," *Biotechnol. Bioeng.*, vol. 41, no. 11, pp. 1101–6, May 1993.
- [131] A. Kumar, I. Y. Galaev, and B. Mattiasson, "Metal chelate affinity precipitation: a new approach to protein purification," *Bioseparation*, pp. 185–194, 1999.
- [132] F. Moure, "Coupling process for plasma protein fractionation using ethanol precipitation and ion exchange chromatography," *Meat Sci.*, vol. 64, no. 4, pp. 391–398, Aug. 2003.
- [133] R. K. Scopes, *Protein Purification: Principles and Practice 2nd ed.* Springer Verlag, New York, 1987.
- [134] A. Bhambhani, J. M. Kissmann, S. B. Joshi, D. B. Volkin, and R. S. Kashi, "Formulation Design and High-Throughput Excipient Selection Based on Structural Integrity and Conformational Stability of Dilute and Highly Concentrated IgG1 Monoclonal Antibody," vol. 101, no. 3, pp. 1120–1135, 2012.
- [135] T. J. Kamerzell, R. Esfandiary, S. B. Joshi, C. R. Middaugh, and D. B. Volkin, "Protein-excipient interactions: mechanisms and biophysical characterization applied to protein formulation development.," *Adv. Drug Deliv. Rev.*, vol. 63, no. 13, pp. 1118–59, Oct. 2011.
- [136] C. E. Glatz, M. Hoare, and J. Landa-Vertiz, "The formation and growth of protein precipitates in a continuous stirred-tank reactor," *AIChE J.*, vol. 32, no. 7, pp. 1196–1204, Jul. 1986.
- [137] M. Boström, D. Williams, and B. Ninham, "Specific Ion Effects: Why DLVO Theory Fails for Biology and Colloid Systems," *Phys. Rev. Lett.*, vol. 87, no. 16, p. 168103, Oct. 2001.
- [138] A. Saluja and D. S. Kalonia, "Nature and consequences of protein-protein interactions in high protein concentration solutions.," *Int. J. Pharm.*, vol. 358, no. 1–2, pp. 1–15, Jun. 2008.
- [139] L. Brown and C. Glatz, "Aggregate breakage in protein precipitation," *Chem. Eng. Sci.*, vol. 42, no. 1, 1987.
- [140] M. Hoare, P. Dunnill, and D. J. Bell, "Reactor design for protein precipitation and its effect on centrifugal separation.," *Ann. N. Y. Acad. Sci.*, vol. 413, pp. 254–69, Jan. 1983.
- [141] E. Y. Chi, S. Krishnan, T. W. Randolph, and J. F. Carpenter, "Physical stability of proteins in aqueous solution: mechanism and driving forces in nonnative protein aggregation.," *Pharm. Res.*, vol. 20, no. 9, pp. 1325–36, Sep. 2003.
- [142] D. J. Bell, M. Hoare, and P. Dunnill, *The Formation of Protein Precipitates and Their Centrifugal Recovery*. 1983, pp. 1–72.
- [143] P. D. Virkar, M. Hoare, M. Y. Chan, and P. Dunnill, "Kinetics of the acid precipitation of soya protein in a continuous-flow tubular reactor.," *Biotechnol. Bioeng.*, vol. 24, no. 4, pp. 871–87, Apr. 1982.
- [144] T. R. Camp and P. C. Stein, "Velocity gradients and internal work in fluid motion," *J. Bost. Soc. Civ. Eng.*, vol. 85, pp. 219–237, 1943.
- [145] J. H. Rushton and E. W. Costich, "Power characteristics of mixing impellers. 1," *Chem. Eng. Prog.*, vol. 46, pp. 395–404, 1950.
- [146] D. J. Bell and P. Dunnill, "Shear disruption of soya protein precipitate particles and the effect of aging in a stirred tank.," *Biotechnol. Bioeng.*, vol. 24, no. 6, pp. 1271–85, Jun. 1982.

- [147] R. R. Fisher and C. E. Glatz, "Polyelectrolyte precipitation of proteins: II. Models of the particle size distributions.," *Biotechnol. Bioeng.*, vol. 32, no. 6, pp. 786–96, Sep. 1988.
- [148] D. J. Bell and P. Dunnill, "The influence of precipitation reactor configuration on the centrifugal recovery of isoelectric soya protein precipitate.," *Biotechnol. Bioeng.*, vol. 24, no. 11, pp. 2319–36, Nov. 1982.
- [149] N. Hutchinson, N. Bingham, N. Murrell, S. Farid, and M. Hoare, "Shear Stress Analysis of Mammalian Cell Suspensions for Prediction of Industrial Centrifugation and Its Verification," *Methods*, 2006.
- [150] R. Biddlecombe and S. Pleasance, "Automated protein precipitation by filtration in the 96-well format.," *J. Chromatogr. B. Biomed. Sci. Appl.*, vol. 734, no. 2, pp. 257–65, Nov. 1999.
- [151] A. P. Watt, D. Morrison, K. L. Locker, and D. C. Evans, "Higher throughput bioanalysis by automation of a protein precipitation assay using a 96-well format with detection by LC-MS/MS.," *Anal. Chem.*, vol. 72, no. 5, pp. 979–84, Mar. 2000.
- [152] W. a Duetz, "Microtiter plates as mini-bioreactors: miniaturization of fermentation methods.," *Trends Microbiol.*, vol. 15, no. 10, pp. 469–75, Oct. 2007.
- [153] M. Micheletti, T. Barrett, S. Doig, F. Baganz, M. Levy, J. Woodley, and G. Lye, "Fluid mixing in shaken bioreactors: Implications for scale-up predictions from microlitre-scale microbial and mammalian cell cultures," *Chem. Eng. Sci.*, vol. 61, no. 9, pp. 2939–2949, May 2006.
- [154] J. I. Betts, S. D. Doig, and F. Baganz, "Characterization and application of a miniature 10 mL stirred-tank bioreactor, showing scale-down equivalence with a conventional 7 L reactor.," *Biotechnol. Prog.*, vol. 22, no. 3, pp. 681–8, 2006.
- [155] F. Kensy, et al, "Oxygen transfer phenomena in 48-well microtiter plates: determination by optical monitoring of sulfite oxidation and verification by real-time measurement during microbial growth.," *Biotechnol. Bioeng.*, vol. 89, no. 6, pp. 698–708, Mar. 2005.
- [156] C. Knevelman, J. Davies, L. Allen, and N. J. Titchener-Hooker, "High-throughput screening techniques for rapid PEG-based precipitation of IgG4 mAb from clarified cell culture supernatant.," *Biotechnol. Prog.*, vol. 26, no. 3, pp. 697–705, 2009.
- [157] M. Boychyn, S. S. S. Yim, M. Bulmer, J. More, D. G. Bracewell, and M. Hoare, "Performance prediction of industrial centrifuges using scale-down models.," *Bioprocess Biosyst. Eng.*, vol. 26, no. 6, pp. 385–91, Dec. 2004.
- [158] J. P. Welsh, M. G. Petroff, P. Rowicki, H. Bao, T. Linden, D. J. Roush, and J. M. Pollard, "A practical strategy for using miniature chromatography columns in a standardized high-throughput workflow for purification development of monoclonal antibodies.," *Biotechnol. Prog.*, vol. 30, no. 3, pp. 626–35, 2014.
- [159] M. Bensch, P. Schulze Wierling, E. von Lieres, and J. Hubbuch, "High Throughput Screening of Chromatographic Phases for Rapid Process Development," *Chem. Eng. Technol.*, vol. 28, no. 11, pp. 1274–1284, Nov. 2005.
- [160] J. P. Aucamp, A. M. Cosme, G. J. Lye, and P. a Dalby, "High-throughput measurement of protein stability in microtiter plates.," *Biotechnol. Bioeng.*, vol. 89, no. 5, pp. 599–607, Mar. 2005.
- [161] J. P. Aucamp, R. J. Martinez-Torres, E. G. Hibbert, and P. a Dalby, "A microplate-based evaluation of complex denaturation pathways: structural stability of Escherichia coli transketolase.," *Biotechnol. Bioeng.*, vol. 99, no. 6, pp. 1303–10, Apr. 2008.

- [162] G. J. Mannall, J. P. Myers, J. Liddell, N. J. Titchener-Hooker, and P. a Dalby, "Ultra scale-down of protein refold screening in micro-wells: challenges, solutions and application.," *Biotechnol. Bioeng.*, vol. 103, no. 2, pp. 329–40, Jun. 2009.
- [163] C. Kitchen, A. Wang, D. Musson, A. Yang, and A. Fisher, "A semi-automated 96-well protein precipitation method for the determination of montelukast in human plasma using high performance liquid chromatography/fluorescence detection," *J. Pharm. Biomed. Anal.*, vol. 31, no. 4, pp. 647–654, Mar. 2003.
- [164] J. Gabrielsson, N.-O. Lindberg, and T. Lundstedt, "Multivariate methods in pharmaceutical applications," *J. Chemom.*, vol. 16, no. 3, pp. 141–160, Mar. 2002.
- [165] T. Lundstedt, E. Seifert, L. Abramo, B. Thelin, Å. Nyström, J. Pettersen, and R. Bergman, "Experimental design and optimization," *Chemom. Intell. Lab. Syst.*, vol. 42, no. 1–2, pp. 3–40, Aug. 1998.
- [166] P. Richardson, M. Hoare, and P. Dunnill, "A new biochemical engineering approach to the fractional precipitation of proteins.," *Biotechnol. Bioeng.*, vol. 36, no. 4, pp. 354–66, Aug. 1990.
- [167] H. Zhang, S. R. Lamping, S. C. R. Pickering, G. J. Lye, and P. A. Shamlou, "Engineering characterisation of a single well from 24-well and 96-well micro-titre plates," *Biochem. Eng. J.*, vol. 40, no. 1, pp. 138–149, May 2008.
- [168] M. P. Nunes, P. C. B. Fernandes, and M. H. L. Ribeiro, "Microtiter plates versus stirred mini-bioreactors in biocatalysis: a scalable approach.," *Bioresour. Technol.*, vol. 136, pp. 30–40, May 2013.
- [169] S. D. Doig, S. C. R. Pickering, G. J. Lye, and F. Baganz, "Modelling surface aeration rates in shaken micro-titre plates using dimensionless groups," *Chem. Eng. Sci.*, vol. 60, no. 10, pp. 2741–2750, May 2005.
- [170] W. Duetz and B. Witholt, "Effectiveness of orbital shaking for the aeration of suspended bacterial cultures in square-deep-well microtiter plates.," *Biochem. Eng. J.*, vol. 7, no. 2, pp. 113–115, Mar. 2001.
- [171] W. Klöckner, S. Tissot, F. Wurm, and J. Büchs, "Power input correlation to characterize the hydrodynamics of cylindrical orbitally shaken bioreactors," *Biochem. Eng. J.*, vol. 65, pp. 63–69, Jun. 2012.
- [172] A. J. Nealon, R. D. O’Kennedy, N. J. Titchener-Hooker, and G. J. Lye, "Quantification and prediction of jet macro-mixing times in static micro-well plates," *Chem. Eng. Sci.*, vol. 61, no. 15, pp. 4860–4870, Aug. 2006.
- [173] H. V. Iyer and T. M. Przybycien, "Protein precipitation: Effects of mixing on protein solubility," *AIChE J.*, vol. 40, no. 2, pp. 349–360, Feb. 1994.
- [174] J. Baldyga and R. Pohorecki, "Turbulent micromixing in chemical reactors - a review," *Chem. Eng. J.*, vol. 58, pp. 183–195, 1995.
- [175] W. Klöckner and J. Büchs, "Advances in shaking technologies.," *Trends Biotechnol.*, vol. 30, no. 6, pp. 307–14, Jun. 2012.
- [176] E. L. McGown and D. G. Hafeman, "Multichannel pipettor performance verified by measuring pathlength of reagent dispensed into a microplate.," *Anal. Biochem.*, vol. 258, no. 1, pp. 155–7, Apr. 1998.

[177] R. Raweerith and K. Ratanabanangkoon, "Fractionation of equine antivenom using caprylic acid precipitation in combination with cationic ion-exchange chromatography," *J. Immunol. Methods*, vol. 282, no. 1–2, pp. 63–72, Nov. 2003.

[178] J. Queiroz, C. T. Tomaz, and J. M. Cabral, "Hydrophobic interaction chromatography of proteins.," *J. Biotechnol.*, vol. 87, no. 2, pp. 143–59, May 2001.